Biologic Interconversion of Hydrogen and Formate

Cláudia Alhinho Mourato

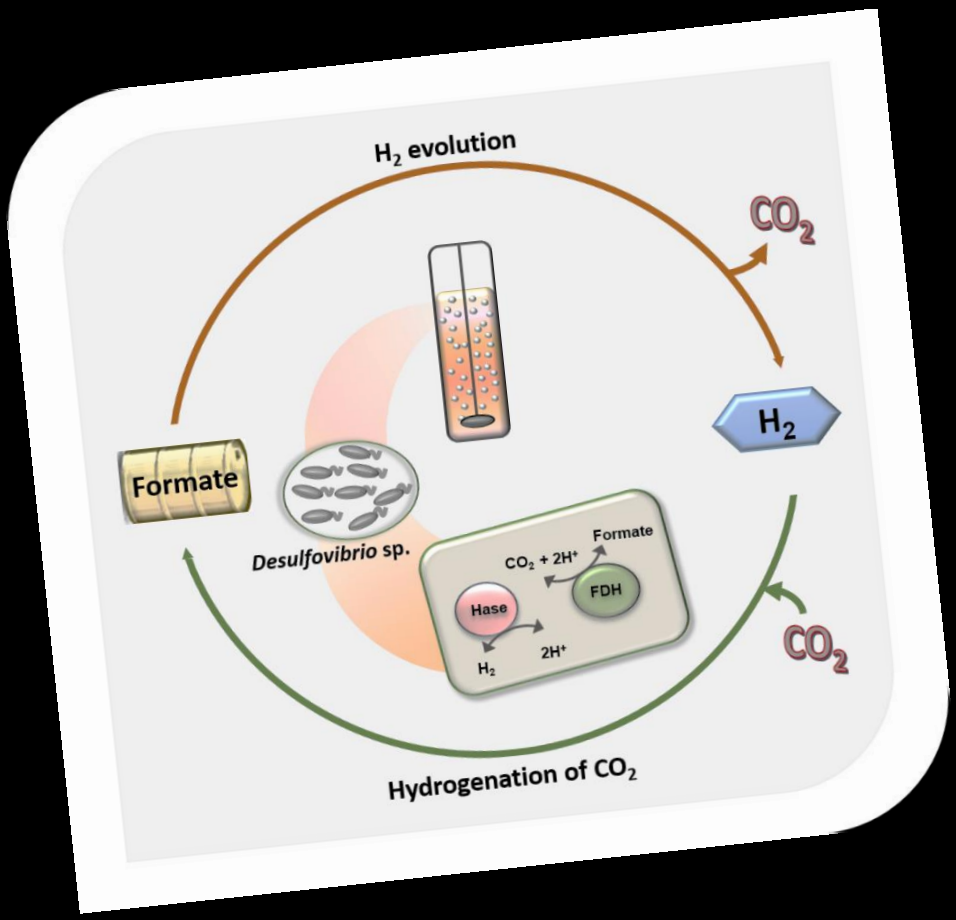

Dissertation presented to obtain the Ph.D degree in Biochemistry

Instituto de Tecnologia Química e Biológica António Xavier | Universidade Nova de Lisboa

Oeiras,
March, 2017

UNIVERSIDADE NOVA DE LISBOA

ITQB-UNL | Av. da República, 2780-157 Oeiras, Portugal
Tel (+351) 214 469 100 | Fax (+351) 214 411 277

www.itqb.unl.pt

Biologic Interconversion of Hydrogen and Formate

Cláudia Alhinho Mourato

Dissertation presented to obtain the Ph.D degree in Biochemistry – speciality in Biotechnology

Instituto de Tecnologia Química e Biológica António Xavier | Universidade Nova de Lisboa

Supervisor: Doctor Inês A.C. Pereira

Co-supervisor: Doctor Mónica Martins

Oeiras, March, 2017

The work presented in this thesis was carried out under the ITQB PhD program at the Instituto de Tecnologia Química e Biológica António Xavier (ITQB NOVA) from Universidade Nova de Lisboa under the supervision of Doctor Inês Cardoso Pereira and co-supervision of Doctor Mónica Martins.

Financial support was given by the PhD fellowship SFRH/BD/86442/2012 and two grants PTDC/BIA-MIC/104030/2008 and PTDC/BBB-EBB/2723/2014, from Fundação para a Ciência e Tecnologia (FCT).

ACKNOWLEDGMENTS

To Doctor Inês Cardoso Pereira for the guidance, help and support provided throughout all of these years. For all the knowledge and advices transmitted during this work. Thank you for accepting me in your group and for the trust deposited in me all this time.

To Mónica for all the advices and teachings transmitted all this time. For the work, help and companionship in my thesis but especially for the friendship that you gave me and that accompany me these years. Thank you so much for everything Monica! =)

To my current colleagues in the Bacterial Energy Metabolism lab, Ana Rita, Sónia, Américo, Sofia, Delfim, Carla, Sara, to whom I am grateful for all the moments and to share with me this moment. Sónia e Américo thank you for the funny and happy moments! To previous members of the lab: to Marta, who introduced me the protein purification world and with whom I shared truly happy and funny moments; to Raquel that taught me the tools needed for the molecular biology work; to Gonçalo, that although briefly was a good companion in the lab.

To Sofia Silva for the teaching and help during the qRT-PCR work. To Fábio and Cátia for their collaboration in the work during my PhD.

To Isabel Pacheco and João Carita for the help and support in the lab.

To the colleagues from the 3rd floor labs with I could always count for help or a technical advice.

To Professor Cláudio Soares and Professor Carlos Salgueiro for all the support and useful discussions during this thesis.

To Prof. Gerrit Voordouw, Judy D. Wall and Claudina Rodrigues-Pousada for their collaboration in the work and for providing the hydrogenases and formate-dehydrogenases mutants.

To Professor Silke Leimkühler for accepting in her lab in Potsdam and for the wonderful experience. To Tobias Hartmann for teaching me new things on genetic recombination and for all the guidance.

To friends …

Às minhas grandes amigas Catarina e Sofia pela amizade, pelo companheirismo e por todo o apoio que sempre me deram. Adoro-vos!

Às minhas amigas e companheiras de "viagem" Mariana e Andreia, com as quais partilhei muitos momentos desta longa jornada e fora dela e que sempre me deram força e ânimo para continuar. Foram um pilar!

Ao André... não tenho muito a dizer a não ser que foste um excelente colega e companheiro neste percurso e que és um grande amigo. À Inês por me ter recebido de braços e portas abertas e por agora já sermos "primas".

À minha Ritinha, que apesar de já ter aparecido numa fase final desta jornada, foi sem dúvida uma grande ajuda, uma grande colega e uma amiga extraordinária. =D

Ao Luís pela ajuda e amizade durante este tempo.

... and family

Às minhas irmãs, cunhados e aos meus sobrinhos pelo carinho, amizade e apoio. Adoro-vos! À minha avó pela sua fé e amor.

Aos meus pais por todo o amor, carinho e apoio incondicional que sempre me deram ao longo da minha vida, pelos sacrifícios que fizeram para eu chegar até aqui e por me ajudarem a alcançar os meus sonhos. ♥

Ao César, pelo apoio, companheirismo, amizade e amor partilhados ao longo de todos estes anos. ♥

A todos, Muito Obrigada!

THESIS PUBLICATIONS

Martins, M., Mourato C., and Pereira I.A.C. 2015. *Desulfovibrio vulgaris* growth coupled to formate-driven H_2 production. Environ Sci Technol. 49(24): 14655-14662.

Martins M.*, Mourato C.*, Morais-Silva F.O., Rodrigues-Pousada C., Voordouw G., Wall, J.D., Pereira I.A.C. 2016. Electron transfer pathways of formate-driven H_2 production in *Desulfovibrio*. Appl. Microbiol. Biotechnol. 100(18): 8135-8146. (*co-first authors)

Cláudia Mourato, Mónica Martins, Sofia M. da Silva, Inês A. C. Pereira. A continuous system for biocatalytic hydrogenation of CO_2 to formate. Bioresource Technology. Accepted. (doi.org/10.1016/j.biortech.2017.03.091)

Additional publications during the PhD not included in this thesis:

Martins M., Mourato C., Sanches, S., Noronha, J.P., Barreto Crespo, M.T., Pereira I.A.C. 2017. Biogenic platinum and palladium nanoparticles as new catalysts for the removal of pharmaceutical compounds. Water Res. 108:160-168.

THESIS ABSTRACT

Hydrogen (H_2) is one of the most promising energy vehicles in alternative to the use of fossil fuels. However, in order to use H_2 as energy carrier it is necessary to find a safe, economically viable, and reasonably sized solution to store and transport it. Formate has emerged as an ideal storage compound for H_2 as it is a safe compound, liquid at room temperature, which can be easily stored and transported, and furthermore it allows the sequestration of CO_2 in a valuable commodity chemical. Nevertheless, for the implementation of a H_2 and formate economy it is crucial to find efficient processes that can be used either for the use of formate as storage material for H_2 production or for the conversion of H_2 and CO_2 to formate.

Biotechnological processes using microorganisms as biological catalysts are an inexpensive and "greener" alternative for the conversion of CO_2 to formate and for biologic hydrogen production from one carbon compounds such as formate.

The main aim of the work presented in this thesis was to investigate the potential of sulfate reducing bacteria (SRB) as biocatalysts for formate-driven H_2 production, as well as, for the conversion of H_2 and CO_2 to formate. SRB are notorious for expressing a high level of formate-dehydrogenases (FDHs) and hydrogenases (Hases), the enzymes responsible for the reversible reactions of H_2 and formate production, making them good candidates for production of H_2 and formate.

In the first part of the work, a new lab-scale H_2 production process was designed to investigate the potential of the model organism *Desulfovibrio vulgaris* as a biocatalyst for H_2 production from formate. In the optimal conditions high volumetric and specific H_2 production rates (125 mL L^{-1} h^{-1} and 2500 mL g_{dcw}^{-1} h^{-1}) were achieved demonstrating that the non-conventional H_2-producing organism *D. vulgaris* is a good biocatalyst for converting formate to H_2. Moreover, the capacity of *D. vulgaris* to be used for continuous H_2 production from formate was also demonstrated. Furthermore, a bioreactor with gas sparging was used to demonstrate for the first time that H_2 production from formate can be coupled with growth of *D. vulgaris* in the absence of sulfate or a syntrophic partner. This is the first report of a single mesophilic organism that can grow while catalyzing the oxidation of formate to H_2 and bicarbonate.

Besides *D. vulgaris*, the potential for H_2 production of other *Desulfovibrio* strains was also evaluated. Among the strains tested (*D. vulgaris, D. desulfuricans*, *D. alaskensis* G20, *D. fructosivorans* and *D. gigas) D. vulgaris* showed the highest H_2 productivity and *D. gigas* the lowest one. Moreover, the electron transfer pathways involved in formate-driven H_2 production were also investigated in these two microorganisms through the study of deletion mutants of Hases and FDHs. This work demonstrated that the electron transfer pathways are species-specific. In *D. vulgaris*, the periplasmic FdhAB was shown to be the key enzyme for formate oxidation and that two pathways are involved in the production of H_2 from formate: a direct one only involving periplasmic enzymes, in which the Hys [NiFeSe] Hase is the main enzyme responsible for H_2 production; and a second one that involves transmembrane

electron transfer and may allow energy conservation. In contrast, H_2 production in *D. gigas* occurs exclusively in the periplasm not involving the cytoplasmic Ech Hase.

In the second part of the work SRB were investigated as novel biocatalysts for formate production through the hydrogenation of CO_2. Among the three *Desulfovibrio* strains tested (*D. vulgaris, D. alaskensis* G20 and *D. desulfuricans*), *D. desulfuricans* showed the highest capacity to reduce CO_2 to formate. This strain was used as whole cell biocatalyst in a new bioprocess developed for continuous production of formate. This is the first report of a process for continuous biocatalytic production of formate, in which more than 45 mM of formate were produced with a maximum specific formate production rate of 14 mM g_{dcw}^{-1} h^{-1}. Gene expression analysis indicated that the cytoplasmic FdhAB and the periplasmic HydAB [FeFe] are the main enzymes expressed in *D. desulfuricans* during formate production.

This work showed that SRB are suitable microorganisms to be used as whole cells biocatalysts in the biologic interconversion of H_2 and formate.

RESUMO DA TESE

O hidrogénio (H_2) é um dos veículos energéticos mais promissores em alternativa ao uso de combustíveis fósseis. No entanto, para a utilização do H_2 como transportador de energia é necessário encontrar uma forma segura e economicamente viável de o armazenar e transportar. Neste sentido, o formato tem surgido como um composto ideal para o armazenamento de H_2, dado que é líquido à temperatura ambiente, seguro, pode ser facilmente armazenado e transportado, e que permite a sequestração de CO_2 num produto químico de valor acrescentado. Contudo, para a implementação de uma economia à base de H_2 e formato é crucial encontrar processos eficientes que utilizem formato como material de partida para a produção de H_2 ou para a conversão de H_2 e CO_2 em formato.

A utilização de microrganismos como catalisadores biológicos em processos biotecnológicos é uma alternativa mais verde e económica para a conversão de CO_2 em formato e para produção de hidrogénio biológico a partir de compostos com apenas um carbono, como o formato.

O principal objetivo do trabalho apresentado nesta tese foi o de investigar o potencial de bactérias redutoras de sulfato (BRS) como biocatalisadores para a produção de H_2 a partir de formato, assim como, para a conversão de H_2 e CO_2 em formato. As BRS expressam um elevado número de formato-desidrogenases (FDHs) e hidrogenases (Hases), enzimas responsáveis pelas reações reversíveis de produção de H_2 e formato, o que as torna excelentes candidatos a ser utilizados para a produção de H_2 e formato.

Na primeira parte do trabalho, foi desenvolvido um novo processo à escala laboratorial para a produção de H_2 a partir de formato usando o organismo modelo *Desulfovibrio vulgaris* como biocatalisador. Nas condições de trabalho otimizadas, foram obtidas elevadas taxas volumétricas e específicas de produção de H_2 (125 mL L^{-1} h^{-1} e 2500 mL g_{dcw}^{-1} h^{-1}), demonstrando que um organismo não convencionalmente usado, *D. vulgaris,* é um promissor biocatalisador para a conversão de formato a H_2. Em paralelo foi também demonstrada a capacidade de *D. vulgaris* para ser usado na produção contínua de H_2 a partir de formato. Para além disso, usando um bioreator com dispersão de gás, demonstrou-se pela primeira vez que a produção de H_2 a partir de formato pode ser acoplada ao crescimento de *D. vulgaris,* na ausência de sulfato e de um organismo sintrófico. Com este trabalho, foi observado pela primeira vez que um organismo mesófilo pode crescer, individualmente, pela conversão de formato a H_2 e bicarbonato.

Posteriormente, a produção de H_2 por outras espécies de *Desulfovibrio* foi também investigada. Entre as espécies testadas (*D. vulgaris, D. desulfuricans*, *D. alaskensis* G20, *D. fructosivorans* e *D. gigas), D. vulgaris* foi a estirpe com maior produtividade enquanto que *D. gigas* foi a estirpe com menor produção de H_2. No seguimento deste estudo, foram investigadas as vias metabólicas envolvidas na produção de H_2 a partir de formato nestes dois organismos usando mutantes de deleção de Hases e FDHs. Este trabalho demonstrou que as vias de transferência de eletrões são específicas de cada espécie. Em *D. vulgaris*, foi observado que a FdhAB periplasmática é a principal enzima responsável pela oxidação de formato e que duas vias estão envolvidas na produção de H_2 a partir de formato: uma via direta em que apenas as enzimas

periplasmáticas estão envolvidas e na qual a Hys [NiFeSe] Hase é a principal enzima responsável pela produção de H_2; e uma segunda via que envolve a transferência de eletrões através da membrana e que pode permitir conservação de energia. Por outro lado, a produção de H_2 em *D. gigas* ocorre exclusivamente no periplasma não envolvendo a Hase citoplasmática Ech.

Numa segunda parte do trabalho, as BRS foram investigadas como novos biocatalisadores para a produção de formato através da hidrogenação de CO_2. Entre as três espécies de *Desulfovibrio* testadas (*D. vulgaris, D. alaskensis* G20 e *D. desulfuricans*), *D. desulfuricans* apresentou a maior capacidade para reduzir CO_2 a formato. Esta estirpe foi também utilizada como biocatalisador num novo bioprocesso desenvolvido para produção de formato. Para além disso, neste estudo implementou-se também pela primeira vez um processo que permite a produção contínua de formato conseguindo produzir mais de 45 mM de formato com uma taxa máxima específica de 14 mM g_{dcw}^{-1} h^{-1}. Neste estudo, a análise da expressão genética evidenciou que a FdhAB citoplasmática e a HydAB [FeFe] periplasmática são as principais enzimas expressas em *D. desulfuricans* durante a produção de formato.

Assim, o presente trabalho demonstrou que as BRS são microrganismos com elevado potencial para serem utilizados como biocatalisadores na interconversão biológica de H_2 e formato.

LIST OF ABBREVIATIONS

A. woodii	*Acetobacterium woodii*
ASTR	Anaerobic stirred tank reactor
ATP	Adenosine triphosphate
$BioH_2$	Biological hydrogen
BRS	Bactérias redutoras de sulfato
C. boidinii	*Candida boidinii*
C. carboxidivorans	*Clostridium carboxidivorans*
Coo	CooMKLXUH CO-induced hydrogenase
Cys	Cysteine
ΔG	Gibbs free energy change
D. alaskensis	*Desulfovibrio alaskensis* G20
D. desulfuricans	*Desulfovibrio desulfuricans* ATCC 27774
D. fructosivorans	*Desulfovibrio fructosivorans*
D. gigas	*Desulfovibrio gigas*
D. vulgaris	*Desulfovibrio vulgaris* Hildenborough
dcw	Dry cell weight
E. coli	*Escherichia coli*
Ech	Energy conserving hydrogenase
[FeFe] Hase	Iron-iron hydrogenase
Fd	Ferredoxin
FDH	Formate-dehydrogenase
FdhAB	Formate-dehydrogenase AB
$FdhABC_3$	Formate-dehydrogenase ABC_3
FdhABD	Formate-dehydrogenase ABD
FHL	Formate-hydrogen lyase
Fw	Forward
GC	Gas chromatography
Hase	Hydrogenase
HPLC	High performance liquid chromatography
HRT	Hydraulic retention time
Hyd or HydAB	[FeFe] hydrogenase AB
HynAB-1	$[NiFe]_1$ hydrogenase AB
HynAB-2	$[NiFe]_2$ hydrogenase AB
Hys or HysAB	[NiFeSe] hydrogenase
M. arboriphilus AZ	*Methanobrevibacter arboriphilus* AZ
M. extorquians	*Methylobacterium extorquens*
MECs	Microbial electrolysis cells

METC	Membrane-bound electron transfer complexes
MFCs	Microbial fuel cells
Mo-FDH	Molybdenum-containing FDH
MOPS	3-(N-morpholino)propanesulfonic acid buffer
NAD/NADH	Nicotinamide adenine dinucleotide
$NADP^+$/NADPH	Nicotinamide adenine dinucleotide phosphate
Nase	Nitrogenase
[NiFe] Hase	Nickel-iron hydrogenase
[NiFeSe] Hase	Nickel iron selenium hydrogenase
OD	Optical density
P_{H2}	H_2 partial pressure
P_{CO2}	CO_2 partial pressure
P. furiosus	*Pyrococcus furiosus*
PFL	Pyruvate formate-lyase
PFOR	Pyruvate ferredoxin oxidoreductase
PS	Photosystem
PSI	Photosystem I
PSII	Photosystem II
Q_{AR}	Argon flow rate
Qrc	Quinone reductase complex
qRT-PCR	Quantitative real time polymerase chain reaction
rRNA	Ribossomic ribonucleic acid
Rv	Reverse
SeCys	Selenocysteine
sp.	species
SRB	Sulfate-reducing bacteria
TOF	Turnover frequency
TON	Turnover number
Tris	Tris(hydroxymethyl)aminomethane
T. onnurineus	*Thermococcus onnurineus*
TCD	Thermal conductivity detector
Tmc	Transmembrane complex
UV	Ultraviolet
W-FDH	Tungsten-containing FDH
wt	wild-type

TABLE OF CONTENTS

ACKNOWLEDGMENTS ..... **v**

THESIS PUBLICATIONS ..... **vii**

THESIS ABSTRACT ..... **ix**

RESUMO DA TESE ..... **xiii**

LIST OF ABBREVIATIONS ..... **xvii**

CHAPTER 1 – INTRODUCTION

1. INTERCONVERSION OF H_2 AND FORMATE 2

1.1 BIOLOGICAL H_2 PRODUCTION 6

1.1.1 MICROORGANISMS AS BIOCATALYSTS FOR H_2 PRODUCTION 7

1.1.1.1 BIO-PHOTOLYSIS PROCESS 8

1.1.1.2 FERMENTATION PROCESSES 10

1.1.1.3 ELECTRICALLY DRIVEN BIOHYDROGEN PRODUCTION 13

1.1.1.4 DARK-FERMENTATION IMPROVEMENT APPROACHES 14

1.1.2 HYDROGENASES - THE ENZYMES INVOLVED IN H_2 PRODUCTION 17

1.2 BIOLOGICAL FORMATE PRODUCTION 20

1.2.1 MICROORGANISMS AS BIOCATALYSTS FOR FORMATE PRODUCTION 22

1.2.2FORMATE-DEHYDROGENASES – THE ENZYMES RESPONSIBLE FOR FORMATE PRODUCTION 23

1.3 SULFATE-REDUCING BACTERIA FOR H_2 AND FORMATE PRODUCTION 26

1.4 AIM OF THE THESIS 31

REFERENCES 32

CHAPTER 2 – *DESULFOVIBRIO VULGARIS* GROWTH COUPLED TO FORMATE-DRIVEN H_2 PRODUCTION

2. ABSTRACT **48**
2.1 INTRODUCTION **48**
2.2 MATERIALS AND METHODS **51**
2.2.1 BACTERIAL STRAINS AND GROWTH CONDITIONS 51
2.2.2 BIOREACTOR ASSAYS 51
2.2.4 ANALYTICAL METHODS 54
2.2.5 THERMODYNAMIC CALCULATIONS 55
2.3 RESULTS **55**
2.3.1 STIRRED TANK REACTOR ASSAYS 55
2.3.2 COLUMN REACTOR ASSAYS 61
2.3.3 BIOH_2 PRODUCTION ON FED-BATCH MODE 65
2.4 DISCUSSION **66**
2.4.1 HYDROGEN PRODUCTION 66
2.4.2 BACTERIAL GROWTH ON FORMATE 70
ACKNOWLEDGMENTS **72**
REFERENCES **73**

CHAPTER 3 - ELECTRON TRANSFER PATHWAYS OF FORMATE-DRIVEN H_2 PRODUCTION IN *DESULFOVIBRIO*

3. ABSTRACT **78**
3.1 INTRODUCTION **79**
3.2 MATERIAL AND METHODS **81**
3.2.1 STRAINS AND GROWTH CONDITIONS 81
3.2.2 H_2 PRODUCTION ASSAYS IN SERUM BOTTLES 82
3.2.3 H_2 PRODUCTION IN A BIOREACTOR WITH GAS SPARGING 83
3.2.4 ANALYTICAL METHODS 84
3.2.5 HASE ACTIVITY-STAINED NATIVE GELS 85
3.2.6 STATISTICAL ANALYSIS 85
3.3 RESULTS **86**

3.3.1 H_2 PRODUCTION BY DIFFERENT *DESULFOVIBRIO* SPECIES 86
3.3.2 EFFECT OF FDH INACTIVATION ON H_2 PRODUCTION BY *D. VULGARIS* 89
3.3.3 EFFECT OF HASE INACTIVATION ON H_2 PRODUCTION BY *D. VULGARIS* 90
3.3.4 ANALYSIS OF *D. VULGARIS* HASES BY ACTIVITY-STAINED GELS 94
3.3.5 EFFECT OF HASE INACTIVATION ON H_2 PRODUCTION BY *D. GIGAS* 95
3.3.6 GROWTH OF *D. VULGARIS* MUTANTS BY FORMATE TO H_2 CONVERSION ..98
3.4 DISCUSSION 100
ACKNOWLEDGEMENTS 110
REFERENCES 111

CHAPTER 4 - A CONTINUOUS SYSTEM FOR BIOCATALYTIC HYDROGENATION OF CO_2 TO FORMATE

4. ABSTRACT 118
4.1 INTRODUCTION 118
4.2 MATERIALS AND METHODS 121
4.2.1 BACTERIAL STRAINS AND GROWTH CONDITIONS 121
4.2.2FORMATE PRODUCTION BY WHOLE CELLS IN SERUM BOTTLES 121
4.2.3 FORMATE PRODUCTION IN A COLUMN BIOREACTOR 122
4.2.4 RNA ISOLATION AND QUANTITATIVE RT-PCR ANALYSIS (qRT-PCR) 123
4.2.5 ANALYTICAL METHODS 125
4.2.6 THERMODYNAMIC AND SOLUBILITY CALCULATIONS 125
4.2.7 STATISTICAL ANALYSIS 127
4.3 RESULTS AND DISCUSSION 127
4.3.1 FORMATE PRODUCTION BY *DESULFOVIBRIO* WHOLE CELLS IN BATCH CONDITIONS 127
4.3.2 FORMATE PRODUCTION BY *D. DESULFURICANS* WHOLE CELLS IN A BIOREACTOR 129
4.3.2.1. FORMATE PRODUCTION PROFILE 130
4.3.2.2. OPTIMIZATION OF BIOREACTOR CONDITIONS 131
4.3.3 FORMATE PRODUCTION IN CONTINUOUS CONDITIONS 133
4.3.4 EXPRESSION ANALYSIS OF FDHS AND HASES 135

4.3.4.1 FORMATE DEHYDROGENASES GENES 136
4.3.4.2 HYDROGENASES GENES 138
4.3.5 OVERVIEW OF FORMATE PRODUCTION STUDIES 141
4.4 CONCLUSIONS 143
ACKNOWLEDGEMENTS 143
REFERENCES 144

CHAPTER 5 - CONCLUDING REMARKS

5. CONCLUDING REMARKS 150

CHAPTER 1

INTRODUCTION

1. INTERCONVERSION OF H_2 AND FORMATE

Fossil fuels are the main global energy resource, used for electric power generation, industry and transportation [1]. Due to the great dependence on these non-renewable resources and consequent emission of greenhouse gases there has been an increasing awareness of the need to reduce their use, since the greenhouse effect is the main responsible for global climate change [2,3] and the carbon dioxide (CO_2) levels have been increasing more rapidly in the recent years. The rate of CO_2 emissions has been steadily increasing, going to 2.25 ppm/year in recent years, which corresponds to 12 billion tons of CO_2/year [4,5]. These high levels of CO_2 not only contribute to climate change, but also lead to ocean acidification, with unpredictable consequences for life in our planet. Therefore, finding new alternative energy sources for the replacement of fossil fuels and developing sustainable processes to reduce the levels of CO_2 is a critical issue nowadays. Among others, two promising areas of research have been developed: (i) the use of hydrogen (H_2) as an alternative energy carrier, with no negative impact on the environment [6–8], and (ii) the recycling of CO_2 by its conversion to added-value compounds that can be used as fuels or chemical feedstocks, like formate [9–12].

H_2 is one of the most attractive candidates to be used as energy carrier. As a carbon-neutral molecule, H_2 is a source of clean energy and can be produced from renewable biomass. Due to its clean combustion with only water as its end-product, and its high energy content of 122 KJ/g (2.75-fold greater than hydrocarbon fuels), H_2 represents a promising alternative to the use of fossil

fuels [6,8,9,13]. Therefore, research on H_2 production and usage has received a growing attention from scientists during the last decades [14]. H_2 has a great potential in the transport sector and in domestic and industrial applications, where it is being explored for use in combustion engines and fuel-cell electric vehicles [6,8,15].

Although H_2 is a strong candidate as an alternative energy carrier, there is still no safe, economically viable, and reasonably sized solution to store and transport it. The conventional methods for H_2 storage, such as high-pressure gas containers or cryogenic liquid containers, have safety issues [16] and storage of H_2 in its elemental form as a gas or a liquid has safety implications due to its low volumetric energy density and flammable nature, and the need to keep it under pressure [8,9]. Thus, developing a viable H_2 storage system is very important for the implementation of H_2 as energy carrier. A possible method for its storage has been explored using formate as storage system (Figure 1.1) [9,17]. Formate or formic acid has been considered one of the most promising candidates as storage material for H_2 production. Formate is liquid at room temperature, non-toxic and non-flammable and can thus be handled, stored and transported easily [9,18], providing a renewable low price and efficient source for large scale or *in situ* H_2 production.

The formate based H_2 storage system provides not only a viable way to produce and store H_2 in a safe and efficient compound, but also a means of CO_2 sequestration by reducing it to a value-added compound like formate. In fact, the reduction of CO_2 to generate value-added compounds as fuels and chemical feedstocks is an essential requirement for a carbon-neutral

sustainable energy economy. In the first step of the proposed system, formate is formed by hydrogenation of CO_2, and later H_2 can be generated from formate liberating CO_2 as the only byproduct. Thus, this cycle is carbon-neutral [9,17,18].

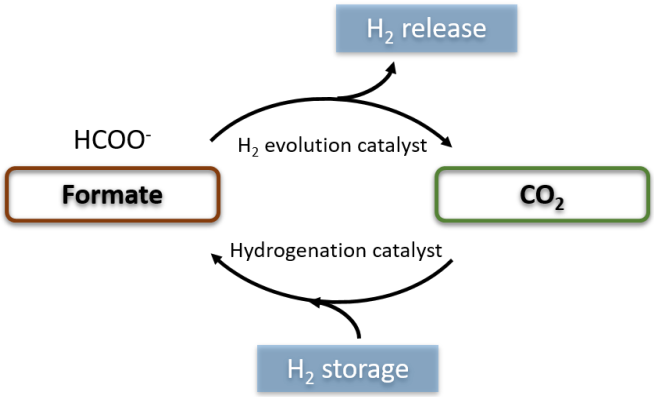

Figure 1.1. Formate-based H_2 storage system (created according to [9,18]).

For the implementation of a H_2 and formate economy it is very important to find efficient processes and suitable catalysts that can be used for the production of formate as storage material and for H_2 release from formate. An important problem is also the need to produce H_2 as this gas is not naturally available and there are currently no inexpensive methods to produce it. Many of the technologies to produce H_2 still rely on non-sustainable and energy-intensive processes. Extensive studies have been carried out on the use of homogeneous and heterogeneous chemical catalysts for H_2 and formate production [9,11,18–21]. However, most of these catalysts require too expensive and demanding operation conditions, like the use of precious metals

such as iridium (Ir), ruthenium (Ru) and rhodium (Rh), high temperatures and high pressures (see examples in Table 1.1), not making them suitable for a sustainable economy.

Table 1.1. Examples of most used metal catalysts for H_2 and formate production.

Catalysts	Substrate	Performance	T (°C)	Pressure (atm)	Ref
Hydrogen production					
$[IrH_3(PPh_3)_3]$	Formate	TOF=8890 h^{-1}	118	n.r.	[22]
$RuBr_3.H_2O/3PPh_3$		TOF=3630 h^{-1}	40	n.r.	[23]
$(^{Ph}I_2P^{2-})Al(THF)H$		TOF=5200 h^{-1}	65	n.r.	[24]
$[Cp^*Ir(N9)(OH_2)]^{2+}$		TON=2 050 000	60	n.r.	[25]
$[RuCl_2(p\text{-}cymene)]_2$	Isopropanol	TOF=up to 519 h^{-1}	90	n.r.	[26]
$[RuH_2(N_2)(PPh_3)_3]$	Alcohols (ethanol, ethylene, buthanol)	TOF=148-523 h^{-1}	150	n.r.	[21]
$[RuH_2(PPh_3)_4]$		TOF=150-527 h^{-1}	150	n.r.	
Formate production					
$[RuCl(OAc)PMe_3)_4]$	Carbon dioxide	TOF=95000 h^{-1}	50	70 H_2/120 CO_2	[27]
$[RuCl_2(TPPMS)_2]_2$		TOF=9600 h^{-1}	80	60 H_2/35 CO_2	[28]
$(PN^{Py}P)IrH_3$		TOF=150000 h^{-1}	200	25 H_2/25 CO_2	[29]
$[Cp^*Ir(OH_2)(6HBPY)]^{2+}$		TOF=25200 h^{-1}	120	5 H_2/5 CO_2	[30]
$RuCl_2(PTA)_4$		TON=750	60	50 H_2/50 CO_2	[31]
RuH(Cl)(CO)(P3)		TOF=1100000 h^{-1}	120	30 H_2/10 CO_2	[32]
$[\{RuCl_2(benzene)\}_2]$	Sodium bicarbonate	TON=1731	70	50 H_2/30 CO	[10]
	Potassium bicarbonate	TON=1592	70		

TOF, turnover frequency; TON, turnover number; n.r. = not reported

As a result, biological systems may provide an alternative and a sustainable process for H_2 and formate production. The use of biological catalysts that can use renewable resources would constitute an inexhaustible, clean and sustainable process to produce H_2 and/or formate [7,33].

1.1 BIOLOGICAL H_2 PRODUCTION

The most common processes used for H_2 production include electrolysis of water, thermocatalytic reformation of H_2-rich organic compounds and thermal processes such as steam reforming of natural gas or methane [34]. Since the majority of H_2 production is predominantly derived from fossil fuels or is very energy intensive, there is still no large scale sustainable production process. Currently, the production of H_2 exceeds 1 billion m^3/day worldwide, of which 48% derives from natural gas, 30% from oil, 18% from coal, and the remaining 4% is produced from H_2O-splitting electrolysis [14,35,36]. On the other hand, the emergence of biological processes for H_2 production using waste materials provides renewable, environmental friendly and less energy intensive processes. These bioprocesses rely on less expensive and demanding operation settings and can be operated under mild conditions (at ambient temperature and pressure with minimal energy consumption) [13,34,37] using microorganisms as biocatalysts.

1.1.1 MICROORGANISMS AS BIOCATALYSTS FOR H_2 PRODUCTION

The biological H_2 ($bioH_2$) production is known to be conducted by a diverse group of microorganisms and can be achieved by using pure cultures with defined substrates or with mixed consortia [35]. Several microorganisms such as obligate anaerobes, thermophiles, methanogens and facultative anaerobes are capable of producing H_2, whereas others only produce H_2 from specific metabolic routes under defined conditions [35]. This is the case of anaerobic, photosynthetic prokaryotes (heterotrophic and autotrophic) and microalgae [35,38]. Besides, in most microorganisms, the generation of molecular H_2 is an essential part of their energy metabolism, and provides a way of eliminating excess electrons.

In biological systems, H_2 can be generated from a variety of renewable resources and a wide range of approaches for $bioH_2$ production are available including bio-photolysis, photo-fermentation, dark-fermentation and microbial electrolysis (Figure 1.2) [7,14,33,37].

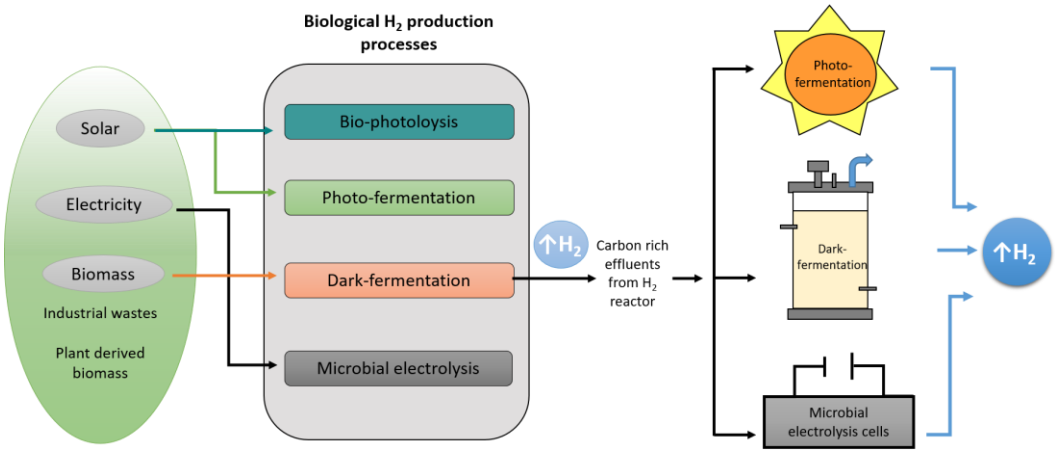

Figure 1.2. Schematic representation of the biological processes integrated with secondary routes for effective H_2 production (created according to [14]).

1.1.1.1 BIO-PHOTOLYSIS PROCESS

The mechanism of **bio-photolysis**, also known as water-splitting photosynthesis, involves plant-type photosynthesis, that uses sunlight to split water for H_2 formation [35,39,40]. This bioprocess occurs in photoautotrophic microorganisms such as eukaryotic microalgae like *Chlamydomonas reinhardtii* sp. [41,42] and *Chlorella* sp. [43,44] or in prokaryotic bacteria from soil or natural water like cyanobacteria *Anabaena* sp. [45,46]. These organisms use sunlight and CO_2 as the only energy and carbon sources and the reducing power for cellular photosynthesis and/or bio-photolysis comes from water oxidation under light irradiation [39]. In a plant-like oxygenic photosynthesis,

the sunlight energy is captured and absorbed by photosynthetic systems (PSI and PSII) [47]. The photons from sunlight are adsorbed by the PSII resulting in the production of oxidizing equivalents used for water oxidation to protons (H^+), electrons (e^-) and molecular oxygen (O_2) [35,39,48]. The electrons are then transferred through the electron transport chain through a series of electron carriers to PSI which also adsorbs photons leading to the reduction of the oxidized ferredoxin (Fd) and/or nicotinamide adenine dinucleotide phosphate ($NADP^+$) [39,48]. In this process, adenosine triphosphate (ATP) is produced via ATP synthase through the generation of a proton gradient formed across the cellular membrane and atmospheric CO_2 is reduced with ATP and NADPH via Calvin cycle for cell growth [39,48]. The excess reduced carbon is stored inside the cells as carbohydrates and/or lipids [39]. However, under anaerobic and dark conditions, the reduced Fd also serves as electron donor for hydrogenases (Hases) or nitrogenases (Nases) which will reduce protons to H_2 leading to bio-photolysis [14,39,48]. H_2 production by bio-photolysis takes place in anaerobic conditions to induce activation of enzymes involved in hydrogen metabolism (Hases and Nases), since these two enzymes are sensitive to the O_2 evolved during photosynthesis [39,49].

There are two types of bio-photolysis: direct and indirect bio-photolysis (Figure 1.3) [35,39,40]. In both processes, the light energy adsorpt by the PSII generates a proton gradient and electrons from water splitting that are used to produce H_2. However, in indirect bio-photolysis the reducing equivalents can also be derived from the fermentation of organic molecules (starch or carbohydrates reserves formed during photosynthesis) and not only directly

from water splitting [14,35,39]. Indirect bio-photolysis has the advantage of separating the photosynthesis for carbohydrate accumulation from the dark-fermentation of the carbon reserves for H_2 production. In this way, the oxygen and hydrogen evolutions are separated [39].

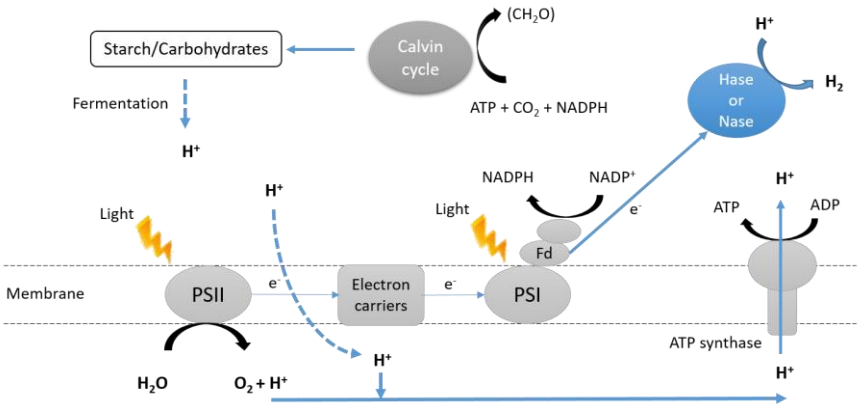

Figure 1.3. Schematic mechanism of H_2 evolution through direct and indirect bio-photolysis (created according to [14,35,39]).

1.1.1.2 FERMENTATION PROCESSES

Fermentation processes, contrarily to bio-photolysis, have a higher stability and efficiency regarding H_2 production [35]. These processes can use a variety of organic wastes (i.e. biomass, agricultural and domestic wastes) as a substrate, so can play the dual role of waste reduction and energy production [13,35,40]. In the case of **photo-fermentation**, a group of photosynthetic bacteria (e.g. purple non-sulfur bacteria) use sunlight as source of energy to convert organic substrates into H_2 and CO_2 [14,35,40,50]. This conversion of

small organic compounds, like acetate, lactate and butyrate, to H_2 is performed under anaerobic conditions by anoxygenic photosynthesis where water is not used as an electron donor and thus no O_2 is produced [14,35]. Thus, photo-fermentation circumvents the oxygen sensitivity issue of bio-photolysis process.

H_2 production by photo-fermentation has been shown in purple non-sulfur bacteria such as *Rhodobacter sphaeroides* [51,52], *Rhodopseudomonas palustris* [53,54] and *Rhodopseudomonas faecalis* [55,56]. In photo-fermentation (Figure 1.4) , the electrons generated during oxidation of organic substrates are transferred through a series of electron carriers, during which protons are pumped through a ATP synthase creating a proton gradient leading to ATP synthesis [50]. The electrons are then transferred to Fd and delivered to a Nase, that functions as a Hase under limited nitrogen source conditions, for H_2 production using ATP [50].

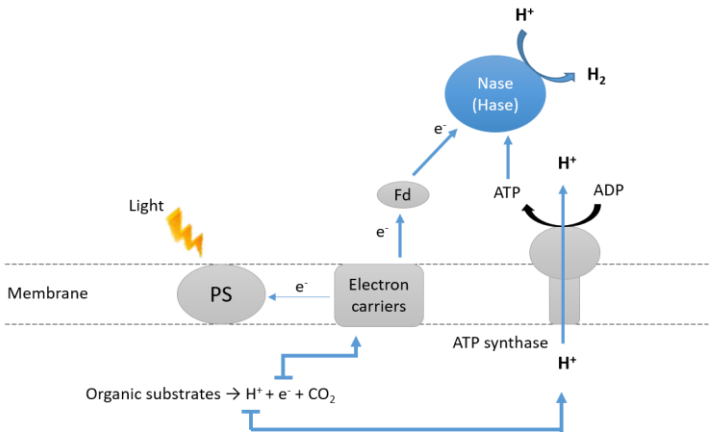

Figure 1.4. Schematic mechanism of H_2 evolution through photo-fermentation (created according to [35,50]).

In contrast, in **dark-fermentation**, the conversion of organic substrates to H_2 occurs under anaerobic conditions in the absence of light [14,37,40]. In this process, obligate anaerobes such as *Clostridium* [57,58] or facultative anaerobes like *Enterobacter* [59,60] are able to produce H_2 and volatile fatty acids from carbohydrates like glucose or complex organic feedstocks such as organic wastes and wastewaters [14,61].

In the case of glucose fermentation, this is converted to pyruvate through glycolysis. Under anaerobic conditions, this pyruvate is converted to fermentation products (short chain fatty acids like lactic acid, acetic acid and butyric acid) producing also H_2. Thus, the process of dark-fermentation can occur in two pathways (Figure 1.5): (1) in obligate anaerobic organisms, in which the decarboxylation of pyruvate into acetyl-CoA and CO_2 occurs by pyruvate ferredoxin oxidoreductase (PFOR), which generates reduced Fd that transfer electrons to a Hase producing H_2; and (2) in facultative anaerobic organisms, in which the conversion of pyruvate to acetyl-CoA and formate occurs by the action of pyruvate formate-lyase (PFL), and then the production of H_2 from formate with the catalysis of the formate-hydrogen lyase (FHL), a complex comprising a formate-dehydrogenase (FDH) together with a Hase [14,62,63]. The electrons generated during glycolysis are channeled trough several electron carriers to Fd which donates the electron for the reduction of protons, released from the redox mediator NADH with NADH dehydrogenase, to H_2 by the action of a Hase [14,35,63].

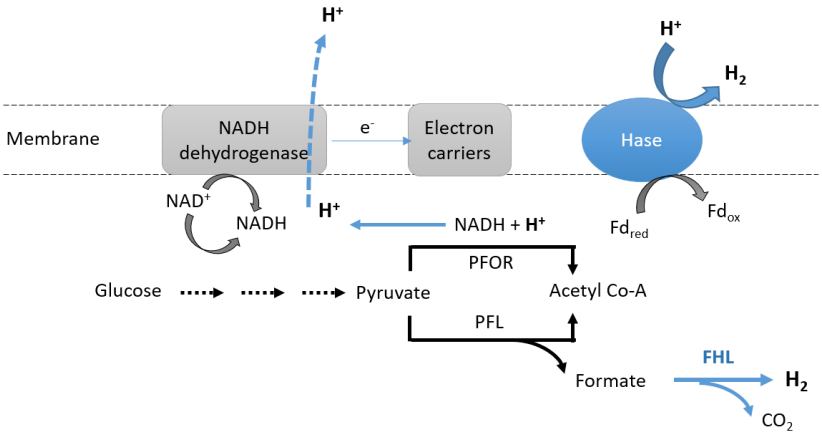

Figure 1.5. Schematic mechanism of H_2 evolution through dark-fermentation (created according to [14,35]).

1.1.1.3 ELECTRICALLY DRIVEN BIOHYDROGEN PRODUCTION

Another H_2 production technique that can use a wide variety of substrates to produce H_2 are microbial electrolysis cells (MECs) [64]. MECs are a bioelectrochemical technology that has been used for biological H_2 production as an alternative electrically driven H_2 production bioprocess [14,35,65]. MECs are adapted microbial fuel cells (MFCs), in which the conversion of a wide range of organic compounds into H_2 occurs by combining microbial metabolism of organic matter with bio-electrochemical reactions under a small input of external potential [66–68]. Bacteria will oxidize the organic substrate releasing CO_2 and protons into solution and electrons to the anode. Then, the electrons flow from the anode through a electrical wire to the cathode electrode. By applying a small voltage and generating a current

between the anode and cathode, H_2 is produced in the cathode through the reduction of protons [14,65,69].

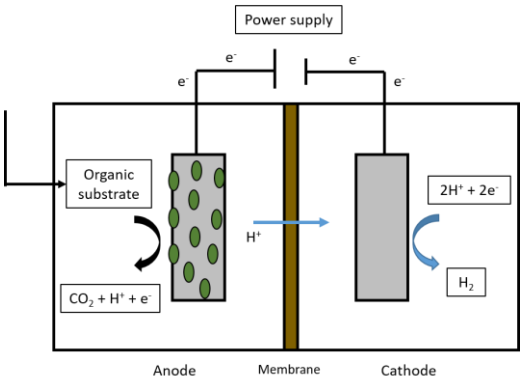

Figure 1.6. Schematic of a two chamber MEC system construction and operation (created according to [65,69]).

1.1.1.4 DARK-FERMENTATION IMPROVEMENT APPROACHES

Despite the advantageous features of the different bioprocesses for H_2 production such as the use of a inexhaustible substrate (water) in the case of biophotolysis, the nearly complete substrate conversion in photo-fermentation or the variety of wastes that can be used for H_2 production in dark fermentation, there are still several technical challenges to be overcome [70]. Of the biological H_2 production processes previously described, dark-fermentation has received increasing interest due to the: high rates of H_2 production when compared to the other bioprocesses, the continuous production of H_2 in the absence of light, the low energy demand, process

simplicity and easy operation (simple reactor technology, either in batch or continuous mode) and the versatility of the substrates that can be used for this process [7,33,40,70]. However, the main drawback of this fermentative process is the low H_2 yield, due to the co-production of other fermentation products such as carboxylic acids and alcohols, which results in low substrate conversion efficiency [14,33,61]. As a result, several researchers have focused on the development of suitable hybrid processes, such as the two-stage system integration of the dark fermentation process, which can increase the H_2 production by dark-fermentation [14,62,63]. In this integrated approach, additional energy is recovered from the organic products from the first dark-fermentation stage, like formate, butyrate, acetate, ethanol or lactate, and used for further H_2 production during a second stage process that could either be a photo-fermentation process [71,72], MECs [73,74] or a second stage of dark-fermentation (e.g. in anaerobic digestion) (Figure 1.2) [75,76]. With a two-system approach, the total energy recovery is maximized making the entire process more economically and industrially viable [14]. Moreover, three-stage fermentation systems have also been investigated for H_2 and also methane production (anaerobic digestion) [77,78].

Despite the positive advantages of dark-fermentation, bioH_2 production is yet to compete with the existent processes derived from fossil fuels in terms of cost, efficiency and reliability [7,14]. Thus, besides developing hybrid systems for higher H_2 production, the design of H_2 producing bioreactors and the selection of appropriate feedstocks and suitable and efficient microbial strains as biocatalysts is extremely important for bioH_2 production [62]. Significant

advances have been made in identifying H_2-producing microorganisms, and optimizing systems to maximize H_2 production. Several studies have shown the potential of these as biocatalysts for bioH_2 production from different substrates such as lactate, butyrate, acetate and formate [53,79–81] . Of these, the use of formate in bioH_2 production studies has been an attractive area of research, due to the emergence of formate as a good H_2 storage material. Formate is also a key metabolite for bacteria, functioning as a growth substrate or being a metabolic product of bacterial fermentations. Moreover, since formate is also a by-product of dark-fermentation, the formation of H_2 from this substrate can be coupled to a two stage system. Formate-driven H_2 production has been observed by many organisms [38]. In *Escherichia coli*, in which formate-driven H_2 production is well studied, the production of H_2 has been observed with agar-immobilized cells, as well as by applying genetic engineering for higher H_2 productivity [60,82–84]. Studies with *Enterobacter* species [85,86] and hyperthermophile organisms like *Thermococcus onnurineus* and recombinant strains of *Pyrococcus furiosus* [84,87,88] have also demonstrated the capacity of these microorganisms for H_2 production from formate. In addition, H_2 production using formate was also reported in sulfate-reducing bacteria (SRB), either by using these bacteria in bio-electrodes in MEC [80,89], or by using a low cost technology like an anaerobic stirred tank reactor (ASTR) [81].

1.1.2 HYDROGENASES - THE ENZYMES INVOLVED IN H_2 PRODUCTION

BioH_2 production as a product of microbial metabolism is achieved by H_2 producing enzymes, mostly hydrogenases (Hases), that catalyze the simple and reversible reaction of H_2 production (equation 1.1) [90–92].

$$2H^+ + 2e^- \rightleftharpoons H_2 \qquad \text{(equation 1.1)}$$

Hydrogenases are the enzymes that mediate H_2 metabolism in Bacteria, Archea and Eucarya [90,91,93]. Different types of Hases can be found in these microorganisms and the difference among these enzymes is based on the metal composition of their active site which divides Hases in di-iron [FeFe], nickel-iron [NiFe], and iron-sulfur cluster free [Fe] only enzymes [91,92]. Among the [NiFe] Hases, some organisms also contain [NiFeSe] Hases, a sub-group of the [NiFe] Hases where a selenocysteine (SeCys) residue is a terminal Ni ligand instead of a cysteine [94,95].

Most Hases are bidirectional and their reversible action allows the generation of molecular H_2, as well as its consumption, depending on the reaction conditions, and in general their physiological function is associated with their location in the cell. Hases present in the periplasm (either soluble or associated with the membrane), are generally considered uptake Hases and utilize H_2 as electron source. In contrast, cytoplasmic Hases are usually proton reduction enzymes as a way of disposing of excess electrons, leading to the production of H_2 [93,96]. Accordingly, the [NiFe] Hases are usually involved in H_2 oxidation,

whereas [FeFe] Hases are often more active for the production of H_2 [93]. Moreover, the [NiFeSe] Hases also display a higher H_2 production than H_2 oxidation activity [94,95,97].

Hases usually work independently, but in some organisms, these enzymes can also function together with formate-dehydrogenases (FDHs), the enzymes responsible for formate production/oxidation (see FDHs in section 1.2.2). In those organisms, like *E. coli*, formate-driven H_2 production is catalyzed by the formate-hydrogen lyase (FHL) complex, where a cytoplasmic membrane bound [NiFe] Hase is coupled to a FDH (FDH-H) [82,98–100].

A growing interest has arisen in using Hases as biotechnological tools for H_2 production, either by modifying these enzymes for high performance or by applying them in electrocatalytic or photocatalytic devices. In other cases, the optimization of H_2 production in whole cell biocatalysts is achieved through genetic engineering of Hases by heterologous expression of Hases or FHL complexes [84,101] or by overexpression of Hase genes [82,102,103]. In addition, molecular studies on Hases, through directed mutagenesis, have also been carried out in order to engineer Hases with low sensitivity to O_2 [104,105] since some of these enzymes can be irreversibly inactivated during catalysis in the presence of O_2 [96]. Furthermore, the relevance of Hases for H_2 production has also been demonstrated by applying these enzymes in electrochemical and catalytic assays. Some studies have shown the applicability of [FeFe] Hases for H_2 production due to their high catalytic activity [106]. The potential of a [FeFe] Hase from the organism *Desulfovibrio desulfuricans* to be used in H_2-producing

devices coupled to solar-powered water splitting was shown [107], whereas the use of a [FeFe] Hase from *Chlamydomonas reinhardtii* inside of a redox polymer (hydrogel) was demonstrated in a fuel cell for H_2 production [108]. However, due to [FeFe] Hases sensitivity to O_2, many studies have also been performed using [NiFe] Hases, which react reversibly with O_2 and among these, the [NiFeSe] Hases have been further studied since they have been shown to display a high H_2 production activity and show less product inhibition by H_2 [95,97,109–111]. Reisner *et al*. have demonstrated an efficient system for photocatalytic H_2 production using a [NiFeSe] Hase from the organism *Desulfomicrobium baculatum* [110]. This system functions under non-strict anaerobic conditions by adsorption of the Hase on TiO_2 nanoparticles for photocatalytic H_2 production by visible light [110]. In another study, it was also shown that [NiFeSe] Hase from *Desulfovibrio vulgaris* Hildenborough had a good electrocatalytic current for H_2 production when bound to a gold electrode [112]. This [NiFeSe] Hase had already shown a high H_2 production activity [94,97] and the capacity to be immobilized on electrodes allowing for direct electron transfer [113]. Recently, in a new study, the photocatalytic production of H_2 from water and sunlight was also observed using the [NiFeSe] Hase from *D. vulgaris* and an inorganic semiconductor able to absorb in the visible light spectral range [114].

1.2 BIOLOGICAL FORMATE PRODUCTION

The production of formate has emerged as an important area of research due to the increased awareness of using formate as a favorable energy and H_2 carrier. However, similarly to H_2 production, the production of value-added chemicals like formate, currently depends almost entirely on fossil carbons or simple sugars [115]. Therefore, there is an urgent need to develop less energy intensive methods that may utilize available and cheap resources for the production of formate (Figure 1.7).

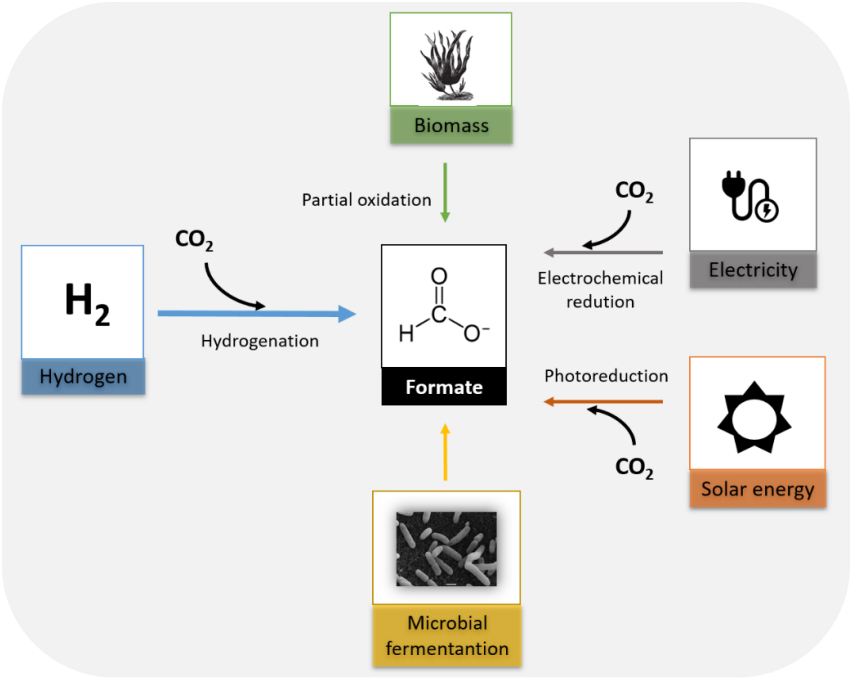

Figure 1.7. A schematic representation of formate production processes from renewable sources (created according to [115].

One of the approaches for sustainable formate production is through biomass processing by oxidative conversion of biomass with overpressure of O_2 to give formate [116,117]. In this process, polyoxometalate catalysts are able to convert carbohydrate based biomass (e.g. glucose) or even water-insoluble biomass (e.g. cellulose, lignin, waste paper or microorganisms such as cyanobacteria) to formate in the presence of O_2 [116,117]. However, it requires high temperatures and pressures of O_2 to work [116,117]. Furthermore, it is also known that formate can be a sub-product generated during metabolic fermentation by many microorganisms like *E. coli*, *Enterobacter*, *Clostridium* during dark-fermentation [118,119]. On the other hand, an approach that has attracted much attention is the use of CO_2 as renewable material for its conversion to formate [17,115,120,121]. This works as a strategy to both decrease the levels of CO_2 and to produce a valuable compound to be used as H_2 storage material. In this sense, the use of electricity for electrochemical reduction of CO_2 to formate is an option where direct electron transfer from the electrode to living cells or enzymes is carried out [122–125]. In another process, photoreduction of CO_2 provides a direct process for formate production using light-driven photocatalysts (based on ruthenium and rhenium) for the reduction of CO_2 to form formate with high selectivity using a wide range of wavelengths of visible light [126,127]. Moreover, another process that has gained attention is the production of formate through the reduction of CO_2 with molecular H_2 [9,115]. Several processes using chemical catalysts can be used for reduction of CO_2 to formate (as mentioned in section 1), but these technologies require expensive metals

and demanding conditions to work [10–12,31,121]. An alternative approach is found in biologic systems, using whole cell biocatalysts, which offer a green and potent alternative for efficient CO_2 conversion to formate (including hydrogenation of CO_2) [128–130].

1.2.1 MICROORGANISMS AS BIOCATALYSTS FOR FORMATE PRODUCTION

The use of microorganisms in formate production constitutes an attractive biotechnological application and there is a great interest in finding new biocatalysts for the reduction of CO_2. Until now, only a few studies have shown the capacity and efficiency of different organisms as biological systems for the production of formate [100,128–131]. Whole cells of the acetogen *Acetobacterium woodii* were demonstrated to be able to produce formate from hydrogenation of CO_2 under defined growth conditions [128]. Acetogens possess a carbon fixation pathway producing acetate (the Wood-Ljungdahl pathway), in which the first step involves reduction of CO_2 to formate [132]. The formate production observed in *A. woodii* was only possible after disrupting its energy metabolism for acetate production. In addition, formate production was also shown in the sulfate-reducing bacterium *D. vulgaris* Hildenborough when this organism was fed with CO_2 and H_2 [131] and in *E. coli* cells, from CO_2 or bicarbonate and H_2 [100,129].

In biological studies, different approaches can be applied to enhance the formate productivity of bacteria. The use of genetic engineering for the

modification of FDHs present in bacteria is one of the target processes regarding the use of whole cell for formate production. Deletion of formate oxidizing FDHs, overexpression of FDHs which act towards CO_2 reduction, as well as, the heterologous expression of FDHs for formate production in more efficient biological systems are all promising mechanisms to achieve higher formate production performances. This last approach was shown in a previous study where recombinant *E. coli* cells harboring FDHs from different organisms, such as *Clostridium carboxidivorans*, *Methanobacterium thermoformicicum* and *P. furiosus,* demonstrated an improvemet in formate productivity from H_2 and bicarbonate [129].

Most recently, a new approach using electro-biocatalytic assays was also performed for formate production in *Methylobacteria* oxygen-stable cells [130]. An electrochemical reactor was operated using *Methylobacteria* species with CO_2 as carbon source and electricity as a reducing agent instead of H_2 [130].

1.2.2 FORMATE-DEHYDROGENASES – THE ENZYMES RESPONSIBLE FOR FORMATE PRODUCTION

In biological systems, the production of formate is carried out by formate-dehydrogenases (FDHs). FDHs comprise a heterogeneous group of enzymes that can be found both in eukaryotes and prokaryotes [133]. These enzymes are most often found to physiologically catalyze formate oxidation and the

release of CO_2. However, FDHs are reversible and can catalyze both formate oxidation and CO_2 reduction to formate (equation 1.2) [133–136].

$$CO_2 + H^+ + 2e^- \rightleftharpoons HCOO^- \qquad \text{(equation 1.2)}$$

Two main types of FDHs are described, FDHs containing a nicotinamide adenine dinucleotide (NAD^+) cofactor known as NAD^+-dependent FDHs and the metal-containing FDHs [119]. NAD^+-dependent FDHs can be found in aerobic organisms, yeasts, fungi and plants and are oxygen-tolerant enzymes [135]. These FDHs contain a NAD^+ cofactor at the active site and catalyze the concomitant reduction of NAD^+ to NADH and formate oxidation to CO_2 [119,135,136]. The metal-containing FDHs are NAD^+-independent enzymes which contain redox active molybdenum (Mo) or tungsten (W) prosthetic groups, iron-sulfur clusters and selenium in the form of SeCys [134,137]. According to their metal content, FDHs can sub-divided as molybdenum-containing FDH (Mo-FDH) and tungsten-containing FDH (W-FDH). These metallo-FDHs are broadly distributed throughout the bacterial kingdom, but due to the presence of oxidizable cofactors, they are most commonly found in anaerobic organisms. Similarly to other type of enzymes, the function of FDHs is also thought to be linked with their cellular location. The FDHs that mainly act as CO_2 reductases are found in the cytoplasm of many microorganisms, whereas periplasmic FDHs usually function towards the oxidation of formate [134–136].

FDHs that catalyze CO_2 reduction are of interest for the capture of CO_2 and for the production of formate as a stabilized form of H_2. The enzymatic CO_2 reductase activity of W and Mo containing FDHs enzymes, as well as NAD^+-dependent FDHs enzymes, has been successfully demonstrated *in vitro* [100,124,138–142]. FDHs from acetogenic organisms have been characterized and found to be capable of catalyzing CO_2 reduction to formate under thermodynamically favorable conditions [128,139,143–145]. Recently, a FDH from the acetogen *C. carboxidivorans* was recombinantly expressed in *E. coli* and shown to display a high CO_2 reducing activity [139]. Furthermore, a new FDH from *A. woodii* was also described and found to directly convert CO_2 to formate using H_2 as an electron donor and it is responsible for formate production *in vivo* [128]. This FDH is part of the hydrogen-dependent CO_2 reductase complex, where FDH is coupled to a [FeFe] Hase [128]. Moreover, non-acetogenic FDHs, which are known to catalyze formate oxidation have also been found to be capable of reducing CO_2 to formate [100,124,125,140,141]. Recently, it was demonstrated that the FDH from the FHL complex in *E. coli* can also reduce CO_2 to formate [100]. The potential for CO_2 reduction of the FDH from *E. coli*, as well as, of W-FDHs from *Syntrophobacter fumaroxidans* and *Methylobacterium extorquens* were also described by electrochemical studies [124,125,141]. These enzymes operated as thermodynamically reversible catalysts and maintained high catalytic performance immobilized in an electrode [124,125,141]. An oxygen-tolerant Mo-dependent FDH from *Rhodobacter capsulatus* was also reported to catalyse the reduction of CO_2 with NADH [140]. In a recent study, the reduction

of CO_2 by a FDH from the sulfate-reducing bacterium *D. desulfuricans,* was also demonstrated [138].

All of these kinetic and electrochemical studies demonstrate the potential of FDHs in biotechnological processes for the conversion of CO_2 to formate. Nevertheless, the catalytic properties of these enzymes as biocatalysts vary greatly depending on the source organism.

1.3 Sulfate-Reducing Bacteria for H_2 and Formate Production

Sulfate-reducing bacteria (SRB) are a group of environmental anaerobic microorganisms that play a key role in the global cycles of carbon and sulfur. These organisms are widespread in anoxic habitats, where they use sulfate as terminal electron acceptor for the degradation of organic compounds to sulfide as the major metabolic end product. These organisms are phylogenetically diverse and metabolically versatile. Regarding their metabolism, SRB utilize a wide range of substrates as energy sources (e.g., molecular hydrogen, short chain fatty acids, alcohols, hydrocarbons, sugars, etc) and besides the use of sulfate as electron acceptor, many SRB can also use additional compounds as electron acceptors such as sulfite, thiosulfate or nitrate [146–148]. These organisms can be found in many anoxic environments where sulfate is present, such as marine sediments, freshwaters, soils, hydrothermal vents, hydrocarbon seeps and mud volcanoes and in hypersaline microbial mats [146].

SRB are very important organisms involved in several biotechnological applications like bioremediation of heavy metals and wastewater treatment [146,149]. Recently, the potential of these bacteria as biocatalysts in a H_2 production process was also demonstrated [80,81,89], mainly using formate as substrate [81].

H_2 and formate are important energy sources for SRB in natural habitats. These substrates play a central role in the energy metabolism of SRB of the genus *Desulfovibrio,* the most studied SRB [147,149]. H_2 and formate produced by fermentative organisms are used by SRB as energy source and since they are the most efficient H_2 consumers they can outcompete other organisms, like methanogens, if sulfate is present [146,147]. However, although SRB are normally considered as H_2 consumers they can also produce H_2 in the absence of sulfate [148] as described in previous studies with *Desulfovibrio* species [81,150].

In 2013, Martins and Pereira demonstrated the potential of *D. vulgaris* Hildenborough for H_2 production from formate in the absence of sulfate [81]. In this study, the capacity of *D. vulgaris* for formate-driven H_2 production was optimized by evaluating several parameters (pH, metal cofactors, substrate concentration, and cell load) in batch conditions and by using an anaerobic stirred tank reactor (ASTR) [81]. *D. vulgaris* was shown to convert formate to H_2 with 100 % efficiency producing 15 mL L^{-1} h^{-1} of H_2 (with a specific rate of 7 mmol g_{dcw}^{-1} h^{-1}) [81]. The H_2 production capacity demonstrated by *D. vulgaris* highlighted the potential of these microorganisms as H_2 producers in second-stage dark-fermentation process and the importance of exploring SRB

for biotechnological applications in further studies. However, in this work the production of H_2 from formate was not coupled to bacterial growth [81]. In fact, growth coupled to formate-driven H_2 production has been only observed in a single hyperthermophile organism *T. onnurineus* [151] or in syntrophy with the methanogenic *Methanobrevibacter arboriphilus* AZ and a sulfate-reducing bacterium *Desulfovibrio* strain G11 [152].

The growth of SRB coupled to H_2 production was only previously observed in syntrophy with methanogenic organisms through the consumption of H_2 by these organisms, which keep the H_2 partial pressure low [152,153]. It is known that due to their versatile metabolism, SRB are also present in sulfate-limited habitats where they ferment organic acids and alcohols while producing H_2, acetate and CO_2, by forming syntrophic associations with H_2-consuming organisms [154]. In these conditions, it was shown that SRB from *Desulfovibrio* genus were able to grow syntrophically with methanogens such as *Methanococcus maripaludis* strain S2 on lactate [153] and with *M. arboriphilus* AZ on formate [152] by reducing protons to H_2.

The formate-driven H_2 production in SRB results from the high content of Hases and FDHs present in these microorganisms, which are differently distributed among the SRB, where they play an important role in the energy metabolism [147,149,155–158]. In SRB of the genus *Desulfovibrio*, three classes of Hases are described: the [FeFe], the [NiFe] and the [NiFeSe] Hases [97,109,149,157]. These enzymes are either periplasmic or cytoplasmic, and can be soluble or membrane bound with the active site facing the periplasm

or cytoplasm [149,157]. A genomic analysis has shown that periplasmic Hases are found in most SRB, which may function in the uptake of H_2, and a higher number of these enzymes is present in the *Desulfovibrionaceae* family [149]. These Hases can be composed of two subunits, a large catalytic subunit and a small electron-transfer subunit, and transfer electron to one or several cytochromes c. However, a three subunit periplasmic Hase can also be found in some SRB, where the third subunit is a membrane-associated protein responsible for quinone reduction [149]. Among the periplasmic Hases, the soluble periplasmic [NiFe] HynAB Hase is the most common with all the Deltaproteobacteria SRB containing at least one copy of HynAB [149]. Many of these periplasmic Hases, including [NiFe] HynAB, [NiFeSe] HysAB and [FeFe] HydAB Hases, use a Type I cytochrome c_3 ($TpIc_3$) as electron acceptor [156]. In contrast, another [NiFe] $HynABC_3$ Hase, only present in a few organisms, has a cytochrome c_3 encoded next to the *hynAB* genes [149]. Most SRB contain cytoplasmic Hases, either soluble or membrane-bound, which belong to the [NiFe] and [FeFe] Hases families. The two most common are the energy-conserving membrane bound [NiFe] Hases, Ech and Coo [149]. In SRB, FDHs can also be present in the cytoplasm or in the periplasm and their cellular location is related to their function [134–136]. Moreover, these enzymes can have a large diversity in their co-factor composition and structure. The soluble periplasmic FDHs can contain only the catalytic and small subunits (FdhAB) or in other cases have a dedicated cytochrome c_3 ($FdhABC_3$) [159,160]. In the case of FdhAB, the physiological electron acceptor is likely to be the soluble TpIc3 [161,162]. Periplasmic FDHs can also be membrane-associated, in which

a subunit for quinone reduction is present: with a NarI-like cytochrome b (FdhABC) or a larger protein of the NrfD family (FdhABD) [149]. Most FDHs in SRB have a Mo or W co-factor, and depending on the metal availability different FDHs are expressed, as already reported in *D. vulgaris* Hildenborough and *Desulfovibrio alaskensis* NCIMB 13491 [163,164]. Cytoplasmic FDHs are also present in almost all SRB, which can be NAD(P)H-linked FDH, ferredoxin (Fd)-dependent FDH or even part of a soluble FHL complex. Both Hases and FDHs are fundamental in understanding the cellular H_2 and formate metabolism in SRB, and although they are generally found working independently, in some SRB, like *Desulfovibrio alaskensis* G20 (Table 1), they are also found as a FHL complex [149]. This enzymatic system identified in SRB by genome analysis is soluble, and includes an [FeFe] Hase, a FDH and two four-cluster electron-transfer proteins [149].

1.4 AIM OF THE THESIS

Due to the importance of implementing a H_2 and formate economy, there is a need to find new and alternative biological processes and biocatalysts for the production of these two energy carriers. The potential of SRB for H_2 production from formate was reported in a previous study, where *D. vulgaris* Hildenborough was shown to have a high H_2 productivity. This has highlighted the importance of using these bacteria as biocatalysts in further fundamental and applied H_2 production studies. In addition, due to the reversible action of Hases and FDHs, which are abundant enzymes in SRB, the potential of these microorganisms for the production of formate could also be explored. Thus, studies on H_2 and formate production by SRB were conducted in this thesis:

- Design and optimize a new bioprocess for H_2 production **(Chapter 2)**
- Evaluate if there is growth coupled to formate-driven H_2 production in a single mesophilic organism **(Chapter 2)**
- Investigate the electron transfer mechanisms involved in formate-driven H_2 production **(Chapter 3)**
- Explore the capacity of SRB for formate production by hydrogenation of CO_2 and develop a new bioprocess for it **(Chapter 4)**
- Investigate the metabolic pathways involved in formate production**(Chapter4)**

REFERENCES

1. Nejat P, Jomehzadeh F, Taheri MM, Gohari M, Abd. Majid MZ. A global review of energy consumption, CO_2 emissions and policy in the residential sector (with an overview of the top ten CO_2 emitting countries). Renew Sustain Energy Rev. 2015;43: 843–862.
2. De Silva GPD, Ranjith PG, Perera MSA. Geochemical aspects of CO_2 sequestration in deep saline aquifers: A review. Fuel. 2015;155: 128–143.
3. Cheah WY, Ling TC, Juan JC, Lee DJ, Chang JS, Show PL. Biorefineries of carbon dioxide: From carbon capture and storage (CCS) to bioenergies production. Bioresour Technol. 2016;215: 346–356.
4. Omae I. Recent developments in carbon dioxide utilization for the production of organic chemicals. Coord Chem Rev. 2012;256: 1384–1405.
5. U.S. Department of Commerce, National Oceanic & Atmospheric Administration Earth System Research Laboratory, Global Monitoring Division, Trends in Atmospheric Carbon Dioxide, Recent Mauna Loa CO_2 [Internet]. Available: www.esrl.noaa.gov/gmd/ccgg/trends/gr.h
6. Kotay SM, Das D. Biohydrogen as a renewable energy resource - Prospects and potentials. Int J Hydrogen Energy. 2008;33: 258–263.
7. Show KY, Lee DJ, Tay JH, Lin CY, Chang JS. Biohydrogen production: Current perspectives and the way forward. Int J Hydrogen Energy. 2012;37: 15616–15631.
8. Dutta S. A review on production, storage of hydrogen and its utilization as an energy resource. J Ind Eng Chem. 2014;20: 1148–1156.
9. Enthaler S, von Langermann J, Schmidt T. Carbon dioxide and formic acid—the couple for environmental-friendly hydrogen storage? Energy Environ Sci. 2010;3: 1207–1217.
10. Boddien A, Gärtner F, Federsel C, Sponholz P, Mellmann D, Jackstell R, *et al*. CO_2 -"neutral" hydrogen storage based on bicarbonates and formates. Angew Chemie. 2011;50: 6411–6414.
11. Appel AM, Bercaw JE, Bocarsly AB, Dobbek H, DuBois DL, Dupuis M, *et al*. Frontiers, opportunities, and challenges in biochemical and chemical catalysis of CO_2 fixation. Chem Rev. 2013;113: 6621–6658.

12. Aresta M, Dibenedetto A, Quaranta E. State of the art and perspectives in catalytic processes for CO_2 conversion into chemicals and fuels: The distinctive contribution of chemical catalysis and biotechnology. J Catal. 2016;343: 2–45.

13. Kapdan IK, Kargi F. Bio-hydrogen production from waste materials. Enzyme and Microbial Technology. 2006. pp. 569–582.

14. Chandrasekhar K, Lee Y-J, Lee D-W. Biohydrogen production: strategies to improve process efficiency through microbial routes. Int J Mol Sci. 2015;16: 8266–8293.

15. Singh S, Jain S, PS V, Tiwari AK, Nouni MR, Pandey JK, *et al*. Hydrogen: A sustainable fuel for future of the transport sector. Renew Sustain Energy Rev. 2015;51: 623–633.

16. Schlapbach L, Züttel A. Hydrogen-storage materials for mobile applications. Nature. 2001;414: 353–358.

17. Pereira IAC. An enzymatic route to H_2 storage. Science. 2013;342: 1329–1330.

18. Loges B, Boddien A, Gärtner F, Junge H, Beller M. Catalytic generation of hydrogen from formic acid and its derivatives: useful hydrogen storage materials. Top Catal. 2010;53: 902–914.

19. Mellmann D, Sponholz P, Junge H, Beller M. Formic acid as a hydrogen storage material – development of homogeneous catalysts for selective hydrogen release. Chem Soc Rev. 2016;45: 3954–3988.

20. Wang W-H, Himeda Y, Muckerman JT, Manbeck GF, Fujita E. CO_2 hydrogenation to formate and methanol as an alternative to photo- and electrochemical CO_2 reduction. Chem Rev. 2015;115: 12936–12973.

21. Johnson TC, Morris DJ, Wills M. Hydrogen generation from formic acid and alcohols using homogeneous catalysts. Chem Soc Rev. 2010;39: 81–88.

22. Coffey RS. The decomposition of formic acid catalysed by soluble metal complexes. Chem Commun. 1967; 923b.

23. Boddien A, Loges B, Junge H, Beller M. Hydrogen generation at ambient conditions: application in fuel cells. ChemSusChem. 2008;1: 751–758.

24. Myers TW, Berben L A. Aluminium–ligand cooperation promotes selective dehydrogenation of formic acid to H_2 and CO_2. Chem Sci. 2014;5: 2771.

25. Wang W-H, Ertem MZ, Xu S, Onishi N, Manaka Y, Suna Y, *et al*. Highly robust hydrogen generation by bioinspired Ir complexes for dehydrogenation of formic acid in water: experimental and theoretical mechanistic investigations

at different pH. ACS Catal. 2015;5: 5496–5504.

26. Junge H, Loges B, Beller M. Novel improved ruthenium catalysts for the generation of hydrogen from alcohols. Chem Commun. 2007; 522–524.

27. Munshi P, Main AD, Linehan JC, Tai C-C, Jessop PG. Hydrogenation of carbon dioxide catalyzed by ruthenium trimethylphosphine complexes: The accelerating effect of certain alcohols and amines. J Am Chem Soc. 2002;124: 7963–7971.

28. Elek J, Nádasdi L, Papp G, Laurenczy G, Joó F. Homogeneous hydrogenation of carbon dioxide and bicarbonate in aqueous solution catalyzed by water-soluble ruthenium(II) phosphine complexes. Appl Catal A Gen. 2003;255: 59–67.

29. Tanaka R, Yamashita M, Nozaki K. Catalytic hydrogenation of carbon dioxide using Ir(III)−pincer complexes. J Am Chem Soc. 2009;131: 14168–14169.

30. Wang W-H, Hull JF, Muckerman JT, Fujita E, Himeda Y. Second-coordination-sphere and electronic effects enhance iridium(iii)-catalyzed homogeneous hydrogenation of carbon dioxide in water near ambient temperature and pressure. Energy Environ Sci. 2012;5: 7923.

31. Moret S, Dyson PJ, Laurenczy G. Direct synthesis of formic acid from carbon dioxide by hydrogenation in acidic media. Nat Commun. 2014;5: 4017.

32. Filonenko GA, van Putten R, Schulpen EN, Hensen EJM, Pidko EA. Highly efficient reversible hydrogenation of carbon dioxide to formates using a ruthenium PNP-pincer catalyst. ChemCatChem. 2014;6: 1526–1530.

33. Hallenbeck PC, Abo-Hashesh M, Ghosh D. Strategies for improving biological hydrogen production. Bioresour Technol. 2012;110: 1–9.

34. Levin DB, Pitt L, Love M. Biohydrogen production: Prospects and limitations to practical application. Int J Hydrogen Energy. 2004;29: 173–185.

35. Mohan SV, Pandey A. Biohydrogen production. In: Pandey A, Chang J-S, Hallenbeck P, Larroche C, editors. Biohydrogen. Elsevier; 2013. pp. 1–24.

36. Sinha P, Pandey A. An evaluative report and challenges for fermentative biohydrogen production. Int J Hydrogen Energy. 2011;36: 7460–7478.

37. Das D. Hydrogen production by biological processes: a survey of literature. Int J Hydrogen Energy. 2001;26: 13–28. doi:10.1016/S0360-3199(00)00058-6

38. Rittmann SK-MR, Lee HS, Lim JK, Kim TW, Lee J-H, Kang SG. One-carbon substrate-based biohydrogen production: Microbes, mechanism, and

productivity. Biotechnol Adv. 2015;33: 165–177.

39. Yu J, Takahashi P. Biophotolysis-based hydrogen production by cyanobacteria and green microalgae. Commun Curr Res Educ Top Trends Appl Microbiol. 2007;1: 79–89.

40. Azwar MY, Hussain MA, Abdul-Wahab AK. Development of biohydrogen production by photobiological, fermentation and electrochemical processes: A review. Renew Sustain Energy Rev. 2014;31: 158–173.

41. Tamburic B, Zemichael FW, Maitland GC, Hellgardt K. Parameters affecting the growth and hydrogen production of the green alga *Chlamydomonas reinhardtii*. Int J Hydrogen Energy. 2011;36: 7872–7876.

42. Tamburic B, Zemichael FW, Maitland GC, Hellgardt K. Effect of the light regime and phototrophic conditions on growth of the H_2-producing green alga *Chlamydomonas reinhardtii*. Energy Procedia. 2012;29: 710–719.

43. Chader S, Hacene H, Agathos SN. Study of hydrogen production by three strains of *Chlorella* isolated from the soil in the Algerian Sahara. Int J Hydrogen Energy. 2009;34: 4941–4946.

44. Hwang J-H, Kim H-C, Choi J-A, Abou-Shanab RAI, Dempsey B a, Regan JM, *et al*. Photoautotrophic hydrogen production by eukaryotic microalgae under aerobic conditions. Nat Commun. 2014;5: 3234.

45. Berberoğlu H, Jay J, Pilon L. Effect of nutrient media on photobiological hydrogen production by *Anabaena variabilis* ATCC 29413. Int J Hydrogen Energy. 2008;33: 1172–1184.

46. Ferreira AF, Marques AC, Batista AP, Marques PASS, Gouveia L, Silva CM. Biological hydrogen production by *Anabaena* sp. – Yield, energy and CO_2 analysis including fermentative biomass recovery. Int J Hydrogen Energy. 2012;37: 179–190.

47. Kruse O, Rupprecht J, Mussgnug JH, Dismukes GC, Hankamer B. Photosynthesis: a blueprint for solar energy capture and biohydrogen production technologies. Photochem Photobiol Sci. 2005;4: 957.

48. Allakhverdiev SI, Thavasi V, Kreslavski VD, Zharmukhamedov SK, Klimov V V., Ramakrishna S, *et al*. Photosynthetic hydrogen production. J Photochem Photobiol C Photochem Rev. 2010;11: 101–113.

49. Melis A, Zhang L, Forestier M, Ghirardi ML, Seibert M. Sustained photobiological hydrogen gas production upon reversible inactivation of oxygen evolution in the green alga *Chlamydomonas reinhardtii*. Plant Physiol.

2000;122: 127–136.

50. Androga DD, Ozgur E, Eroglu I, Gunduz U, Yucel M. Photofermentative hydrogen production in outdoor conditions. Hydrogen Energy - Challenges and Perspectives. InTech; 2012. pp. 77–120.

51. Kim D-H, Cha J, Kang S, Kim M-S. Continuous photo-fermentative hydrogen production from lactate and lactate-rich acidified food waste. Int J Hydrogen Energy. 2013;38: 6161–6166.

52. Seifert K, Waligorska M, Laniecki M. Brewery wastewaters in photobiological hydrogen generation in presence of *Rhodobacter sphaeroides* O.U. 001. Int J Hydrogen Energy. 2010;35: 4085–4091.

53. Lo Y-C, Chen C-Y, Lee C-M, Chang J-S. Photo fermentative hydrogen production using dominant components (acetate, lactate, and butyrate) in dark fermentation effluents. Int J Hydrogen Energy. 2011;36: 14059–14068.

54. Lee C-M, Hung G-J, Yang C-F. Hydrogen production by *Rhodopseudomonas palustris* WP 3-5 in a serial photobioreactor fed with hydrogen fermentation effluent. Bioresour Technol. Elsevier Ltd; 2011;102: 8350–8356.

55. Liu B-F, Xie G-J, Guo W-Q, Ding J, Ren N-Q. Optimization of photo-hydrogen production by immobilized *Rhodopseudomonas faecalis* RLD-53. Nat Resour. 2011;2: 1–7.

56. Xie G-J, Liu B-F, Guo W-Q, Ding J, Xing D-F, Nan J, *et al*. Feasibility studies on continuous hydrogen production using photo-fermentative sequencing batch reactor. Int J Hydrogen Energy. 2012;37: 13689–13695.

57. Ho K-L, Chen Y-Y, Lee D-J. Biohydrogen production from cellobiose in phenol and cresol-containing medium using *Clostridium* sp. R1. Int J Hydrogen Energy. 2010;35: 10239–10244.

58. Lo Y-C, Chen X-J, Huang C-Y, Yuan Y-J, Chang J-S. Dark fermentative hydrogen production with crude glycerol from biodiesel industry using indigenous hydrogen-producing bacteria. Int J Hydrogen Energy. 2013;38: 15815–15822.

59. Shin J-H, Yoon JH, Ahn EK, Kim M-S, Sim SJ, Park TH. Fermentative hydrogen production by the newly isolated *Enterobacter asburiae* SNU-1. Int J Hydrogen Energy. 2007;32: 192–199.

60. Seol E, Manimaran A, Jang Y, Kim S, Oh Y-K, Park S. Sustained hydrogen production from formate using immobilized recombinant *Escherichia coli* SH5. Int J Hydrogen Energy. 2011;36: 8681–8686.

61. Hallenbeck PC, Ghosh D. Advances in fermentative biohydrogen production: the way forward? Trends in Biotechnology. 2009; 27: 287–297.

62. Khanna N, Das D. Biohydrogen production by dark fermentation. Wiley Interdiscip Rev Energy Environ. 2013;2: 401–421.

63. Tapia-Venegas E, Ramirez-Morales JE, Silva-Illanes F, Toledo-Alarcón J, Paillet F, Escudie R, *et al*. Biohydrogen production by dark fermentation: scaling-up and technologies integration for a sustainable system. Rev Environ Sci Bio/Technology. 2015;14: 761–785.

64. Kadier A, Simayi Y, Kalil MS, Abdeshahian P, Hamid AA. A review of the substrates used in microbial electrolysis cells (MECs) for producing sustainable and clean hydrogen gas. Renew Energy. 2014;71: 466–472.

65. Logan BE, Call D, Cheng S, Hamelers HVM, Sleutels THJA, Jeremiasse AW, *et al*. Microbial electrolysis cells for high yield hydrogen gas production from organic matter. Environ Sci Technol. 2008;42: 8630–8640.

66. Hu H, Fan Y, Liu H. Hydrogen production using single-chamber membrane-free microbial electrolysis cells. Water Res. 2008;42: 4172–4178.

67. Lu L, Ren N, Zhao X, Wang H, Wu D, Xing D. Hydrogen production, methanogen inhibition and microbial community structures in psychrophilic single-chamber microbial electrolysis cells. Energy Environ Sci. 2011;4: 1329.

68. Catal T. Comparison of various carbohydrates for hydrogen production in microbial electrolysis cells. Biotechnol Biotechnol Equip. 2016;30: 75–80.

69. Escapa A, Mateos R, Martínez EJ, Blanes J. Microbial electrolysis cells: An emerging technology for wastewater treatment and energy recovery. From laboratory to pilot plant and beyond. Renew Sustain Energy Rev. 2016;55: 942–956.

70. Hallenbeck PC. Microbial paths to renewable hydrogen production. Biofuels. 2011;2: 285–302.

71. Laurinavichene T V., Belokopytov BF, Laurinavichius KS, Khusnutdinova AN, Seibert M, Tsygankov AA. Towards the integration of dark- and photo-fermentative waste treatment. 4. Repeated batch sequential dark- and photofermentation using starch as substrate. Int J Hydrogen Energy. 2012;37: 8800–8810.

72. Chookaew T, O-Thong S, Prasertsan P. Biohydrogen production from crude glycerol by two stage of dark and photo fermentation. Int J Hydrogen Energy. 2015;40: 7433–7438.

73. Babu M Lenin, Subhash G Venkata, Sarma PN, Mohan S Venkata. Bio-electrolytic conversion of acidogenic effluents to biohydrogen: An integration strategy for higher substrate conversion and product recovery. Bioresour Technol. 2013;133: 322–331.

74. Chookaew T, Prasertsan P, Ren ZJ. Two-stage conversion of crude glycerol to energy using dark fermentation linked with microbial fuel cell or microbial electrolysis cell. N Biotechnol. 2014;31: 179–184.

75. Hwang JH, Choi JA, Abou-Shanab RAI, Min B, Song H, Kim Y, *et al*. Feasibility of hydrogen production from ripened fruits by a combined two-stage (dark/dark) fermentation system. Bioresour Technol. 2011;102: 1051–1058.

76. Wieczorek N, Kucuker MA, Kuchta K. Fermentative hydrogen and methane production from microalgal biomass (*Chlorella vulgaris*) in a two-stage combined process. Appl Energy. 2014;132: 108–117.

77. Abd-Alla MH, Morsy FM, El-Enany A-WE. Hydrogen production from rotten dates by sequential three stages fermentation. Int J Hydrogen Energy. 2011;36: 13518–13527.

78. Kim D-H, Kim M-S. Development of a novel three-stage fermentation system converting food waste to hydrogen and methane. Bioresour Technol. 2013;127: 267–274.

79. Lazaro CZ, Vich DV, Hirasawa JS, Varesche MBA. Hydrogen production and consumption of organic acids by a phototrophic microbial consortium. Int J Hydrogen Energy. 2012;37: 11691–11700.

80. Yu L, Duan J, Zhao W, Huang Y, Hou B. Characteristics of hydrogen evolution and oxidation catalyzed by *Desulfovibrio caledoniensis* biofilm on pyrolytic graphite electrode. Electrochim Acta. 2011;56: 9041–9047.

81. Martins M, Pereira IAC. Sulfate-reducing bacteria as new microorganisms for biological hydrogen production. Int J Hydrogen Energy. 2013;38: 12294–12301.

82. Yoshida A, Nishimura T, Kawaguchi H, Inui M, Yukawa H. Enhanced hydrogen production from formic acid by formate hydrogen lyase-overexpressing *Escherichia coli* strains. Appl Environ Microbiol. 2005;71: 6762–6768.

83. Maeda T, Sanchez-Torres V, Wood TK. Hydrogen production by recombinant *Escherichia coli* strains. Microb Biotechnol. 2012;5: 214–225.

84. Lipscomb GL, Schut GJ, Thorgersen MP, Nixon WJ, Kelly RM, Adams MWW. Engineering hydrogen gas production from formate in a hyperthermophile by

heterologous production of an 18-subunit membrane-bound complex. J Biol Chem. 2014;289: 2873–2879.

85. Seol E, Kim S, Raj SM, Park S. Comparison of hydrogen-production capability of four different *Enterobacteriaceae* strains under growing and non-growing conditions. Int J Hydrogen Energy. 2008;33: 5169–5175.

86. Shin J-H, Yoon JH, Lee SH, Park TH. Hydrogen production from formic acid in pH-stat fed-batch operation for direct supply to fuel cell. Bioresour Technol. 2010;101: S53–S58.

87. Bae SS, Kim TW, Lee HS, Kwon KK, Kim YJ, Kim MS, *et al*. H_2 production from CO, formate or starch using the hyperthermophilic archaeon, *Thermococcus onnurineus*. Biotechnol Lett. 2012;34: 75–79.

88. Bae SS, Lee HS, Jeon JH, Lee J-H, Kang SG, Kim TW. Enhancing bio-hydrogen production from sodium formate by hyperthermophilic archaeon, *Thermococcus onnurineus* NA1. Bioprocess Biosyst Eng. 2015;38: 989–993.

89. Aulenta F, Catapano L, Snip L, Villano M, Majone M. Linking bacterial metabolism to graphite cathodes: electrochemical insights into the H_2-producing capability of *Desulfovibrio* sp. ChemSusChem. 2012;5: 1080–1085.

90. Constant P, Hallenbeck PC. Hydrogenase. In: Pandey A, Chang J-S, Hallenbeck P, Larroche C, editors. Biohydrogen. Elsevier; 2013. pp. 75–102.

91. Lubitz W, Ogata H, Rudiger O, Reijerse E. Hydrogenases. Chem Rev. 2014;114: 4081–4148.

92. Peters JW, Schut GJ, Boyd ES, Mulder DW, Shepard EM, Broderick JB, *et al*. [FeFe]- and [NiFe]-hydrogenase diversity, mechanism, and maturation. Biochim Biophys Acta - Mol Cell Res. 2015;1853: 1350–1369.

93. Vignais PM, Billoud B. Occurrence, classification, and biological function of hydrogenases: An overview. Chemical Reviews. 2007. pp. 4206–4272.

94. Baltazar CSA, Marques MC, Soares CM, DeLacey AM, Pereira IAC, Matias PM. Nickel-iron-selenium hydrogenases - An overview. Eur J Inorg Chem. 2011;2011: 948–962.

95. Wombwell C, Caputo CA, Reisner E. [NiFeSe]-hydrogenase chemistry. Acc Chem Res. 2015;48: 2858–2865.

96. Rousset M, Liebgott P. Engineering hydrogenases for H_2 production: Bolts and Goals. In: Zannoni D, De Philippis R, editors. Microbial BioEnergy: Hydrogen Production. Dordrecht: Springer Netherlands; 2014. pp. 43–77.

97. Valente FMA, Oliveira ASF, Gnadt N, Pacheco I, Coelho A V., Xavier A V., *et al*. Hydrogenases in *Desulfovibrio vulgaris* Hildenborough: structural and physiologic characterisation of the membrane-bound [NiFeSe] hydrogenase. JBIC J Biol Inorg Chem. 2005;10: 667–682.

98. Sawers RG. Formate and its role in hydrogen production in *Escherichia coli*. Biochem Soc Trans. 2005;33: 42–46.

99. McDowall JS, Murphy BJ, Haumann M, Palmer T, Armstrong FA, Sargent F. Bacterial formate hydrogenlyase complex. Proc Natl Acad Sci U S A. 2014;111: E3948–E3956.

100. Pinske C, Sargent F. Exploring the directionality of *Escherichia coli* formate hydrogenlyase: a membrane-bound enzyme capable of fixing carbon dioxide to organic acid. Microbiol Open. 2016;5: 721–737.

101. Song W, Cheng J, Zhao J, Zhang C, Zhou J, Cen K. Enhancing hydrogen production of *Enterobacter aerogenes* by heterologous expression of hydrogenase genes originated from *Synechocystis* sp. Bioresour Technol. 2016;216: 976–980.

102. Seol E, Jang Y, Kim S, Oh YK, Park S. Engineering of formate-hydrogen lyase gene cluster for improved hydrogen production in *Escherichia coli*. Int J Hydrogen Energy. 2012;37: 15045–15051.

103. Bai L, Wu X, Jiang L, Liu J, Long M. Hydrogen production by over-expression of hydrogenase subunit in oxygen-tolerant *Klebsiella oxytoca* HP1. Int J Hydrogen Energy. 2012;37: 13227–13233.

104. Dementin S, Leroux F, Cournac L, Lacey AL de, Volbeda A, Léger C, *et al*. Introduction of methionines in the gas channel makes [NiFe] hydrogenase aero-tolerant. J Am Chem Soc. 2009;131: 10156–10164.

105. Huang G-F, Wu X-B, Bai L-P, Liu K, Jiang L-J, Long M-N, *et al*. Improved O_2-tolerance in variants of a H_2-evolving [NiFe]-hydrogenase from *Klebsiella oxytoca* HP1. FEBS Lett. 2015;589: 910–918.

106. Vincent KA, Parkin A, Armstrong FA. Investigating and exploiting the electrocatalytic properties of hydrogenases. Chem Rev. 2007;107: 4366–4413.

107. Rodríguez-Maciá P, Birrell JA, Lubitz W, Rüdiger O. Electrochemical investigations on the inactivation of the [FeFe]-Hydrogenase from *Desulfovibrio desulfuricans* by O_2 or light under hydrogen producing conditions. Chempluschem. 2016; 1–6.

108. Oughli AA, Conzuelo F, Winkler M, Happe T, Lubitz W, Schuhmann W, *et al*. A

redox hydrogel protects the O_2-sensitive [FeFe]-Hydrogenase from *Chlamydomonas reinhardtii* from oxidative damage. Angew Chemie Int Ed. 2015;54: 12329–12333.

109. Valente FMA, Almeida CC, Pacheco I, Carita J, Saraiva LM, Pereira IAC. Selenium is involved in regulation of periplasmic hydrogenase gene expression in *Desulfovibrio vulgaris* Hildenborough. J Bacteriol. 2006;188: 3228–3235.

110. Reisner E, Fontecilla-Camps JC, Armstrong F a. Catalytic electrochemistry of a [NiFeSe]-hydrogenase on TiO_2 and demonstration of its suitability for visible-light driven H_2 production. Chem Commun. 2009; 550–552.

111. Parkin A, Goldet G, Cavazza C, Fontecilla-Camps JC, Armstrong FA. The difference a Se makes? Oxygen-tolerant hydrogen production by the [NiFeSe]-hydrogenase from *Desulfomicrobium baculatum*. J Am Chem Soc. 2008;130: 13410–13416.

112. Rüdiger O, Gutiérrez-Sánchez C, Olea D, Pereira IAC, Vélez M, Fernández VM, *et al*. Enzymatic anodes for hydrogen fuel cells based on covalent attachment of NiFe hydrogenases and direct electron transfer to SAM-modified gold electrodes. Electroanalysis. 2010;22: 776–783.

113. Gutiérrez-Sánchez C, Olea D, Marques M, Fernández VM, Pereira IAC, Vélez M, *et al*. Oriented immobilization of a membrane-bound hydrogenase onto an electrode for direct electron transfer. Langmuir. 2011;27: 6449–6457.

114. Tapia C, Zacarias S, Pereira IAC, Conesa JC, Pita M, De Lacey AL. In Situ determination of photobioproduction of H_2 by In_2S_3-[NiFeSe] hydrogenase from *Desulfovibrio vulgaris* Hildenborough using only visible light. ACS Catal. 2016;6: 5691–5698.

115. Yishai O, Lindner SN, Gonzalez de la Cruz J, Tenenboim H, Bar-Even A. The formate bio-economy. Curr Opin Chem Biol. 2016;35: 1–9.

116. Wölfel R, Taccardi N, Bösmann A, Wasserscheid P. Selective catalytic conversion of biobased carbohydrates to formic acid using molecular oxygen. Green Chem. 2011;13: 2759.

117. Albert J, Wölfel R, Bösmann A, Wasserscheid P. Selective oxidation of complex, water-insoluble biomass to formic acid using additives as reaction accelerators. Energy Environ Sci. 2012;5: 7956.

118. Muller V. Bacterial fermentation. Encyclopedia of Life Sciences. Chichester, UK: John Wiley & Sons, Ltd; 2008. pp. 1–7.

119. Crable BR, Plugge CM, McInerney MJ, Stams AJM. Formate Formation and

Formate Conversion in Biological Fuels Production. Enzyme Res. 2011;2011: 1–8.

120. Hawkins AS, McTernan PM, Lian H, Kelly RM, Adams MW. Biological conversion of carbon dioxide and hydrogen into liquid fuels and industrial chemicals. Curr Opin Biotechnol. 2013;24: 376–384.

121. Yuan Z, Eden MR, Gani R. Toward the development and deployment of large-scale carbon dioxide capture and conversion processes. Ind Eng Chem Res. 2016;55: 3383–3419.

122. Jhong H-R "Molly," Ma S, Kenis PJ. Electrochemical conversion of CO_2 to useful chemicals: current status, remaining challenges, and future opportunities. Curr Opin Chem Eng. 2013;2: 191–199.

123. Lovley DR, Nevin KP. A shift in the current: New applications and concepts for microbe-electrode electron exchange. Curr Opin Biotechnol. 2011;22: 441–448.

124. Bassegoda A, Madden C, Wakerley DW, Reisner E, Hirst J. Reversible interconversion of CO_2 and formate by a molybdenum-containing formate dehydrogenase. J Am Chem Soc. 2014;136: 15473–15476.

125. Sakai K, Kitazumi Y, Shirai O, Kano K. Bioelectrocatalytic formate oxidation and carbon dioxide reduction at high current density and low overpotential with tungsten-containing formate dehydrogenase and mediators. Electrochem commun. 2016;65: 31–34.

126. Tamaki Y, Morimoto T, Koike K, Ishitani O. Photocatalytic CO_2 reduction with high turnover frequency and selectivity of formic acid formation using Ru(II) multinuclear complexes. Proc Natl Acad Sci. 2012;109: 15673–15678.

127. Nakada A, Koike K, Nakashima T, Morimoto T, Ishitani O. Photocatalytic CO_2 reduction to formic acid using a Ru(II)–Re(I) supramolecular complex in an aqueous solution. Inorg Chem. 2015;54: 1800–1807.

128. Schuchmann K, Muller V. Direct and reversible hydrogenation of CO_2 to formate by a bacterial carbon dioxide reductase. Science. 2013;342: 1382–1385.

129. Alissandratos A, Kim HK, Easton CJ. Formate production through carbon dioxide hydrogenation with recombinant whole cell biocatalysts. Bioresour Technol. 2014;164: 7–11.

130. Hwang H, Yeon YJ, Lee S, Choe H, Jang MG, Cho DH, *et al.* Electro-biocatalytic production of formate from carbon dioxide using an oxygen-stable whole cell

biocatalyst. Bioresour Technol. 2015;185: 35–39.

131. da Silva SM, Voordouw J, Leitão C, Martins M, Voordouw G, Pereira IAC. Function of formate dehydrogenases in *Desulfovibrio vulgaris* Hildenborough energy metabolism. Microbiology. 2013;159: 1760–1769.

132. Schuchmann K, Müller V. Autotrophy at the thermodynamic limit of life: a model for energy conservation in acetogenic bacteria. Nat Rev Microbiol. 2014;12: 809–821.

133. Gonzalez PJ, Rivas MG, Mota CS, Brondino CD, Moura I, Moura JJG. Periplasmic nitrate reductases and formate dehydrogenases: Biological control of the chemical properties of Mo and W for fine tuning of reactivity, substrate specificity and metabolic role. Coordination Chemistry Reviews. 2013; 257: 315–331.

134. Hartmann T, Schwanhold N, Leimkühler S. Assembly and catalysis of molybdenum or tungsten-containing formate dehydrogenases from bacteria. Biochim Biophys Acta - Proteins Proteomics. 2015;1854: 1090–1100.

135. Maia LB, Moura JJG, Moura I. Molybdenum and tungsten-dependent formate dehydrogenases. J Biol Inorg Chem. 2015;20: 287–309.

136. Maia LB, Moura I, Moura JJG. Molybdenum and tungsten-containing formate dehydrogenases: aiming to inspire a catalyst for carbon dioxide utilization. Inorganica Chim Acta. 2017;455: 350–363.

137. Grimaldi S, Schoepp-Cothenet B, Ceccaldi P, Guigliarelli B, Magalon A. The prokaryotic Mo/W-bisPGD enzymes family: A catalytic workhorse in bioenergetic. Biochim Biophys Acta - Bioenerg. 2013;1827: 1048–1085.

138. Maia LB, Fonseca L, Moura I, Moura JJG. Reduction of carbon dioxide by a molybdenum-containing formate dehydrogenase: A kinetic and mechanistic study. J Am Chem Soc. 2016;138: 8834–8846.

139. Alissandratos A, Kim HK, Matthews H, Hennessy JE, Philbrook A, Easton CJ. *Clostridium carboxidivorans* strain P7T recombinant formate dehydrogenase catalyzes reduction of CO_2 to formate. Appl Environ Microbiol. 2013;79: 741–744.

140. Hartmann T, Leimkühler S. The oxygen-tolerant and NAD^+-dependent formate dehydrogenase from *Rhodobacter capsulatus* is able to catalyze the reduction of CO_2 to formate. FEBS J. 2013;280: 6083–6096.

141. Reda T, Plugge CM, Abram NJ, Hirst J. Reversible interconversion of carbon dioxide and formate by an electroactive enzyme. Proc Natl Acad Sci. 2008;105:

10654–10658.

142. Choe H, Joo JC, Cho DH, Kim MH, Lee SH, Jung KD, *et al.* Efficient CO_2-reducing activity of NAD-dependent formate dehydrogenase from *Thiobacillus* sp. KNK65MA for formate production from CO_2 Gas. PLoS One. 2014;9: e103111.

143. Thauer RK. CO_2-reduction to formate by NADPH. The initial step in the total synthesis of acetate from CO_2 in *Clostridium thermoaceticum*. FEBS Lett. 1972;27: 111–115.

144. Thauer RK. CO_2 reduction to formate in *Clostridium* acidi-urici. J Bacteriol. 1973;114: 443–444.

145. Jungermann K, Kirchniawy H, Thauer RK. Ferredoxin dependent CO_2 reduction to formate in *Clostridium pasteurianum*. Biochem Biophys Res Commun. 1970;41: 682–689.

146. Muyzer G, Stams AJM. The ecology and biotechnology of sulphate-reducing bacteria. Nat Rev Microbiol. 2008;6: 441–454.

147. Rabus R, Hansen TA, Widdel F. Dissimilatory sulfate- and sulfur-reducing prokaryotes. In The Prokaryotes: Prokaryotic Physiology and Biochemistry. Berlin: Springer-Verlag; 2013. pp. 309–404.

148. Rabus R, Venceslau SS, Wöhlbrand L, Voordouw G, Wall JD, Pereira IAC. A post-genomic view of the ecophysiology, catabolism and biotechnological relevance of sulphate-reducing prokaryotes. In: Poole RK, editor. Advances in Microbial Physiology. 2015. pp. 55–321.

149. Pereira IAC, Ramos AR, Grein F, Marques MC, da Silva SM, Venceslau SS. A comparative genomic analysis of energy metabolism in sulfate reducing bacteria and archaea. Front Microbiol. 2011;2: 1–18.

150. Carepo M, Baptista JF, Pamplona A, Fauque G, Moura JJG, Reis MAM. Hydrogen metabolism in *Desulfovibrio desulfuricans* strain New Jersey (NCIMB 8313) - Comparative study with *D. vulgaris* and *D. gigas* species. Anaerobe. 2002;8: 325–332.

151. Kim YJ, Lee HS, Kim ES, Bae SS, Lim JK, Matsumi R, *et al*. Formate-driven growth coupled with H_2 production. Nature. 2010;467: 352–355.

152. Dolfing J, Jiang B, Henstra AM, Stams AJM, Plugge CM. Syntrophic growth on formate: a new microbial niche in anoxic environments. Appl Environ Microbiol. 2008;74: 6126–6131.

153. Walker CB, He Z, Yang ZK, Ringbauer JA, He Q, Zhou J, *et al*. The electron

transfer system of syntrophically grown *Desulfovibrio vulgaris*. J Bacteriol. 2009;191: 5793–5801.

154. Plugge CM, Zhang W, Scholten JCM, Stams AJM. Metabolic flexibility of sulfate-reducing bacteria. Front Microbiol. 2011;2.

155. Heidelberg JF, Seshadri R, Haveman SA, Hemme CL, Paulsen IT, Kolonay JF, *et al*. The genome sequence of the anaerobic, sulfate-reducing bacterium *Desulfovibrio vulgaris* Hildenborough. Nat Biotechnol. 2004;22: 554–559.

156. Matias PM, Pereira IAC, Soares CM, Carrondo MA. Sulphate respiration from hydrogen in *Desulfovibrio* bacteria: A structural biology overview. Progress in Biophysics and Molecular Biology. 2005. pp. 292–329.

157. Voordouw G, Niviere V, Ferris FG, Fedorak PM, Westlake DWS. Distribution of hydrogenase genes in *Desulfovibrio* spp. and their use in identification of species from the oil field environment. Appl Environ Microbiol. 1990;56: 3748–3754.

158. da Silva SM, Voordouw J, Leitão C, Martins M, Voordouw G, Pereira IAC. Function of formate dehydrogenases in *Desulfovibrio vulgaris* Hildenborough energy metabolism. Microbiology. 2013;159: 1760–1769.

159. Almendra MJ, Brondino CD, Gavel O, Pereira AS, Tavares P, Bursakov S, *et al*. Purification and characterization of a tungsten-containing formate dehydrogenase from *Desulfovibrio gigas*. Biochemistry. 1999;38: 16366–16372.

160. Sebban C, Blanchard L, Bruschi M, Guerlesquin F. Purification and characterization of the formate dehydrogenase from *Desulfovibrio vulgaris* Hildenborough. FEMS Microbiol Lett. 1995;133: 143–9.

161. Venceslau SS, Lino RR, Pereira IAC. The Qrc membrane complex, related to the alternative complex III, is a menaquinone reductase involved in sulfate respiration. J Biol Chem. 2010;285: 22774–22783.

162. ElAntak L, Morelli X, Bornet O, Hatchikian C, Czjzek M, Dolla A, *et al*. The cytochrome c_3 -[Fe]-hydrogenase electron-transfer complex: structural model by NMR restrained docking. FEBS Lett. 2003;548: 1–4.

163. da Silva SM, Pimentel C, Valente FMA, Rodrigues-Pousada C, Pereira IAC. Tungsten and molybdenum regulation of formate dehydrogenase expression in *Desulfovibrio vulgaris* Hildenborough. J Bacteriol. 2011;193: 2909–2916.

164. Mota CS, Valette O, González PJ, Brondino CD, Moura JJG, Moura I, *et al*. Effects of molybdate and tungstate on expression levels and biochemical

characteristics of formate dehydrogenases produced by *Desulfovibrio alaskensis* NCIMB 13491. J Bacteriol. 2011;193: 2917–2923.

CHAPTER 2

DESULFOVIBRIO VULGARIS GROWTH COUPLED TO FORMATE-DRIVEN H_2 PRODUCTION

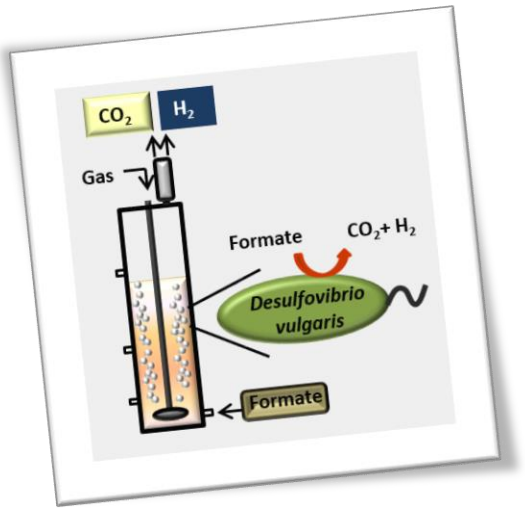

The work presented in this chapter was published in:

Mónica Martins, **Cláudia Mourato**, and Inês A. C. Pereira. 2015. *Desulfovibrio vulgaris* growth coupled to formate-driven H_2 production. Environmental Science and Technology. 49 (24): 14655-62.

Cláudia Mourato was involved in all the bioreactor assays, namely on the motorization of H_2 production and cell growth.

2. ABSTRACT

Formate is recognized as a superior substrate for biological H_2 production by several bacteria. However, the growth of a single organism coupled to this energetic pathway has not been shown in mesophilic conditions. In the present study, a bioreactor with gas sparging was used, where we observed for the first time that H_2 production from formate can be coupled with growth of the model sulfate-reducing bacterium *Desulfovibrio vulgaris* in the absence of sulfate or a syntrophic partner. In these conditions, *D. vulgaris* had a maximum growth rate of 0.078 h^{-1} and a doubling time of 9 h, and the ΔG of the reaction ranged between −21 and −18 kJ mol^{-1}. This is the first report of a single mesophilic organism that can grow while catalyzing the oxidation of formate to H_2 and bicarbonate. Furthermore, high volumetric and specific H_2 production rates (125 mL L^{-1} h^{-1} and 2500 mL g_{dcw}^{-1} h^{-1}) were achieved in a new bioreactor designed and optimized for H_2 production. This high H_2 production demonstrates that the nonconventional H_2-producing organism *D. vulgaris* is a good biocatalyst for converting formate to H_2.

2.1 INTRODUCTION

Formate is considered to be an environmentally friendly H_2 storage compound [1,2]. Consequently, extensive efforts have been directed to the development of chemical catalysts for its conversion to H_2 [2–4]. As an alternative to

chemical processes, formate can be biologically converted to H_2 according to the reaction:

$$HCOO^- + H_2O \rightarrow HCO_3^- + H_2 \quad \Delta G^{\circ\prime} = +1.3\ \text{kJ mol}^{-1} \quad \text{(equation 2.1)}$$

Although a large number of microorganisms catalyze the oxidation of formate to H_2 and bicarbonate, this reaction had not been considered energetic enough to support growth of microorganisms until the discovery of the hyperthermophilic archaeon *Thermococcus onnurineus* NA1, which can grow by this conversion [5–8]. The high growth temperature of this organism coupled with tolerance to high concentrations of formate favors the bioenergetics of the reaction ($\Delta G' = -2.6$ kJ mol^{-1} at 80 °C), enabling growth. The growth of *T. onnurineus* NA1 by converting formate to H_2 and CO_2 was recently shown to be coupled to ATP synthesis. This involves a formate-hydrogen lyase (FHL; comprising a formate dehydrogenase (FDH) and a membrane-bound hydrogenase (Hase)), a sodium-proton antiporter and a Na^+-dependent ATP synthase [8]. Oxidation of formate by the FHL complex is associated with H_2 production by the membrane-bound Hase, which couples it with the generation of a proton gradient. The proton gradient is converted to a sodium gradient by the Na^+/H^+ antiporter and this then drives ATP synthesis [8].

In mesophilic conditions, it has never been shown that H_2 production from formate can be coupled with the growth of a single organism. At this temperature range, formate oxidation in the absence of an external electron

acceptor would require very low H_2 concentrations to support growth of microorganisms. To our knowledge, bacterial growth of mesophilic organisms on formate has been reported only for a syntrophic community of a formate-oxidizing sulfate-reducing bacterium (SRB), and a hydrogenotrophic methanogen [9]. This syntrophic growth is sustained by the consumption of H_2 by the methanogen, which keeps the H_2 partial pressure (P_{H2}) low enough to make the reaction thermodynamically favorable [7–10]. The electron transfer chain involved in syntrophic formate oxidation by SRB is not known, but it was proposed to involve a periplasmic FDH coupled to a cytoplasmic energy conserving hydrogenase (Ech) [9]. SRB are notorious for expressing a high level of Hases and FDHs [11] the enzymes responsible for formate-driven H_2 production. Recently, we demonstrated in batch studies that the model organism *Desulfovibrio vulgaris* displays a very high H_2 productivity from formate in the absence of sulfate [12] However, growth coupled to H_2 production was not observed. H_2 evolution pathways are usually regulated by H_2 concentration and the P_{H2} may rapidly reach a level that thermodynamically inhibits H_2 production and bacterial growth [7,13,14]. Thus, in the present work two anaerobic bioreactor designs with gas sparging (one conventional stirred tank reactor and a column reactor designed specifically for H_2 production) were used to enhance H_2 production from formate by *D. vulgaris*, and investigate if this strain can grow by the conversion of formate to H_2 and bicarbonate in the absence of a methanogen. Gas sparging was used to maintain a low P_{H2} in the liquid phase replacing the H_2 consuming syntrophic partner.

2.2 Materials and Methods

2.2.1 Bacterial Strains and Growth Conditions

The present work was performed using *D. vulgaris* Hildenborough (DSM 644). The strain was grown in modified Postgate medium C containing 0.5 g L^{-1} KH_2PO_4, 1 g L^{-1} NH_4Cl, 2.5 g L^{-1} Na_2SO_4, 0.06 g L^{-1} $CaCl_2.2H_2O$, 0.06 g L^{-1} $MgSO_4.7H_2O$, 1 g L^{-1} yeast extract, 0.0071 g L^{-1} $FeSO_4.7H_2O$, 0.3 g L^{-1} sodium citrate tribasic dihydrate, 0.1 g L^{-1} ascorbic acid, 0.1 g L^{-1} sodium thioglycolate, 4.5 g L^{-1} sodium lactate and 0.3 mg L^{-1} resazurin. Bacterial growth was carried out at 37 ˚C using 120 mL serum bottles with a working volume of 50 mL and N_2 as gas headspace. The bottles were sealed with butyl rubber stoppers and aluminum crimp seals.

2.2.2 Bioreactor Assays

H_2 production in the stirred tank reactor was carried out using a conventional Biostat APlus system (Sartorius Stedim, Germany) bioreactor with a 3 L vessel. This reactor was operated with a working volume of 1.5 L, stirring rate of 50 rpm and a N_2 flow rate of 115 mL min^{-1}. The internal temperature was kept at 37 ˚C by a heating blanket and the pH was set at 7.2 by automatic addition of HCl (0.2 M). The medium used for the experiments was the one described above with a few modifications: limiting sulfate concentration (3.5 mM), sodium formate (80 mM) instead of sodium lactate, supplementation with

sodium acetate (20 mM), MOPS buffer (200 mM), nickel chloride (1 µM), sodium selenite (1 µM) and sodium tungstate (0.1 µM). Three control experiments were also performed: (1) bioreactor with N_2 sparging fed with the defined MO medium [15] supplemented with sodium sulfate (3.5 mM), sodium formate (80 mM), sodium acetate (20 mM), MOPS buffer (200 mM) instead of Tris-HCl, nickel chloride (1 µM), sodium selenite (1 µM), sodium tungstate (0.1 µM), ascorbic acid (0.1 g L^{-1}), sodium thioglycolate (0.1 g L^{-1}) and resazurin (0.3 mg L^{-1}), (2) bioreactor fed with Postgate medium operating without N_2 sparging (batch mode), and (3) bioreactor with N_2 sparging fed with Postgate medium without sulfate and continuous additions of sodium sulfide (140 mM) at a flow rate of 0.11 mL min^{-1}.

The sparging column reactor was designed using a glass column (inner diameter 5.5 cm, height 35 cm) equipped with an argon sparging system (gas distribution tube with a borosilicateglass disc with diameter of 3.4 cm and pore size of 100-160 µm) (Figure 2.1). The reactor operated with a working volume of 340 mL and the internal temperature of bioreactor was kept constant by a heating blanket. The column reactor experiments were performed using the medium C described for H_2 production in the stirred tank reactor but with 40 mM sodium formate, 10 mM sodium acetate and 100 mM MOPS buffer. The pH of the medium was adjusted to 7.2 ± 0.1.

In both reactors, the gas outlet was equipped with two H_2S traps in series containing zinc acetate (0.9 M) buffered with glacial acetic acid to pH 4 (Figure 2.1), followed by a H_2 sensor (BlueSens gas sensor, Germany) for online monitoring of H_2 in the exit gas stream. The data were recorded every 5 s by the BioPat®MFC fermentation software (Sartorius Stedim, Germany). In both

bioreactors 10 % (v/v) of inoculum grown in Postgate medium was used for startup.

Several operation parameters were tested in order to attain the optimal conditions for H_2 production in the column reactor: temperature (from 35 to 45 ˚C), initial cell load (from 50 to 215 $mg_{dcw}\ L^{-1}$) and argon flow rate (Q_{Ar}) (from 50 to 100 mL min^{-1}). Fed-batch experiments were also performed in order to investigate the maintenance of H_2 production capability of the SRB cells. For this purpose the reactor was supplied periodically with a nutrient solution containing formate (1 M sodium formate, 2.4 M MOPS and 1.8 % (w/v) yeast extract) and a sulfide solution (200 mM). The solutions were added to achieve 30 mM of formate and 2.5 mM of sulfide in the reactor. Each experiment was carried out at least in duplicate.

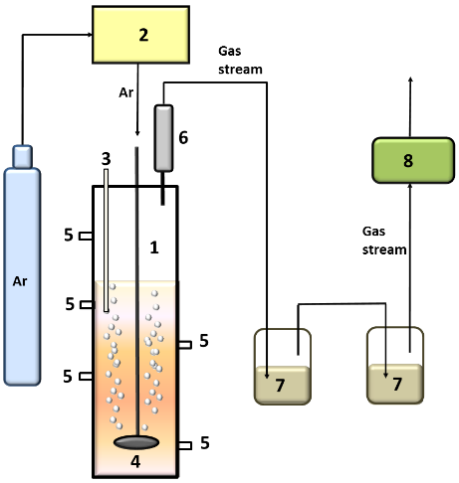

Figure 2.1. Schematic illustration of the sparging column reactor developed for H_2 production: 1, bioreactor; 2, system controller; 3, temperature sensor; 4, system sparging; 5, sampling ports; 6, condenser; 7, H_2S trap; 8, H_2 sensor.

2.2.4 ANALYTICAL METHODS

Cell growth was monitored by measuring optical density at 600 nm (OD_{600}) with a Shimadzu UV/Vis spectrophotometer. Biomass was determined by measuring the dry cell weight (dcw) and correlated with OD_{600} values. One unit value of OD_{600} corresponded to 0.31 g_{dcw} L^{-1} [12]. Liquid samples were periodically collected and filtered (0.22 µM) before analysis. Sulfate was quantified by UV/Vis spectrophotometry at 450 nm using the method of SulfaVer®4 (Hach-Lange, Dusseldorf, Germany). The concentration of formate was determined by high performance liquid chromatography (HPLC) using a Waters system (Waters Chromatography, Milford, MA) and a LKB 2142 differential refractometer detector (LKB, Bromma, Sweden). Chromatographic separation was undertaken using an Aminex HPX-87H column (300 x 7.8 mm), 9 µm particle sizes (Bio-Rad, Hercules, California) at 45 °C. Elution was carried out isocratically with 0.005 N of H_2SO_4 at a flow rate of 0.6 mL min^{-1}. The concentration of bicarbonate in the liquid samples was determined by measuring the CO_2 formed by acidifying samples with H_2SO_4 and heating for 5 min at 100˚C. CO_2 content in the headspace was determined using a Trace GC gas chromatograph (Thermo Finnigan LCC, San Jose, CA) equipped with a CTR-1 column (Althech) and a thermal conductivity detector (TCD). Helium was used as carrier gas at a flow rate of 30 mL min^{-1}.

2.2.5 THERMODYNAMIC CALCULATIONS

The Gibbs free-energy changes for the formate-dependent H_2 production reaction (equation 2.1) were calculated over the course of the experiments in the bioreactor using the Nernst equation and the measured values of P_{H2}, formate and bicarbonate concentrations. The standard Gibbs free-energy was corrected for work temperature using the Gibbs-Helmholtz equation and values of enthalpy energies of formation of products and reactants were taken from the work of Hanselmann [16].

2.3 RESULTS

2.3.1 STIRRED TANK REACTOR ASSAYS

H_2 production by *D. vulgaris* in the presence of N_2 sparging was first tested in a stirred tank reactor (Figure 2.2). We previously reported that inclusion of a small amount of sulfate at start-up is beneficial for formate-driven H_2 production by this organism [12] helping to establish a low redox potential environment and leading to some cell growth. The sulfate present (3.5 mM) is reduced in the first 7 h, leading to an increase of OD_{600} from 0.11 to 0.18. Unexpectedly, growth continued for several hours after sulfate was depleted, leading to a maximum OD_{600} of 0.26 after 12 h. In this period, formate oxidation to H_2 and bicarbonate allowed growth of *D. vulgaris* with a maximum

growth rate of 0.078 h^{-1} and a doubling time of 9 h. Interestingly, H_2 production was observed while sulfate was still being reduced, meaning that the oxidation of formate is not tightly coupled to sulfate reduction, with some of the electrons being channeled both for proton reduction. At this stage 17 mM of formate and 3.6 mM of sulfate were consumed, and 3.0 mM of H_2 were produced, which according to the stoichiometry of the reactions involved (equations 2.1 and 2.2), means that 14 mM of formate (82 %) was used for sulfate reduction, with 3 mM of formate (18 %) being channeled for H_2 production.

$$4HCOO^- + SO_4^{2-} + H^+ \rightarrow HS^- + 4HCO^- \qquad \text{(equation 2.2)}$$

After the depletion of sulfate, H_2 production remained constant at a rate of 15 mL L^{-1} h^{-1} during approximately 3 h suggesting a period of adaptation to the absence of sulfate. Subsequently, the H_2 production rate showed a steep increase, reaching a maximum of 40 mL L^{-1} h^{-1} after 10 h of incubation and this rate was maintained for 3 more hours. After that, the production of H_2 started to decrease reaching a rate of 24 mL L^{-1} h^{-1} in the end of the experiment (27 h), which corresponds to 60 % of the maximum rate observed in the reactor. After sulfate depletion, from 7 to 10 h, the calculated P_{H2} was at 342 Pa and this value increased to 836 Pa at maximum H_2 production (12 h). The concentration of bicarbonate in the bioreactor ranged from 3.3 to 4.7 mM (Table 2.1). Under these conditions, the ΔG values ranged between -21 and -18 kJ mol^{-1} for the conversion of formate (57 to 46 mM) to H_2 and bicarbonate (Figure 2.2 and Table 2.1).

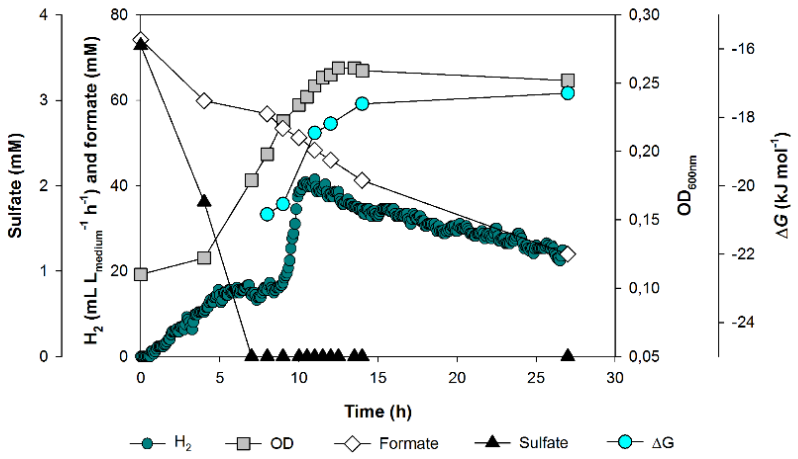

Figure 2.2. Profile of *D. vulgaris* growth and H_2 production from formate in the stirred tank reactor operated with a gas flow rate of 115 mL min^{-1}. Actual Δ*G* values for formate oxidation to H_2 and bicarbonate were calculated at 37˚C at the times indicated (see Table 2.1 for the analytical data).

Table 2.1: Analytical data used for the determination of Gibbs energy values at 37˚C.

Time (h)	Formate (mM)	HCO_3^- (mM)	H_2 (Pa)	ΔG[a] (kJ mol^{-1})
0	74	-	-	-
9	53	3.9	380	-20.5
11	48	3.3	912	-18.5
12	46	3.8	836	-18.2
14	41	4.7	560	-17.6
27	24	4.3	546	-17.3

a) Calculated considering the standard Gibbs energy value ΔG^o = +0.6 kJ mol^{-1} at 37˚C.

To further investigate if the oxidation of formate to H_2 and bicarbonate supports growth of *D. vulgaris*, additional control experiments were performed to test if yeast extract could provide further electron acceptors to support growth, and if the initial sulfate is necessary for this growth to occur. The first experiment used a defined medium in the bioreactor, which was inoculated with a culture grown in modified Postgate medium C. This means that the residual yeast extract in the bioreactor was at most 0.01 %, which is ten times less than in the previous experiments. In these conditions, the H_2 production profile was similar to that observed with yeast extract, reaching a maximum H_2 production rate of 30 mL L^{-1} h^{-1} (Figure 2.3a). Growth of *D. vulgaris* was still observed after sulfate was depleted, leading to a maximum OD_{600} of 0.18 after 15 h. This corresponds to about half the OD increase observed in the presence of 0.1 % yeast extract (Figure 2.2). The maximum growth rate was 0.054 h^{-1} (doubling time 13 h), versus a maximum growth rate of 0.078 h^{-1}, in the presence of 0.1 % yeast extract (doubling time 9 h). Despite this small decrease in growth, these results suggest that the yeast extract is not responsible for providing additional electron acceptors. If this was the reason for the observed growth, then a much stronger growth reduction should have been observed in the presence of a 10-fold decrease of yeast extract.

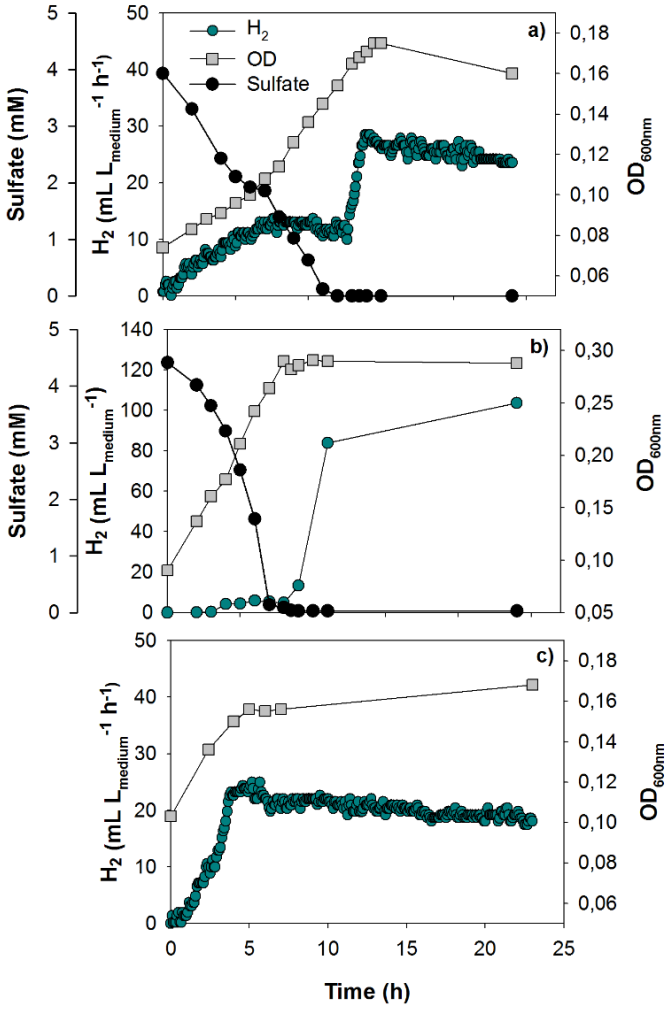

Figure 2.3. Control experiments for *D. vulgaris* growth while producing H_2 from formate in the stirred tank reactor: fed with defined MO medium without yeast extract, but inoculated with cells grown in Postgate medium (a); fed with Postgate medium without sparging (b); and fed with Postgate medium without sulfate (c). In (b) total H_2 produced is reported, whereas in (a) and (c) the H_2 production rate is reported.

An additional experiment was performed where the bioreactor was inoculated with cells that had been transferred several times in a defined lactate/sulfate medium without yeast extract. Sulfate was consumed but almost no growth was detected and no H_2 production was observed (Figure 2.4), so this experiment was not conclusive. A considerable reduction in growth was also observed in batch cultures using the defined MO medium with formate/sulfate. To finally discard that further electron acceptors in yeast extract were supporting growth we performed an additional experiment with modified Postgate medium (with 0.1 % yeast extract), where the bioreactor was operated without gas sparging (Figure 2.3b). In this condition, growth stopped right after sulfate was depleted, indicating that, in the previous experiments, yeast extract is not responsible for growth in the absence of sulfate. Growth coupled to H_2 production in the absence of sulfate is only observed when gas sparging is used to keep a low P_{H2}. In another control experiment the bioreactor was run without the initial presence of sulfate as electron acceptor. Instead of sulfate, it was necessary to add sulfide to ensure a low redox potential (Figure 2.3c). In this condition the H_2 production rate increased steadily right from the start of the experiment, reaching a maximum of 23 mL L^{-1} h^{-1}. This is similar to the rate observed in the bioreactor started with sulfate, if we subtract the H_2 production rate obtained during the reduction of sulfate (Figure 2.2). Growth of *D. vulgaris* was again observed reaching an OD_{600} of 0.17 (from an initial OD_{600} of 0.10), with a maximum growth rate of 0.096 h^{-1} (doubling time 7 h).

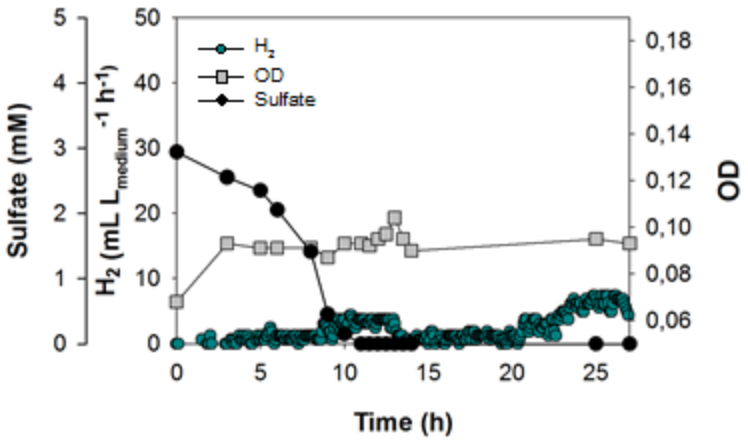

Figure 2.4. Profile of *D. vulgaris* growth and H_2 production from formate in the stirred tank reactor operated fed with MO medium without yeast extract, and inoculated with cells grown also without yeast extract. The reactor operated with a gas flow rate of 115 mL min^{-1}.

2.3.2 COLUMN REACTOR ASSAYS

In order to further optimize H_2 production using *D. vulgaris* as a biocatalyst, a column reactor was designed to improve the efficiency of sparging (Figure 2.1), and several operation parameters were tested in order to find the optimal conditions for H_2 production.

The temperature-profile of the H_2 production is presented in Figure 2.5. As observed in the stirred tank reactor, the H_2 production profile at 35 ˚C can be divided in two stages: one in the presence of sulfate (between 0 and 5 h) and another after sulfate is depleted (5 to 8 h). In the first stage, the H_2 production increased slowly reaching a maximum production rate of 15 mL L^{-1} h^{-1} after 3

hours and this rate was maintained until sulfate was completely reduced. In this stage 2.5 mM of sulfate was reduced and 14 mM of formate was consumed, and so 10 mM of formate (70 %) was used for sulfate reduction, with the remaining 4 mM formate (30 %) being channeled for H_2 production. In the second stage, after sulfate is consumed, the H_2 production rate showed a steep increase, reaching a maximum of 60 mL L^{-1} h^{-1} after 6 h of incubation, and this rate was maintained until the end of the experiment. In the stationary state from 6 to 8 h, 6 mM of H_2 was produced and 6.5 mM of formate was consumed, which is close to a 100 % of conversion of formate to H_2, considering the experimental error of the formate and H_2 quantifications. Growth was observed during the sulfate reduction stage (OD_{600} increased from 0.17 to 0.27), and continued after sulfate was depleted, leading to a maximum OD_{600} of 0.31 after 6 h of incubation.

When the temperature of the reactor was increased from 35 to 41 °C, some differences were observed in the profile of H_2 production. As observed at 35˚C, H_2 production and sulfate reduction occurred simultaneously, but the H_2 production rate reached in this first stage (35 mL L^{-1} h^{-1}) was two times higher than that observed at 35 ˚C (15 mL L^{-1} h^{-1}). In addition, after the depletion of sulfate the H_2 production rate rapidly increased achieving the higher value of 125 mL L^{-1} h^{-1} after 5 hours of incubation, which is also twice of that observed at 35 ˚C. Over the course of the experiment, at 41 °C, 3.5 mM of sulfate and 29 mM of formate were consumed and 17 mM of H_2 were produced. So, sulfate reduction and H_2 production accounts for more than 100 % conversion of formate (due to the analytical error associated with the three quantifications), again suggesting a 100 % conversion of formate to H_2.

However, growth was not observed at this temperature. A further increase from 41 to 46 °C resulted in a decrease in H_2 production rate reaching 60 mL L^{-1} h^{-1} after 8 h of incubation, probably as a result of temperature stress (data not shown).

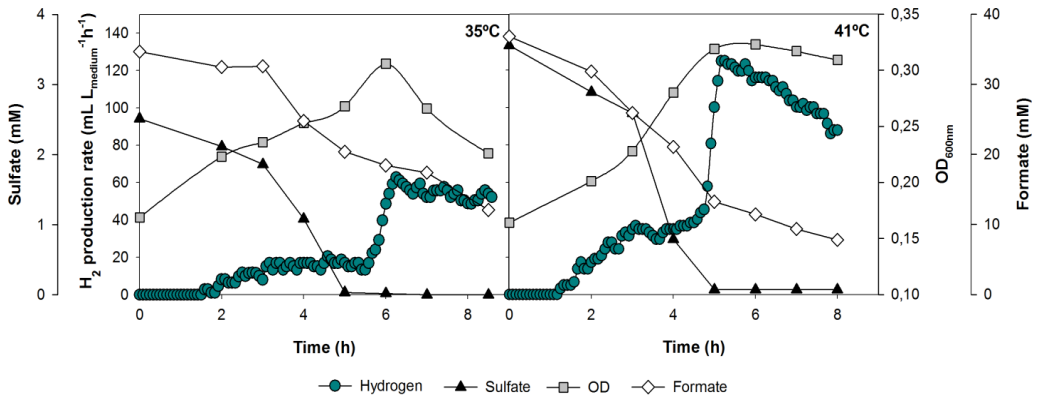

Figure 2.5. Effect of temperature on H_2 production and bacterial growth in the sparging column reactor. The reactor operates with an argon flow rate of 80 mL min^{-1} and an initial cell load of 50 mg_{dcw} L^{-1}.

The effects of increasing the cell load and argon flow rate in H_2 production were also investigated at 41˚C (Figure 2.6). The maximum H_2 production rate was not much affected by the initial cell load, but the incubation time necessary to achieve this maximum rate was different. A H_2 production rate of 125 mL L^{-1} h^{-1} was reached after 5 h of incubation with an initial cell load of 50 mg_{dcw} L^{-1}, while the a similar production rate was achieved after only 3 hours with 130 mg_{dcw} L^{-1} (Figure 2.6a). A further increase from 130 to 215 mg_{dcw} L^{-1}

resulted in a slight increase of the H_2 production rate (145 mL L^{-1} h^{-1}). This corresponds to a maximum specific H_2 production rate of 674 mL g_{dcw}^{-1} h^{-1}, while with a cell load of 50 mg_{dcw} L^{-1} of cells a specific H_2 production rate of 2 500 mL g_{dcw}^{-1} h^{-1} is obtained. Concerning the effect of the argon flow rate on H_2 production (Figure 2.6b), an increase in the H_2 production rate (from 90 to 125 mL L^{-1} h^{-1}) was observed when the Q_{Ar} was increased from 50 to 80 mL min^{-1}. However, a further increase from 80 to 100 mL min^{-1} did not improve the H_2 production rate.

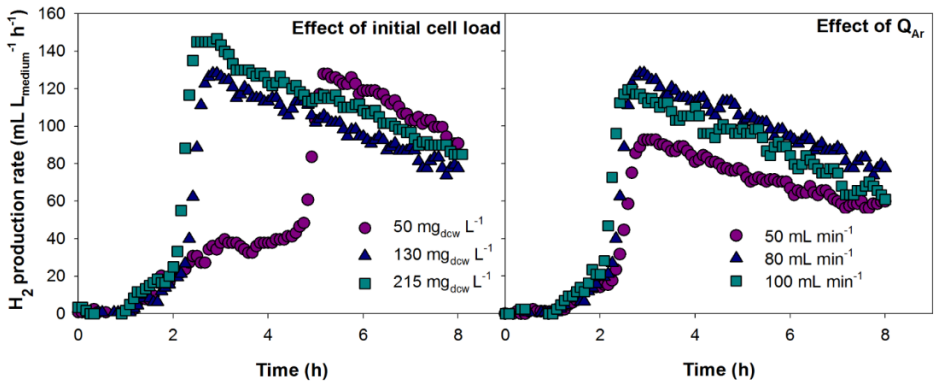

Figure 2.6. Production of H_2 by *D. vulgaris* in the sparging column reactor operated with different initial cell load (a) and argon flow rate (b). Effect of initial cell load was evaluated with Q_{Ar}= 80mL min^{-1}, whereas the effect of Q_{Ar} was evaluated with an initial cell load of 130 mg_{dcw} L^{-1}, both at 41˚C.

2.3.3 BIOH$_2$ PRODUCTION ON FED-BATCH MODE

H_2 production by *D. vulgaris* was also evaluated in fed-batch experiments, where formate was periodically fed to the column reactor (Figure 2.7). After the bioreactor start-up, the H_2 production rate rapidly increased until reaching a maximum plateau (125 mL L^{-1} h^{-1}) after 3 h of operation. This rate was maintained during approximately 4 h, after which the H_2 production rate decreased steadily. After 10 h of continuous production in the reactor, *D. vulgaris* retained the capacity to produce 60 mL L^{-1} h^{-1} of H_2, which is half of the maximum rate achieved. When the H_2 production rated reached zero, formate was again fed to the reactor, resulting in a quick increase in H_2 production to the same maximum rate (125 mL L^{-1} h^{-1}). In two consecutive formate additions the H_2 production profile was closely matched with the initial one.

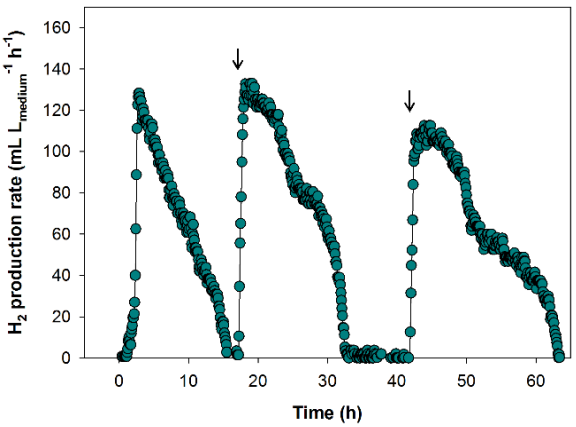

Figure 2.7. Effect of repeated addition of formate (30mM) on H_2 production by *D. vulgaris* in the sparging column reactor operated at 41˚C with an initial cell load of 130 mg_{dcw} L^{-1} and argon flow rate of 80 mL min^{-1}. The addition of formate is represented by the arrows.

2.4 DISCUSSION

Recently, we demonstrated the potential of *D. vulgaris* for H_2 production from formate [12]. However, bacterial growth was not observed in this process. In mesophilic conditions the oxidation of formate to H_2 is slightly endergonic ($\Delta G^{o'}$ = +1.3 kJ mol^{-1}) and thus cannot support bacterial growth, unless the H_2 partial pressure (P_{H2}) is kept very low as it happens in syntrophic growth conditions. In the absence of a H_2-consuming organism, the P_{H2} rapidly reaches a level that thermodynamically inhibits further fermentation. Thus, in order to maintain a low P_{H2}, two anaerobic bioreactor designs, where the liquid culture was continuously purged with gas, were used to improve the production of H_2 from formate and to investigate if this process could be coupled to growth of *D. vulgaris*. A similar approach allow growth of pure cultures of *Pelobacter acetylenicus* on ethanol, *Syntrophothermus lipocalidus* on butyrate and *Aminobacterium colombiense* on alanine [10,17].

2.4.1 HYDROGEN PRODUCTION

Interestingly, in both bioreactors it was observed that H_2 production started while sulfate was still being reduced, which was not observed in the absence of sparging [12]. The simultaneous production of H_2 and reduction of sulfate revealed that both pathways are operating in parallel in *D. vulgaris*, that is electrons resulting from oxidation of formate are being channeled both for sulfate and proton reduction pathways. At this stage 82 % of the electrons were used for sulfate respiration and 18 % for H_2 production in the stirred tank

reactor, while in the column reactor 70 % of the electrons were channeled for sulfate respiration at 35 ˚C. The initial production and subsequent consumption of H_2 in sulfate respiration using lactate or formate as electron donors has been reported when *D. vulgaris* grows with an excess of sulfate [18,19].This phenomenum designed by H_2 burst was suggested to be associated with the generation of low redox potential and sufficient ATP to start sulfate reduction [19]. In this work, we observed that in the presence of a low sulfate concentration and using gas sparging, the production of H_2 was concomitant with sulfate respiration.

The maximum H_2 production rate achieved in the conventional stirred tank (40 mL L^{-1} h^{-1}) is considerably higher than that observed in our previous studies (15 mL L^{-1} h^{-1}), where an identical reactor without gas sparging was used [12] This result can be attributed to the low P_{H2} obtained by gas sparging which favors the thermodynamics of the reaction. The maximum P_{H2} obtained in the stirred tank with sparging was 836 Pa, while without sparging it was 56 kPa. These results are consistent with previous studies where an improvement of H_2 production using fermentative organisms and phototrophic bacteria was achieved using the gas sparging methodology [13,20].

A further enhancement of H_2 production was obtained when *D. vulgaris* was used as biocatalyst in the new column reactor developed specifically for this purpose. The H_2 production obtained in this bioreactor at 35˚C (60 mL L^{-1} h^{-1} after 6 h) is higher and faster than that observed in the conventional stirred tank reactor (40 mL L^{-1} h^{-1} after 10 h) at similar temperature (37˚C). This result is due to the reactor design that allows an efficient liquid-gas transfer of H_2 decreasing the concentration of H_2 in the liquid phase. Optimization of several

operation parameters in the column reactor such as temperature, initial cell load and Q_{gas} improved the maximum H_2 production rate to 125 mL L^{-1} h^{-1} and the specific H_2 production rate to 2 500 mL g_{dcw}^{-1} h^{-1}, at 41 ˚C and with an initial cell concentration of 50 mg_{dcw} L^{-1}. The higher temperature favors the thermodynamics of the reaction.

H_2 production by *D. vulgaris* was also evaluated in fed-batch experiments, where formate was periodically fed to the column reactor. A first formate addition, after H_2 production had stopped, led to a quick rise, achieving the same maximum H_2 production rate (125 mL L^{-1} h^{-1}). In two consecutive formate additions the H_2 production profile was closely matched with the initial one, showing that the cells do not lose the ability to produce H_2. This is an important finding suggesting that *D. vulgaris* can be used as a biocatalyst for H_2 production in continuous mode.

The first reports of H_2 production from formate were obtained with *E.coli* [21,22]. Since then, the capacity of several microorganisms to produce H_2 from formate has been evaluated [23] and some results are highlighted in Table 2.2. An efficient formic acid conversion to H_2 by *Enterobacter asburiae* SNU-1 was reported [24]. A H_2 production rate of 91 mL L^{-1} h^{-1} was obtained with 50 mM of formic acid, which is similar to the substrate concentration used in our study, whereas in the presence of 350 mM of substrate, 491 mL L^{-1} h^{-1} H_2 was achieved [24]. Recently, the hyperthermophilic archaeon *T. onnurineus* NA1 was found to be very efficient in formate-driven H_2 production with a H_2 production rate of 4 mmol L^{-1} h^{-1} [5,6,25], which is similar to the 5 mmol L^{-1} h^{-1} obtained with *D. vulgaris* in the present study. By increasing the temperature (80 ˚C), formate concentration (400 mM) and cell load (OD=1.7) the

production rate by *T. onnurineus* NA1 could be increased to 236 mmol L^{-1} h^{-1} [25]. In addition, the H_2 production rate observed in the present study was similar to that reported for a recombinant strain of *Pyrococcus furiosus* where the FHL complex of *T. onnurineus* was expressed [26] and higher than the ones reported for two SRB species used as bioelectrodes in microbial electrolysis cells (*Desulfovibrio paquesii* 0.3 mmol L^{-1} h^{-1} and *Desulfovibrio caledoniensis* 5.4 µmol L^{-1} h^{-1}) [27,28].

Table 2.2. Hydrogen production from formate by different microorganisms.

Microorganism	H_2 production rate	Specific H_2 production rate	Reference
D. vulgaris	125 mL L^{-1} h^{-1}	2500 mL g_{dcw}^{-1} h^{-1}	this study
	5 mmol L^{-1} h^{-1}	100 mmol g_{dcw}^{-1} h^{-1}	
D. vulgaris	15 mL L^{-1} h^{-1}	7 mmol g_{dcw}^{-1} h^{-1}	[12]
E. coli in agar	710 mL L^{-1} h^{-1}	6 mmol g_{dcw}^{-1} h^{-1}	[29]
Enterobacter asburiae	91 mL L^{-1} h^{-1} [b]	91 mL g_{dcw}^{-1} h^{-1} [b]	[24]
	491 mL L^{-1} h^{-1} [c]	491 mmol g_{dcw}^{-1} h^{-1}	
T. onnurienues NA1	4 mmol L^{-1} h^{-1}	nd [a]	[6]
	236 mmol L^{-1} h^{-1} [d]	nd [a]	[25]
P. furiosus recombinant strain	4 mmol L^{-1} h^{-1}	nd [a]	[26]

[a] nd = not determined. [b] from 50 mM formate. [c] from 350 mM formate. [d] from 400 mM formate.

In the search to find or engineer microorganisms with high H_2 productivities, several efforts have been carried out namely isolation of new species, process development and genetic modification of bacterial strains [5,8,24,26,29–31].

Here, we report a simple and low cost technology for H_2 production from formate with wild-type organism, obtaining comparable results and showing that *D. vulgaris*, a non-conventional H_2 producer microorganism, has potential to be used as biocatalyst for H_2 production from formate. Future studies involving genetic engineering may further improve this productivity.

2.4.2 BACTERIAL GROWTH ON FORMATE

This work suggests for the first time that formate oxidation to H_2 and CO_2 can be coupled to growth of a single mesophilic organism. In the conventional stirred tank reactor, formate oxidation to H_2 and bicarbonate allowed the growth of *D. vulgaris* with a maximum growth rate of 0.078 h^{-1} and a doubling time of 9 h. This growth was observed between ΔG values of -21 and -18 kJ mol^{-1}, which are values similar to those reported for syntrophic growth of *Desulfovibrio* sp. strain G11 and *M. arboriphilus* (from -17 to -19 kJ mol^{-1}) [9] These values are close to the estimated biological minimum energy quantum that can be harnessed to support microbial metabolism (-20 kJ mol^{-1}) [32]. However, microbial metabolisms with Δ*G* below this theoretical minimum have been reported, namely under starvation conditions where energy conservation was observed at Δ*G* values ranging from -10 to -15 kJ mol^{-1} of substrate [33,34]. In addition, it was recently demonstrated that the *T. onnurineus* NA1 is capable of growing in the range of -20 to -8 kJ mol^{-1}, which are the lowest values ever reported for a microorganism [7,8]. Although, bacterial growth coupled to H_2 production from formate was observed in both

bioreactors at 35 and 37 ˚C, such growth was no longer observed when the temperature of the column reactor was increased to 41 ˚C. This result may have been due the very fast increase of P_{H2} in these conditions. At 41 ˚C, the P_{H2} after sulfate depletion was 300 Pa and in half hour it increased very rapidly achieving a value of 900 Pa. This is similar to the value reached in the stirred tank reactor when bacterial growth stopped.

The observation that *D. vulgaris* grows while converting formate to H_2 and CO_2, suggests that it can derive energy from this process. Since substrate level phosphorylation is not possible, this indicates that a proton-motive force is generated in the process leading to production of ATP through the ATP synthase. In previous studies, we reported that the periplasmic [NiFeSe] Hase is the main Hase detected in conditions where formate is oxidized in the absence of sulfate, when Se is present [12]. In *D. vulgaris* the FDHs responsible for oxidizing formate are also periplasmic [35]. If H_2 production from formate involved only direct electron transfer between these periplasmic proteins, then growth would not be possible since there would be no generation of a proton-motive force across the membrane. Since growth is observed, this suggests that an energy-conserving membrane-bound Hase facing the cytoplasm is involved in H_2 production (at least partially). *D. vulgaris* has two such Hases, the Ech and the Coo Hases, one or both of which are likely to be involved in the process. This suggestion is similar to the proposal made by Dolfing and colleagues [9] who proposed that in syntrophic culture *Desulfovibrio* sp. strain G11 or *D. vulgaris* can conserve energy via a periplasmic FDH coupled with an energy-conserving Hase or a Hase located at the

cytoplasm, with the resulting proton gradient as the driving force of ATP synthesis.

In conclusion, this work demonstrates that H_2 productivity from formate by *D. vulgaris* can be significantly increased by using a sparging reactor and that the process is further improved at a slightly elevated temperature. The observation that *D. vulgaris* grows while converting formate to H_2 and CO_2 has important bioenergetics implications and should be further investigated.

ACKNOWLEDGMENTS

This research was supported by Post-Doc and PhD fellowships SFRH/BPD/76707/2011 and SFRH/BD/86442/2012, and grants UID/Multi/04551/2013 and PTDC/BBB-BEP/0934/2012 funded by Fundação para a Ciência e Tecnologia (Portugal). We are grateful to Cristina Leitão and Carlos Romão for HPLC and GC analysis support, respectively.

REFERENCES

1. Boddien A, Gärtner F, Federsel C, Sponholz P, Mellmann D, Jackstell R, *et al.* CO_2 -"neutral" hydrogen storage based on bicarbonates and formates. Angew Chemie. 2011;50: 6411–6414.

2. Boddien A, Mellmann D, Gärtner F, Jackstell R, Junge H, Dyson PJ, *et al*. Efficient dehydrogenation of formic acid using an iron catalyst. Science. 2011;333: 1733–1736.

3. Enthaler S, von Langermann J, Schmidt T. Carbon dioxide and formic acid—the couple for environmental-friendly hydrogen storage? Energy Environ Sci. 2010;3: 1207–1217.

4. Johnson TC, Morris DJ, Wills M. Hydrogen generation from formic acid and alcohols using homogeneous catalysts. Chem Soc Rev. 2010;39: 81–88.

5. Kim YJ, Lee HS, Kim ES, Bae SS, Lim JK, Matsumi R, *et al*. Formate-driven growth coupled with H_2 production. Nature. Nature Publishing Group; 2010;467: 352–355.

6. Bae SS, Kim TW, Lee HS, Kwon KK, Kim YJ, Kim MS, *et al*. H_2 production from CO, formate or starch using the hyperthermophilic archaeon, *Thermococcus onnurineus*. Biotechnol Lett. 2012;34: 75–79.

7. Lim JK, Bae SS, Kim TW, Lee JH, Lee HS, Kang SG. Thermodynamics of formate-oxidizing metabolism and implications for H_2 production. Appl Environ Microbiol. 2012;78: 7393–7397.

8. Lim JK, Mayer F, Kang SG, Muller V. Energy conservation by oxidation of formate to carbon dioxide and hydrogen via a sodium ion current in a hyperthermophilic archaeon. Proc Natl Acad Sci. 2014;111: 11497–11502.

9. Dolfing J, Jiang B, Henstra AM, Stams AJM, Plugge CM. Syntrophic growth on formate: a new microbial niche in anoxic environments. Appl Environ Microbiol. 2008;74: 6126–6131.

10. Adams CJ, Redmond MC, David L. Pure-culture growth of fermentative bacteria, facilitated by H_2 removal: bioenergetics and H_2 production. Appl Environ

Microbiol. 2006;72: 1079–1085.

11. Pereira IAC, Ramos AR, Grein F, Marques MC, da Silva SM, Venceslau SS. A comparative genomic analysis of energy metabolism in sulfate reducing bacteria and archaea. Front Microbiol. 2011;2: 1–18.

12. Martins M, Pereira IAC. Sulfate-reducing bacteria as new microorganisms for biological hydrogen production. Int J Hydrogen Energy. 2013;38: 12294–12301.

13. Bastidas-Oyanedel J-R, Mohd-Zaki Z, Zeng RJ, Bernet N, Pratt S, Steyer J-P, *et al*. Gas controlled hydrogen fermentation. Bioresour Technol. 2012;110: 503–509.

14. Heimann A, Jakobsen R, Blodau C. Energetic constraints on H_2-dependent terminal electron accepting processes in anoxic environments: a review of observations and model approaches. Environ Sci Technol. 2010;44: 24–33.

15. Zane GM, Yen HB, Wall JD. Effect of the deletion of qmoABC and the promoter-distal gene encoding a hypothetical protein on sulfate reduction in *Desulfovibrio vulgaris* Hildenborough. Appl Environ Microbiol. 2010;76: 5500–5509.

16. Hanselmann KW. Microbial energetics applied to waste repositories. Cell Mol Life Sci. 1991;47: 645–687.

17. Valentine DL, Reeburgh WS, Blanton DC. A culture apparatus for maintaining H_2 at sub-nanomolar concentrations. J Microbiol Methods. 2000;39: 243–251.

18. Tsuji K, Yagi T. Significance of hydrogen burst from growing cultures of *Desulfovibrio vulgaris* Miyazaki, and the role of hydrogenase and cytochrome *c3* in energy production system. Arch Microbiol. 1980;125: 35–42.

19. Voordouw G. Carbon monoxide cycling by *Desulfovibrio vulgaris* Hildenborough. J Bacteriol. 2002;184: 5903–5911.

20. Liao Q, Qu X-F, Chen R, Wang Y-Z, Zhu X, Lee D-J. Improvement of hydrogen production with *Rhodopseudomonas palustris* CQK-01 by Ar gas sparging. Int J Hydrogen Energy. 2012;37: 15443–15449.

21. Harden A. The chemical action of *Bacillus coli* communis and similar organisms on carbohydrates and allied compounds. J Chem Soc, Trans. 1901;79: 610–628.

22. Pakes WCC, Jollyman WH. XL.The bacterial decomposition of formic acid into carbon dioxide and hydrogen. J Chem Soc Trans. 1901;79: 386–391.

23. Rittmann SK-MR, Lee HS, Lim JK, Kim TW, Lee J-H, Kang SG. One-carbon substrate-based biohydrogen production: Microbes, mechanism, and productivity. Biotechnol Adv. 2015;33: 165–177.

24. Shin J-H, Yoon JH, Lee SH, Park TH. Hydrogen production from formic acid in pH-stat fed-batch operation for direct supply to fuel cell. Bioresour Technol. 2010;101: S53–S58.

25. Bae SS, Lee HS, Jeon JH, Lee J-H, Kang SG, Kim TW. Enhancing bio-hydrogen production from sodium formate by hyperthermophilic archaeon, *Thermococcus onnurineus* NA1. Bioprocess Biosyst Eng. 2015;38: 989–993.

26. Lipscomb GL, Schut GJ, Thorgersen MP, Nixon WJ, Kelly RM, Adams MWW. Engineering hydrogen gas production from formate in a hyperthermophile by heterologous production of an 18-subunit membrane-bound complex. J Biol Chem. 2014;289: 2873–2879.

27. Aulenta F, Catapano L, Snip L, Villano M, Majone M. Linking bacterial metabolism to graphite cathodes: electrochemical insights into the H_2-producing capability of *Desulfovibrio* sp. ChemSusChem. 2012;5: 1080–1085.

28. Yu L, Duan J, Zhao W, Huang Y, Hou B. Characteristics of hydrogen evolution and oxidation catalyzed by *Desulfovibrio caledoniensis* biofilm on pyrolytic graphite electrode. Electrochim Acta. 2011;56: 9041–9047.

29. Seol E, Manimaran A, Jang Y, Kim S, Oh Y-K, Park S. Sustained hydrogen production from formate using immobilized recombinant *Escherichia coli* SH5. Int J Hydrogen Energy. 2011;36: 8681–8686.

30. Seol E, Jang Y, Kim S, Oh Y-K, Park S. Engineering of formate-hydrogen lyase gene cluster for improved hydrogen production in *Escherichia coli.* Int J Hydrogen Energy. 2012;37: 15045–15051.

31. Yoshida A, Nishimura T, Kawaguchi H, Inui M, Yukawa H. Enhanced hydrogen production from formic acid by formate hydrogen lyase-overexpressing *Escherichia coli* strains. Appl Environ Microbiol. 2005;71: 6762–6768.

32. Schink B. Energetics of syntrophic cooperation in methanogenic degradation. Microbiol Mol Biol Rev. 1997;61: 262–280.

33. Hoehler TM. Biological energy requirements as quantitative boundary conditions for life in the subsurface. Geobiology. 2004;2: 205–215.

34. Hoehler TM, Alperin MJ, Albert DB, Martens CS. Apparent minimum free energy requirements for methanogenic Archaea and sulfate-reducing bacteria in an anoxic marine sediment. FEMS Microbiol Ecol. 2001;38: 33–41.

35. da Silva SM, Voordouw J, Leitão C, Martins M, Voordouw G, Pereira IAC. Function of formate dehydrogenases in *Desulfovibrio vulgaris* Hildenborough energy metabolism. Microbiology. 2013;159: 1760–1769.

CHAPTER 3

ELECTRON TRANSFER PATHWAYS OF FORMATE-DRIVEN H_2 PRODUCTION IN *DESULFOVIBRIO*

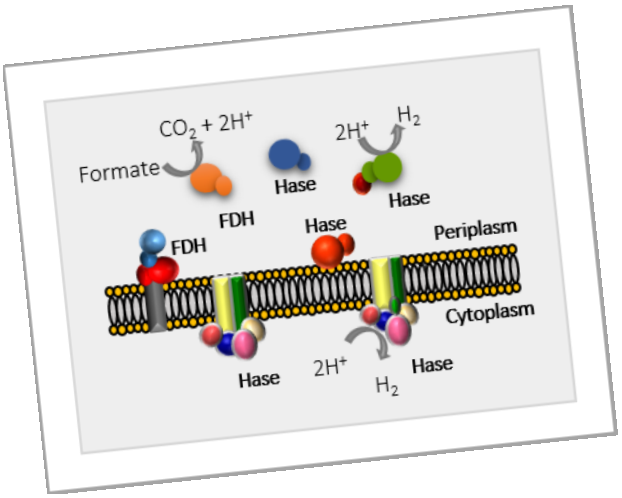

The work presented in this chapter was published in:

Mónica Martins*, **Cláudia Mourato***, Fabio O. Morais-Silva, Claudina Rodrigues-Pousada, Gerrit Voordouw, Judy D. Wall, Inês A. C. Pereira. 2016. Electron transfer pathways of formate-driven H_2 production in *Desulfovibrio*. Applied Microbiology and Biotechnology. 100 (18): 8135-8146. (*co-first authors)

Cláudia Mourato was involved in the experimental procedures, mainly in all the H_2 production studies with the different *Desulfovibrio* species and the mutant strains, and also in the discussion of the work.

3. ABSTRACT

The potential of sulfate-reducing bacteria (SRB) as biocatalysts for H_2 production from formate was recently demonstrated, but the electron transfer pathways involved were not described. In the present work we analyzed the H_2 production capacity of five *Desulfovibrio* strains: *D. vulgaris*, *D. desulfuricans*, *D. alaskensis*, *D. fructosivorans* and *D. gigas*. *D. vulgaris* showed the highest H_2 productivity (865 mL L_{medium}^{-1}), and *D. gigas* the lowest one (374 mL L_{medium}^{-1} of H_2). The electron transfer pathways involved in formate-driven H_2 production by these two organisms were further investigated through the study of deletion mutants of hydrogenases (Hases) and formate dehydrogenases (FDHs). In *D. vulgaris*, the periplasmic FdhAB is the key enzyme for formate oxidation and two pathways are apparently involved in the production of H_2 from formate: a direct one only involving periplasmic enzymes and a second one that involves transmembrane electron transfer and may allow energy conservation. In the presence of selenium, the Hys [NiFeSe] Hase is the main periplasmic enzyme responsible for H_2 production, and the cytoplasmic Coo Hase is apparently involved in the ability of *D. vulgaris* to grow by converting formate to H_2, in sparging conditions. Contrary to *D. vulgaris*, H_2 production in *D. gigas* occurs exclusively by the direct periplasmic route and does not involve the single cytoplasmic Hase, Ech. This is the first report of the metabolic pathways involved in formate metabolism in the absence of sulfate in SRB, revealing that the electron transfer pathways are species-specific.

3.1 INTRODUCTION

Biologic hydrogen production from one carbon compounds such as formate and carbon monoxide can be a promising alternative for a future H_2-based economy [1–3]. Several studies have been performed in recent years to identify H_2-producing microorganisms using formate or CO as substrate and to enhance H_2 productivity by genetic engineering and process development [4–10].

SRB are capable of H_2 production from formate [11], since they contain a high level of Hases and FDHs, the enzymes responsible for H_2 production from formate [12]. In the absence of sulfate, SRB are capable of fermentative metabolism, producing H_2 and growing by syntrophic association with H_2 consuming organisms such as methanogens. Common substrates for syntrophy are lactate (e.g. for *Desulfovibrio*) [13] or propionate (e.g. for *Syntrophobacter*) [14], but syntrophy on formate has also been reported (for *Desulfovibrio*) [15]. In a previous study, we demonstrated that the model SRB *Desulfovibrio vulgaris* Hildenborough displays a high H_2 production from formate when grown in monoculture in the absence of sulfate [11,16]. Recently, it was also suggested that in *D. alaskensis* oxidation of formate coupled to sulfate reduction requires its conversion to H_2 [17]. However, the electron transfer pathways involved in formate oxidation are poorly understood. So far, most studies of fermentative metabolism by SRB have focused on understanding the electron transfer pathways involved in syntrophic association of *Desulfovibrio* spp. with methanogenic organisms using lactate or pyruvate as substrates [13,18–22]. To our knowledge, no

studies have addressed formate oxidation by SRB in the absence of sulfate or a syntrophic partner. However, it is important to understand the metabolic pathway involved in formate-driven H_2 production in order to improve H_2 productivity through genetic engineering.

A recent genomic analysis of energy metabolism genes in several SRB showed a high diversity in number and types of Hases and FDHs, even among strains of the same genus [12]. Thus, in the present work we compared the H_2-production characteristics of five *Desulfovibrio* species (*D. vulgaris* Hildenborough*, D. gigas, D. desulfuricans* ATCC 27774, *D. alaskensis* G20 and *D. fructosivorans*) with quite distinct Hase and FDH compositions. The electron transfer pathways involved in formate-driven H_2 production by two of these organisms, *D. vulgaris* and *D. gigas*, were then further investigated. *D. vulgaris* has three periplasmic-facing FDHs, two of which are soluble ($FdhABC_3$ and FdhAB) and another that is membrane-associated (FdhABD) [23,24]. Among the three, $FdhABC_3$ and FdhAB are the two main FDHs detected in *D. vulgaris* [23]. The genome of *D. vulgaris* encodes seven Hases belonging to the [FeFe] and [NiFe] families. Four of these are periplasmic, including an [FeFe] Hase (Hyd), two [NiFe] Hases (HynAB-1 and HynAB-2), and a [NiFeSe] Hase (Hys), whereas three are in or facing the cytoplasm, namely the two membrane-associated energy-conserving Hases, Ech and Coo, and a soluble [FeFe] Hase [12]. The H_2 production of *D. vulgaris* mutants lacking genes for the two main FDHs, the four periplasmic Hases and the two membrane-associated energy-conserving Hases was compared with the wild-type strain in order to disclose the role of each enzyme in H_2 production from formate. In contrast to *D. vulgaris*, the genome of *D. gigas* [25] shows this organism contains only two

Hases both belonging to the [NiFe] family: a cytoplasmic Ech Hase and a periplasmic dimeric [NiFe] Hase (HynAB-1) [26,27], making *D. gigas* a good model system to study the role of each Hase on H_2 production from formate.

3.2 MATERIAL AND METHODS

3.2.1 STRAINS AND GROWTH CONDITIONS

The strains used in this study are listed in Table 3.1. All strains were grown in modified Postgate medium C containing 0.5 g L^{-1} KH_2PO_4, 1 g L^{-1} NH_4Cl, 2.5 g L^{-1} Na_2SO_4, 0.06 g L^{-1} $CaCl_2.2H_2O$, 0.06 g L^{-1} $MgSO_4.7H_2O$, 1 g L^{-1} yeast extract, 0.0071 g L^{-1} $FeSO_4.7H_2O$, 0.3 g L^{-1} sodium citrate tribasic dihydrate, 0.1 g L^{-1} ascorbic acid, 0.1 g L^{-1} sodium thioglycolate, 4.5 g L^{-1} sodium lactate and 0.3 g L^{-1} resazurin. Bacterial growth was carried out at 37 ˚C in 120 mL serum bottles with a working volume of 50 mL and N_2 as gas headspace. The bottles were sealed with butyl rubber stoppers and aluminum crimp seals.

Table 3.1. Description of the strains used in this study.

Strains	Description	Reference
D. alaskensis	G20	
D. fructosovorans	DSM 3604	
D. desulfuricans	ATCC 27774	
D. vulgaris strains		
D. vulgaris Hildenborough		
D. vulgaris Hildenborough	DSM 644	
Δ*hys*	Δ*hys*AB	[18]
Δ*hyd*/Δ*hyn1*	Δ*hyd*AB Δ*hyn*AB-1	[18]
Δ*hyn2*	Δ*hyn*AB-2	[28]
Δ*fdhAB*	Δf*dh*AB	[29]
Δ*fdhABC*$_3$	Δ*fdh*ABC$_3$	[29]
JW710	*D. vulgaris* wt Δ*upp*	[30]
Δ*coo* (JW5051)	Δ*coo*MKLXUH *hyp*A *coo*F	[13]
Δ*coo*/Δ*ech* (JW5054)	Δ*coo*MKLXUH *hyp*A *coo*F Δ*ech*ABCDEF	[13]
Δ*ech* (JW5060)	Δ*ech*ABCDEF	[13]
D. gigas strains		
D. gigas	ATCC 19364	
Δ*ech*	Δ*ech*BC	[26]
Δ*hyn*	Δ*hyn*AB	[26]

3.2.2 H_2 PRODUCTION ASSAYS IN SERUM BOTTLES

The studies of H_2 production were performed in the medium described above with a few modifications: sodium formate (40 mM) instead of sodium lactate as electron donor, limiting sulfate concentration (3 mM), reduced level of yeast extract (0.2 g L^{-1}), and supplementation with sodium acetate (10 mM) and MOPS buffer (100 mM). The medium pH was adjusted to 7.2 ± 0.1. The effect of metal cofactors of FDHs (Mo and W) and Hases (Fe, Ni and Se) on H_2

production was evaluated by supplementing the medium with 0.1 µM of either sodium molybdate (VI) or sodium tungstate, and 1 µM nickel chloride or 1 µM of both nickel chloride and sodium selenite. The iron content in the medium was 25 µM. Batch experiments were carried out at 37 ˚C using 120 mL serum bottles with a working volume of 20 mL and N_2 as gas headspace. A 10 % (v/v) inoculum was used in all experiments. To monitor H_2 production 30 µL of gas phase were analyzed by GC, and to monitor cell growth 1 mL of liquid sample was collected. The H_2 production rates were calculated taking into account the actual volume at each time point.

3.2.3 H_2 PRODUCTION IN A BIOREACTOR WITH GAS SPARGING

The bioreactor assays were carried out in a conventional Biostat A Plus system (Sartorius Stedim, Göttingen, Germany) with a 3 L vessel, as previously described [16]. The reactor was operated with a working volume of 1.5 L, stirring rate of 50 rpm, a N_2 flow rate of 115 mL min^{-1} and a temperature of 37 ˚C. The gas outlet was equipped with two H_2S traps in series containing zinc acetate (0.9 M) buffered with glacial acetic acid to pH 4, followed by a H_2 sensor (BlueSens gas sensor, Herten, Germany) for online monitoring of H_2. The H_2 data were recorded every 5 s by the BioPat®MFC fermentation software (Sartorius Stedim, Göttingen, Germany). The medium used for the experiments was the one described for H_2 production in serum bottles with a few modifications: 80 mM sodium formate, 20 mM sodium acetate, 200 mM

MOPS buffer, 1 µM nickel chloride, 1 µM sodium selenite and 0.1 µM sodium tungstate. A 10 % (v/v) inoculum was used for bioreactor startup.

3.2.4 ANALYTICAL METHODS

Cell growth was monitored by measuring optical density at 600 nm (OD_{600}) with a Shimadzu UV/Vis spectrophotometer. Biomass was determined by measuring the OD_{600}, which was previously correlated with dry cell weight (dcw). One unit value of OD_{600} corresponded to 0.31 g_{dcw} L^{-1} for *D. vulgaris* and 0.37 g_{dcw} L^{-1} for *D. gigas* [11,26]. Sulfate concentration was determined by UV/Vis spectrophotometry using a modified SulfaVer®4 method (Hach-Lange). The SulfaVer®4 reagent was dissolved in 10 mL of H_2O, and the sulfate concentration was determined by mixing 1 mL of SulfaVer®4 solution with 100 µL of filtered sample. After 10 min the turbidity was measured at 450 nm. The detection limit of this method is 0.2 mM sulfate. The H_2 content in the headspace of the serum bottles was determined using a Trace GC 2000 gas chromatograph (Thermo Corporation) equipped with a MolSieve 5A 80/100 column (Althech) and a thermal conductivity detector (TCD). Nitrogen was used as carrier gas at a flow rate of 10 mL min^{-1}. The specific H_2 production rate (mL g_{dcw}^{-1} h^{-1}) was calculated by dividing the maximum volumetric H_2 production rate (mL L^{-1} h^{-1}) by the maximum biomass concentration (dry cell weight) reached.

3.2.5 HASE ACTIVITY-STAINED NATIVE GELS

Analysis of the Hases was also performed with native gels stained for Hase activity, using crude cell extracts as previously described [31]. Briefly, crude cell extracts were obtained by cell disruption using the BugBuster Plus Lysonase™ Kit (Novagen) according to the manufacturer's instructions. The extracts (5 µg protein) were run in 7.5 % (w/v) polyacrylamide gels containing 0.1 % (v/v) Triton X-100. The gels were incubated in a solution of 50 mM Tris-HCl (pH 7.6), 0.5 mM methyl viologen under a H_2 atmosphere and after development, the bands were fixed with 10 mM 2,3,5-triphenyltetrazolium chloride solution.

3.2.6 STATISTICAL ANALYSIS

Experiments were carried out at least in triplicate and all values are expressed as means ± standard deviation. The production of H_2 by different strains was analyzed using a one-way analysis of variance (ANOVA) and the multiple comparative pairwise Holm-Sidak tests (confidence of 95 %). The statistical analyses were performed with SigmaStat 3.0 and a *p*-value less than 0.05 was considered statistically significant.

3.3 RESULTS

3.3.1 H_2 PRODUCTION BY DIFFERENT *DESULFOVIBRIO* SPECIES

The H_2 production from formate by five *Desulfovibrio* species having different Hase and FDH compositions (*D. vulgaris* Hildenborough, *D. gigas*, *D. alaskensis* G20, *D. desulfuricans* ATCC 27774 and *D. fructosivorans*) was evaluated in two conditions (Figure 3.1): in the presence of Mo or W. These two FDH metal cofactors have been shown to regulate the expression of these enzymes [23]. A limiting sulfate concentration is initially present, as this condition has been shown to enhance H_2 production after sulfate consumption [11]. This was slightly higher for *D. gigas* due to carry-over sulfate from the inoculum. During the initial phase of sulfate reduction a similar increase in cell mass was observed for all strains and growth conditions. The production of H_2 started after sulfate was depleted and all strains were able to produce H_2, although in variable amounts. In the presence of Mo (Figure 3.1a), the highest H_2 production was achieved by *D. vulgaris* and *D. desulfuricans* reaching the maximum values of 735 and 800 mL L_{medium}^{-1}, respectively. In contrast, a low H_2 production (approximately 300 mL L_{medium}^{-1}) was observed for both *D. fructosivorans* and *D. gigas*, whereas 526 mL L_{medium}^{-1} of H_2 were produced by *D. alaskensis*. When Mo was replaced by W an improvement in H_2 production was observed for all strains except for *D. desulfuricans*, where it was reduced from 800 to 220 mL L_{medium}^{-1} of H_2. The highest H_2 production in the presence

of W was achieved by *D. vulgaris*, followed by *D. alaskensis*, *D. fructosivorans* and *D. gigas* producing 865, 660, 448 and 374 mL L_{medium}^{-1} of H_2, respectively. Both *D. vulgaris* and *D. gigas* are genetically tractable and FDH and Hase deletion mutants have been produced [18,26,29,30]. Since these two organisms present quite distinct H_2 production capacities and have different Hase and FDH compositions, we used these mutants to investigate the electron transfer pathways involved in formate conversion to H_2.

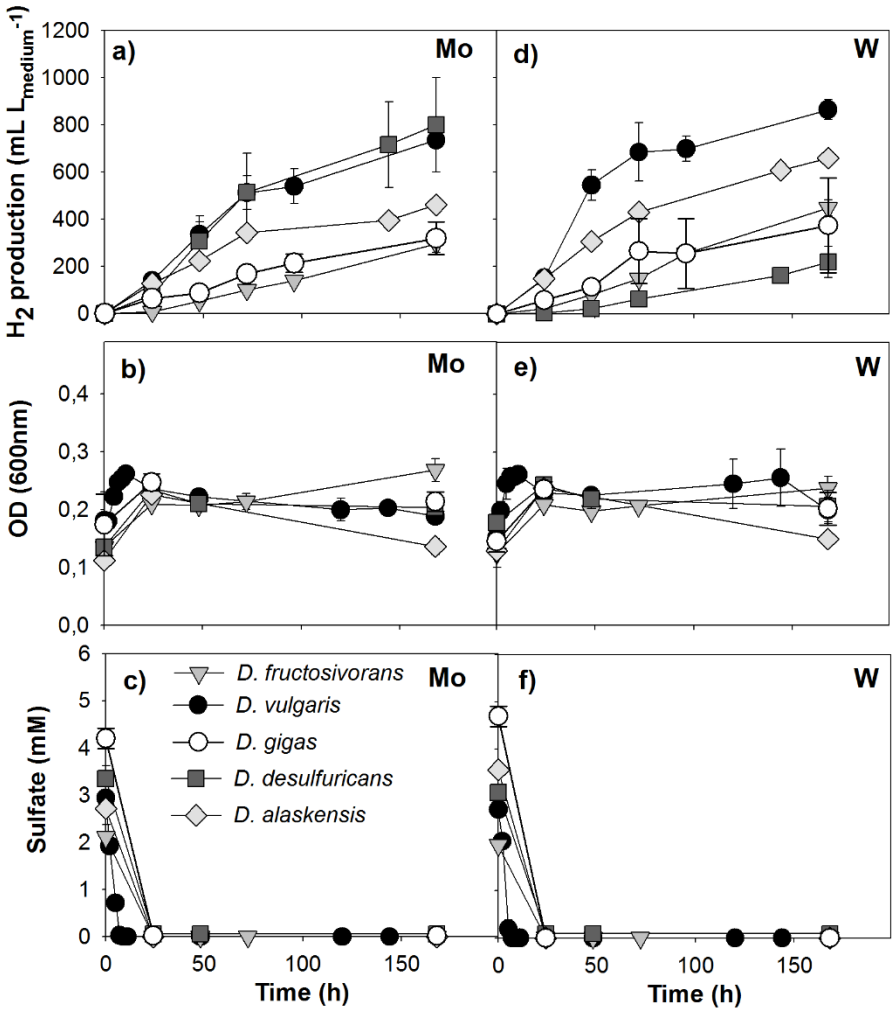

Figure 3.1. Profiles of H_2 production (a and d), cell growth (b and e), and sulfate consumption (c and f) of five *Desulfovibrio* strains in the presence of 40 mM formate and 0.1 µM Mo (left) or 0.1µMW (right). The error bars indicate the standard deviation of triplicate cultures.

3.3.2 EFFECT OF FDH INACTIVATION ON H_2 PRODUCTION BY *D. VULGARIS*

The production of H_2 from formate by *D. vulgaris* mutants of the two main FDHs (Δ*fdhABC*$_3$ and Δ*fdhAB*) was compared with the wild-type strain to investigate the role of each FDH in this metabolic pathway (Figure 3.2). During the initial phase of sulfate reduction there is some growth, reaching a maximum OD_{600} of 0.25 ± 0.01 (initial OD_{600}=0.15), independently of strain and growth condition (Table 3.2). The production of H_2 was differently affected by deletion of each FDH. In the presence of Mo (Figure 3.2a), the production of H_2 by the Δ*fdhABC*$_3$ strain was similar to the wild-type strain achieving the maximum value of 690 and 740 mL L_{medium}^{-1}, respectively, with a H_2 production rate of 90 mL g_{dcw}^{-1} h^{-1} for both. In contrast, the amount of H_2 produced by the Δ*fdhAB* strain was strongly decreased (160 mL L_{medium}^{-1} with a production rate of 22 mL g_{dcw}^{-1} h^{-1}). In the presence of W (Figure 3.2c) a higher H_2 production was observed for both the wild-type and Δ*fdhABC*$_3$ strains, reaching a production of 870 and 740 mL L_{medium}^{-1}, respectively, corresponding to a H_2 production rate of 140 mL g_{dcw}^{-1} h^{-1} for both. The H_2 production by the Δ*fdhAB* strain was negligible in this growth condition.

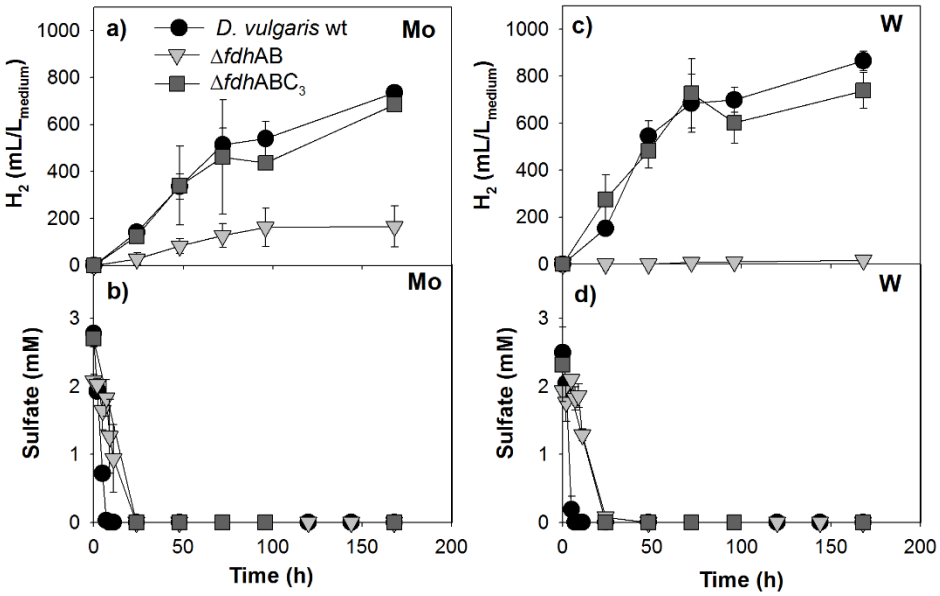

Figure 3.2. Hydrogen production (a and c) and sulfate consumption (b and d) by *D. vulgaris* wild-type and FDH mutants in the presence of 40 mM formate, Fe, Ni, and Se. The medium was supplemented with 0.1 µM Mo (a and b) or 0.1 µM W (c and d). The error bars indicate the standard deviations of triplicate cultures.

3.3.3 Effect of HASE inactivation on H_2 production by *D. vulgaris*

The H_2 production by *D. vulgaris* wild-type and Hase mutants was studied in the presence of W, while varying the metals that affect the expression of Hases, resulting in three conditions: addition of only Fe, Fe plus Ni and Fe plus Ni and Se (Figure 3.3). The *D. vulgaris* mutants *Δhyd, Δhyn1, Δhyn2*, Δ*hys,* Δ*coo*, Δ*ech* and the double mutants Δ*hyd*Δ*hyn2* and Δ*coo*Δ*ech* were investigated.

Similar growth was observed for all strains during the initial stage of sulfate reduction, independently of the medium composition (Table 3.2). In the presence of only Fe (Figure 3.3a), the Δ*hys* and Δ*hyn2* strains showed similar behavior to the wild-type strain producing 650 mL L_{medium}^{-1} of H_2 with a production rate of 70 mL g_{dcw}^{-1} h^{-1}. The H_2 production by the single mutants *Δhyd* and *Δhyn1* was similar to the wild-type strain (data not shown), while the double mutant (*ΔhydΔhyn1)* showed a slightly reduced H_2 production of 425 mL L_{medium}^{-1}, which is still not statistically different to that observed with the wild-type strain (p=0.064). In this condition the mutants of the energy-conserving Ech and Coo cytoplasmic Hases showed a similar behavior to the respective parental strain, JW710 (Figure 3.3d), producing approximately 600 mL L_{medium}^{-1} of H_2.

In the presence of Fe and Ni, the Δ*hyn*2 strain showed a higher H_2 production than the wild-type (850 mL L^{-1}_{medium}, an increase of 26%, corresponding to a production rate of 177 mL g_{dcw}^{-1} h^{-1}) (Figure 3.3b). In this condition, the *D. vulgaris* wild-type strain produced 664 mL L_{medium}^{-1} at a maximum production rate of 70 mL g_{dcw}^{-1} h^{-1}, while the Δ*hys* and Δ*hyd*Δ*hyn1* strains produced 560 mL L_{medium}^{-1} at 62 mL g_{dcw}^{-1} h^{-1} and 538 mL L_{medium}^{-1} with a production rate of 69 mL g_{dcw}^{-1} h^{-1}, respectively. The H_2 production observed by these mutants is not statistically different from the wild-type strain. The single mutants *Δhyd* and *Δhyn1* showed a similar H_2 production profile to the wild-type strain (data not shown). In this condition, the parental JW710 strain had a slightly reduced H_2 production versus the Fe condition, whereas the three cytoplasmic Hase mutant strains had a slightly higher H_2 production (Figure 3.3e). The parental strain produced 448 mL L_{medium}^{-1} at 81 mL g_{dcw}^{-1} h^{-1}, while the Δ*ech* strain

produced 677 mL L_{medium}^{-1} at 78 mL g_{dcw}^{-1} h^{-1}, the Δ*coo* strain, produced 745 mL L_{medium}^{-1} at 105 mL g_{dcw}^{-1} h^{-1} and the Δ*coo*Δ*ech* strain produced 657 mL L_{medium}^{-1} with a production rate of 81 mL g_{dcw}^{-1} h^{-1}.

In the presence of Fe, Ni and Se (Figure 3.3c), the wild-type *D. vulgaris* showed a higher H_2 productivity than in the previous conditions, with 850 mL L_{medium}^{-1} of H_2 at 150 mL g_{dcw}^{-1} h^{-1}. The Δ*hyn2* and Δ*hyd*Δ*hyn1* strains showed similar H_2 production profile to the wild-type strain, while the Δ*hys* strain had a lower performance. This strain produced only 600 mL L_{medium}^{-1} in this condition (30 % less than the wild-type) with a rate of 108 mL g_{dcw}^{-1} h^{-1}. In this condition all mutants of the cytoplasmic Hases showed a similar behavior to the respective parental strain, JW710 (Figure 3.3f), producing approximately 850 mL L_{medium}^{-1} of H_2.

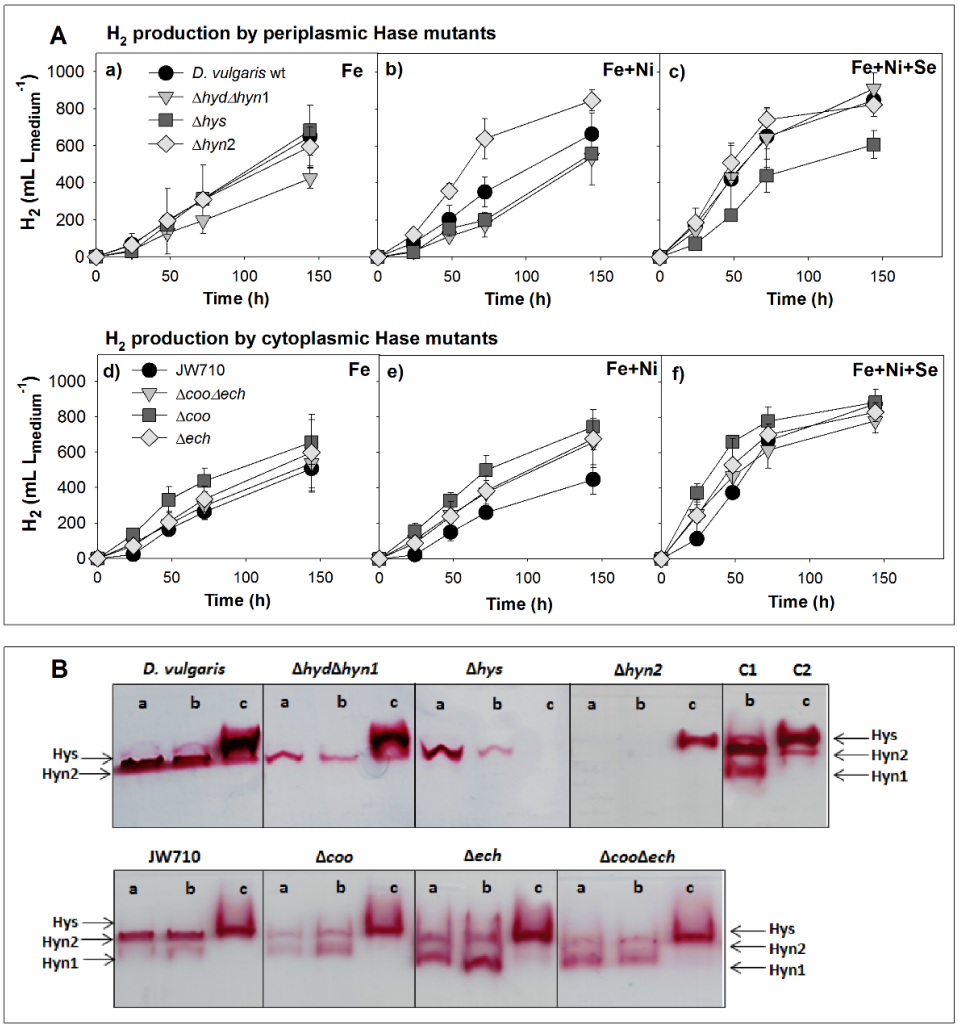

Figure 3.3. Profiles of H_2 production (A) and activity-stained native gels of crude cell extracts (B) of *D. vulgaris* wild-type and Hase mutants in the presence of 40 mM formate and W. A) Cells grown in the presence of only Fe (a and d), Fe and Ni (b and e), and Fe, Ni, and Se (c and f). The error bars indicate the standard deviations of three or six independent cultures. B) Cell extracts were prepared after 6 days of incubation in medium containing Fe (lanes a), Fe and Ni (lanes b), and Fe, Ni, and Se (lanes c). C1, *D. vulgaris* control from cells grown with formate and sulfate, Fe and Ni (contains Hyn1 and Hyn2 Hases); C2, *D. vulgaris* control from cells grown with formate and sulfate, Fe, Ni, and Se (contains Hys Hase).

3.3.4 ANALYSIS OF *D. VULGARIS* HASES BY ACTIVITY-STAINED GELS

Cells of *D. vulgaris* wild type and Hase mutant strains were collected after the experiments described above and cell extracts were analyzed to investigate the relative activity of Hases by activity-stained native gels, where the periplasmic Hases can be detected (Figure 3.3b). In this assay, the membrane-bound cytoplasmic Hases are not usually detected [31], either due to instability or a low expression level. For the *D. vulgaris* wild-type cells incubated with formate in the presence of Fe or Fe plus Ni (Figure 3.3b, lanes a and b), only the HynAB-2 Hase was detected, while the Hys Hase was the major Hase present when Se was also included (lane c). In contrast, in *D. vulgaris* cells grown in respiratory formate/sulfate conditions with Fe and Ni, both the HynAB-1 and HynAB-2 Hases are detected. The Hys Hase was the main Hase observed in cell extracts of all mutant strains grown in the presence of Fe, Ni and Se (lanes c), except obviously for the Δ*hys* strain, where no Hase activity band was observed. In the presence of Fe and Fe plus Ni, HynAB-2 was the main Hase detected for the cell extracts of all mutant strains, as observed for the wild-type strain, except also for the Δ*hyn2* strain, where no Hase activity band was detected (lanes a and b).

Also, in cell extracts of the JW710 strain incubated with formate in the presence of Fe and Fe plus Ni, HynAB-2 is the major Hase present (with HynAB-1 detected with lower activity); whereas, when Se is included, Hys is again the single Hase observed (Figure 3.3b). The cytoplasmic Hase mutant strains (Δ*coo,* Δ*ech* and Δ*coo*Δ*ech*) all showed a similar profile to JW710, but with an

increased activity of the HynAB-1 versus the HynAB-2 Hase, particularly in the case of the Δ*ech* and Δ*coo*Δ*ech* strains.

3.3.5 EFFECT OF HASE INACTIVATION ON H_2 PRODUCTION BY *D. GIGAS*

The H_2 production of *D. gigas* wild-type and single mutants was also studied (Figure 3.4). In this organism there are no [FeFe] or [NiFeSe] Hases, so only the Fe plus Ni condition was studied. Similarly to *D. vulgaris*, H_2 production started after sulfate was depleted and growth was only observed during sulfate reduction, reaching an OD_{600} of 0.22 ± 0.01 (Table 3.2). The Δ*ech* strain showed similar H_2 productivity to the wild type (448 mL L_{medium}^{-1} at 59 mL g_{dcw}^{-1} h^{-1} for the Δ*ech* strain and 356 mL L_{medium}^{-1} at 56 mL g_{dcw}^{-1} h^{-1} for *D. gigas* wild-type). In marked contrast, no H_2 production was detected for the Δ*hyn* strain.

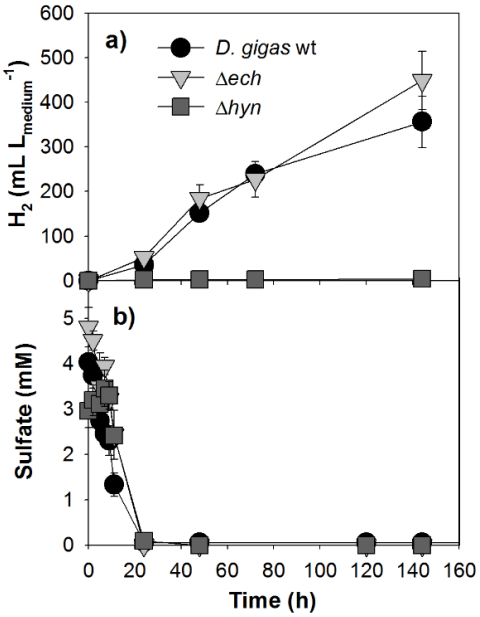

Figure 3.4. Hydrogen production (a) and sulfate consumption (b) by *D.gigas* wild-type and Hase mutants (Δ*ech* and Δ*hyn*) in the presence of 40 mM formate, Fe, Ni, and W. The error bars indicate the standard deviations of triplicate cultures.

Table 3.2. Growth of *D. vulgaris* and *D. gigas* strains used in the study.

Strains		Growth conditions				
			Tungsten		Molybdenum	
	OD_{600nm}[a)]	Fe	Fe + Ni	Fe + Ni + Se	Fe + Ni	Fe + Ni + Se
D. vulgaris						
Wild-type	Initial	0.16 ± 0.00	0.16 ± 0.01	0.15 ± 0.01		0.13 ± 0.00
	Maximum	0.22 ± 0.00	0.23 ± 0.00	0.24 ± 0.01		0.25 ± 0.01
Δ*hyd/hyn1*	Initial	0.17 ± 0.00	0.17 ± 0.01	0.16 ± 0.00		
	Maximum	0.18 ± 0.01	0.19 ± 0.00	0.20 ± 0.01		
Δ*hys*	Initial	0.17 ± 0.00	0.18 ± 0.04	0.18 ± 0.01		
	Maximum	0.23 ± 0.01	0.23 ± 0.01	0.23 ± 0.00		
Δ*hyn2*	Initial	0.14 ± 0.01	0.14 ± 0.00	0.14 ± 0.01		
	Maximum	0.18 ± 0.01	0.20 ± 0.01	0.20 ± 0.00		
JW *D. vulgaris*	Initial	0.16 ± 0.00	0.16 ± 0.01	0.16 ± 0.01		
	Maximum	0.20 ± 0.00	0.20 ± 0.00	0.21 ± 0.01		
Δ*ech*	Initial	0.15 ± 0.03	0.14 ± 0.01	0.14 ± 0.01		
	Maximum	0.20 ± 0.00	0.21 ± 0.01	0.22 ± 0.01		
Δ*coo*	Initial	0.15 ± 0.02	0.16 ± 0.03	0.15 ± 0.01		
	Maximum	0.20 ± 0.01	0.22 ± 0.01	0.21 ± 0.01		
Δ*coo/ech*	Initial	0.14 ± 0.01	0.16 ± 0.01	0.15 ± 0.01		
	Maximum	0.19 ± 0.00	0.20 ± 0.01	0.19 ± 0.02		
Δ*fdhAB*	Initial			0.15 ± 0.03		0.14 ± 0.02
	Maximum			0.25 ± 0.01		0.26 ± 0.01
Δ*fdhABC*$_3$	Initial			0.15 ± 0.01		0.13 ± 0.00
	Maximum			0.24 ± 0.01		0.25 ± 0.01
D. gigas						
Wild-type	Initial		0.15 ± 0.01			
	Maximum		0.21 ± 0.01			
Δ*ech*	Initial		0.20 ± 0.03			
	Maximum		0.23 ± 0.02			
Δ*hyn*	Initial		0.15 ± 0.01			
	Maximum		0.20 ± 0.02			

[a)] The values are the average at least of triplicate cultures.

3.3.6 GROWTH OF *D. VULGARIS* MUTANTS BY FORMATE TO H_2 CONVERSION

Recently, we showed that gas sparging enabled the growth of *D. vulgaris* coupled with the conversion of formate to H_2 in the absence of sulfate or syntrophic partner [16]. Sparging maintains a low P_{H2} in the liquid phase replacing the H_2 consuming syntrophic partner. Thus, the same approach was used in the present work to investigate if the Δ*hys*, Δ*ech,* Δ*coo* and Δ*coo*Δ*ech* strains are able to grow by the conversion of formate to H_2 and bicarbonate in the presence of Fe, Ni and Se. The parental JW710 and JW710-derived strains lacking the cytoplasmic Hases were more sensitive to the bioreactor conditions (to continuous gas sparging and/or stirring), even when grown in presence of sulfate. The studies showed that although all mutants were able to produce H_2 (as observed in serum bottles), only the Δ*hys* and Δ*ech* strains were able to grow by the conversion of formate to H_2 and bicarbonate, as revealed by the continued increase in OD after sulfate is depleted (Figure 3.5). These results suggest that the cytoplasmic Coo Hase (and not Ech) may be essential to allow energy conservation in the oxidation of formate to H_2, which would agree with the work of Walker and colleagues who demonstrated that this Hase is essential for syntrophic growth of *D. vulgaris* with *Methanococcus maripaludis* on lactate [13]. However, since the parental strain JW710 had an erratic behavior in the bioreactor conditions (even in presence of sulfate), some caution is required in interpreting the absence of growth of the Δ*coo* and Δ*coo*Δ*ech* strains, preventing a definite conclusion on the requirement of the Coo Hase.

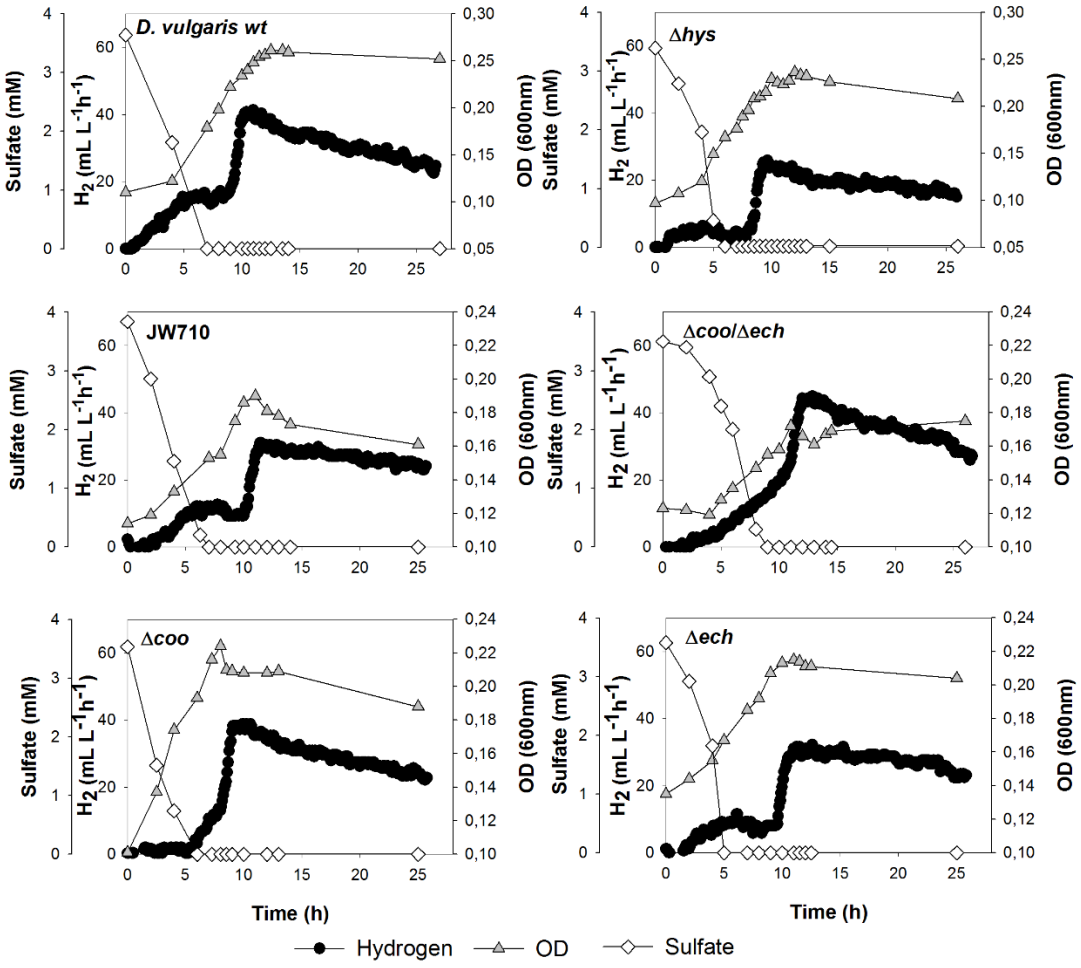

Figure 3.5. Growth and H_2 production profiles of strains *D. vulgaris* wt, JW710, Δ*hys*, Δ*ech*, Δ*coo*, and Δ*coo*Δ*ech* in a bioreactor with gas sparging. The reactor was fed with medium containing 80 mM formate, Fe, Ni, Se, and W and operated with a nitrogen flow rate of 115 mL min^{-1}. The production of H_2 is expressed as H_2 production rate (mL L^{-1} h^{-1}), and not total H_2 produced as in previous figures.

3.4 DISCUSSION

FDHs catalyze the reversible oxidation of formate to carbon dioxide (equation 3.1), and in the absence of sulfate the resulting reducing equivalents may be transferred to Hases, which reduce protons to molecular H_2 (equation 3.2).

$$HCOO^- \overset{FDH}{\leftrightarrow} CO_2 + 2e^- + H^+ \qquad \text{(equation 3.1)}$$

$$H^+ + 2e^- \overset{Hase}{\leftrightarrow} H_2 \qquad \text{(equation 3.2)}$$

The most common FDHs in anaerobic microorganisms are the Mo or W pterin containing enzymes [32,33], which in *Desulfovibrio* are differentially regulated by the availability of these metals [23,32–34]. In addition, FDHs can be cytoplasmic or periplasmic and the cellular localization is usually related to their physiological function [32,33]. Periplasmic FDHs are mostly involved in the oxidation of formate, while the cytoplasmic FDHs usually work as CO_2 reductases [32,33]. In *Deltaproteobacteria* SRB, namely in *Desulfovibrio* spp. the majority of the periplasmic Hases and FDHs are soluble, in contrast to most other bacteria, and share the same soluble electron acceptor, the Type I cytochrome c_3 [35,36]. This unique situation means there is a possible direct link between periplasmic FDHs and Hases through this cytochrome, which may lead to direct periplasmic H_2 production from formate.

Comparing the different *Desulfovibrio* strains, *D. desulfuricans* and *D. vulgaris* showed similar high H_2-production capacity in the presence of Mo (800 and

735 mL L_{medium}^{-1} of H_2, respectively). However, when Mo was replaced by W the production of H_2 by *D. desulfuricans* was 70% reduced (220 mL L_{medium}^{-1}), whereas the opposite effect was observed for the other species. Analysis of the *D. desulfuricans* genome indicates the presence of two periplasmic FDHs (Table 3.3), one of which was characterized as a Mo-containing enzyme [37]. The reduced H_2 production in the presence of W indicates that this metal functions as an antagonist for one of the FDHs, and that a W-binding enzyme is probably not present. The highest H_2 production in the presence of W was observed for *D. vulgaris* followed by *D. alaskensis*. Analysis of the *D. alaskensis* genome reveals the presence of three periplasmic FDHs (Table 3.3). Two of them have been characterized, one of which was found to be a W-FDH, while the other was shown to incorporate either Mo or W [34,38]. These enzymes are probably responsible for the slight improvement of H_2 production by *D. alaskensis* when Mo was replaced by W (526 and 660 mL L_{medium}^{-1} of H_2 were produced in the presence of Mo and W, respectively). In the case of *D. vulgaris,* although the genome indicates the presence of three periplasmic FDHs, only the two soluble enzymes are detected [23]. One of them is a Mo-Fdh ($FdhABC_3$, DVU2809-11), whereas the other (FdhAB, DVU0587-88) can incorporate either Mo or W, like the enzyme from *D. alaskensis* [23]. The results observed with the *D. vulgaris* FDH mutants demonstrate that FdhAB is the main enzyme involved in formate oxidation, in the presence of either Mo or W. Similar results were observed in reverse conditions where H_2 was converted to formate [29], revealing that in *D. vulgaris* FdhAB is the key enzyme in formate metabolism in the absence of sulfate.

D. fructosivorans and *D. gigas* showed similar H_2 production profiles: both produced 300 mL L_{medium}^{-1} of H_2 in the presence of Mo, and this value was slightly increased to approximately 400 mL L_{medium}^{-1} when Mo was replaced by W. The genome of both strains indicates the presence of two periplasmic FDHs [25] (Table 3.3). A W-containing *D. gigas* FDH has already been isolated and characterized [39], and is probably involved in H_2 production in the presence of W. To our knowledge none of the *D. fructosivorans* FDHs has been isolated or characterized, but the increase in H_2 production when Mo was replaced by W suggests the presence of a W-binding enzyme.

Among all the organisms tested, *D. vulgaris* showed the highest H_2-production capacity while *D. gigas* was one of the species with the lowest H_2 production from formate. A similar behavior was observed for the two organisms with lactate as electron donor in sulfate limiting conditions [40]. These two organisms are quite distinct in terms of number, type and localization of Hases (Table 3.3), which is probably linked to the different performances of H_2 production. Only *D. vulgaris* possesses a Hys Hase, which has been shown to have a very high H_2-production activity (6,900 U $mg_{protein}^{-1}$) and some degree of oxygen tolerance [31,41,42], whereas, *D. gigas* HynAB-1 has a specify activity for H_2 production of only 440 U mg $_{protein}^{-1}$ [42,43]. In order to understand the electron transfer pathways involved in formate-driven H_2 production by *D. vulgaris* and *D. gigas,* H_2 production by mutant strains lacking genes for Hases was compared with wild-type strains.

Table 3.3. Comparative analysis of FDH and Hase distribution in the SRB genomes [12,25].

FDHs	Periplasmic			Cytoplasmic	
	Soluble		Membrane associated	FHL	others
	FDHAB	$FDHABC_3$	FDHABD		
Desulfovibrio vulgaris Hildenborough	1	1	1	-	-
Desulfovibrio desulfuricans ATCC 27774	-	1	1	-	1
Desulfovibrio alaskensis G20	3	-	-	1	-
Desulfovibrio fructosivorans	2	-	-	-	1
Desulfovibrio gigas	2	-	-	-	-

Hases	Periplasmic					Cytoplasmic					
	[NiFe]			[NiFeSe]	[FeFe]	[NiFe]		[FeFe]			
	HynAB	HynABC	$HynABC_3$	HysAB	HydAB	Ech	Coo	$[FeFe]_{bif}$	$[FeFe]_{mon}$	FHL	HsfB
Desulfovibrio vulgaris Hildenborough	1	-	1	1	1	1	1	1	-	-	-
Desulfovibrio desulfuricans ATCC 27774	1	1	-	-	1	1	1	-	-	-	-
Desulfovibrio alaskensis G20	1	-	1	1	1	-	-	-	1	1	-
Desulfovibrio fructosivorans	1	-	-	-	1	1	-	2	-	-	1
Desulfovibrio gigas	1	-	-	-	-	1	-	-	-	-	-

$[FeFe]_{bif}$, cytoplasmic NAD(P)-dependent Hases; $[FeFe]_{mon}$, monomeric Fd-dependent Hases

The *D. vulgaris* Hases have distinct kinetic properties and expression conditions [18,31,43]. They are differently regulated by H_2 levels [18] and the metals Ni and Se [31]. In a previous study, we reported that a periplasmic [NiFe] Hase was involved in H_2 production from formate in the absence of Se (with only Fe or Fe and Ni), while the periplasmic [NiFeSe] was the main Hase involved in the presence of Fe, Ni and Se [11]. While similar results were observed here for the wild-type, the present work demonstrates that each of these Hases is not essential for formate-driven H_2 production since the respective deletion strains are still able to produce H_2. This suggests a high level of functional redundancy, with multiple Hases being involved in H_2 production, and/or that deletion of one enzyme is compensated by the action of remaining one(s) by redirection of electron flow. Thus, the high redundancy of Hases in *D. vulgaris*, and their apparent functional overlap makes it very difficult to understand the specific role of each enzyme in H_2 production from formate. A similar situation was observed for *D. alaskensis* strain G20 during syntrophic growth on lactate, where the Hyn [NiFe] Hase was also reported to be the main enzyme responsible for H_2 production, but, the growth of the Δ*hyn* strain in co-culture was similar to the reference strain indicating compensation by the other periplasmic Hases [20].

Although no specific Hases were identified as crucial for formate-driven H_2 production by *D. vulgaris*, the present work suggests that both periplasmic and cytoplasmic Hases may be involved in this metabolism. Interestingly, in the condition where Fe and Ni are present, a higher H_2 production than the wild-type was observed for the Δ*hyn*2 strain. This suggests that HynAB-2 may operate in H_2 oxidation, since its absence leads to higher H_2 levels when

compared to the wild-type strain. Since in this condition no periplasmic Hase is detected in this mutant, the production of H_2 may be taking place mostly in the cytoplasm, and this then diffuses to the periplasm and to outside the cell. The oxidation of H_2 by HynAB-2 indicates that this Hase may be able to recycle H_2 in the cell to avoid loss of reducing power.

In addition, the study of the cytoplasmic-facing energy-conserving Hases gave no clear results regarding an essential role of any of these enzymes in the process. This suggests that the periplasmic enzymes can easily compensate for the absence of Ech or Coo Hases. In fact, both HynAB-1 and HynAB-2 Hases are detected in the activity-stained gels with an increased expression of the HynAB-1 Hase relative to the mutants of the periplasmic Hases. So, in cells that lack the cytoplasmic Hases, the electrons from formate oxidation are probably transferred only to the periplasmic Hases (HynAB-1, HynAB-2 and Hys). Using a direct periplasmic pathway, the cells can dispose the excess reducing power without energy conservation.

When Se is available the Hys Hase is highly expressed and there is a downregulation of other Hases, as reported previously for respiratory conditions [31]. The presence of Se results in the highest H_2 production (850 mL L_{medium}^{-1}) for the wild-type, and a significant decrease is observed for the Δ*hys* strain (600 mL L_{medium}^{-1}, 30% less than wild-type), whereas all other mutant strains showed similar H_2 production profile to the wild-type. This indicates that in the presence of Se the Hys Hase has a significant role in H_2 production. Recently, the Hys Hase was shown to be required for formate oxidation during sulfate respiration by *D. alaskensis* G20 in the presence of Se [17], suggesting the conversion of formate to H_2 is essential for growth on

formate/sulfate. Although no periplasmic Hases were detected in the activity stained gels of Δ*hys* cells, this mutant retains a considerable capacity to produce H_2, suggesting a considerable involvement of cytoplasmic Hases in H_2 production in this condition. Thus, the overall results point to the ability of *D. vulgaris* periplasmic and cytoplasmic Hases to act bidirectionally and with a high degree of functional overlap.

The recent finding that *D. vulgaris* can show some limited growth by the conversion of formate to H_2 was rather unexpected [16], and indicates that this process can be coupled to energy conservation. Direct electron transfer from the periplasmic FDHs to the periplasmic Hases via the Type I cytochrome c_3 would not allow for energy conservation, so an alternative pathway has to be present. We propose that formate is oxidized in the periplasm by FdhAB, and that the generated electrons are transferred, through the Type I cytochrome c_3, part to periplasmic Hases producing H_2 (mostly the Hys Hase when Se is present) and part to membrane-bound electron transfer complexes (METC), probably Qrc or Tmc [44–46] (Figure 3.6a). Through a still unidentified pathway the electrons crossing the membrane can probably lead to reduction of ferredoxin in the cytoplasm, which can be oxidized by one of the energy-conserving Hases contributing to H_2 production in an electrogenic process. The reduction of ferredoxin by H_2 is an endergonic process, and can only occur if the P_{H2} inside the cell is high enough for the process to become favourable, or if flavin-based electron bifurcation is involved [47]. Interestingly, *D. vulgaris* has a cytoplasmic [FeFe] Hase that may be capable of electron bifurcation, as its gene is adjacent to one coding for a pyridine dinucleotide-disulfide oxidoreductase, which may use NAD(P)H as cofactor. So, some proportion of

reducing power derived from formate may be used to (i) either reduce ferredoxin directly or (ii) produce NADH, which coupled with H_2 present inside the cell can lead to reduction of ferredoxin via electron bifurcation. The bioreactor experiments with the *D. vulgaris* mutants suggest that in these conditions, the cytoplasmic Hase responsible for ferredoxin oxidation coupled with energy conservation is the Coo Hase, given the observed growth of the Δ*ech* strain after sulfate is depleted (from 5 to 10 h) and absence of growth of the Δ*coo* strain once sulfate has been consumed. However, the variable response of the reference strain JW710 in the bioreactor prevents definite conclusions on the negative growth of the Δ*coo* strain. Nevertheless, this model is supported by the observation that the Coo Hase is essential for syntrophic growth of *D. vulgaris* with a methanogen on lactate [13], indicating its role in H_2 production also in this fermentative-type metabolism. Further experiments will be required to clarify this point.

In contrast to *D. vulgaris*, only two [NiFe] Hases are presented in *D. gigas*: the energy conserving Ech and the periplasmic HynAB-1 [25,26], making it a simple model to study the role of each Hase on H_2 production. The present work demonstrates that HynAB-1 is the only *D. gigas* Hase involved in H_2 production from formate, since the amount of H_2 produced by the Δ*hyn* strain was negligible and the production of H_2 by the Δ*ech* strain was similar to the wild-type strain. A similar result was observed for pyruvate fermentation by *D. gigas*, where the cells lacking HynAB-1 were unable to produce H_2 [26]. We could not test growth of *D. gigas* in the bioreactor by converting formate to H_2, because the wild-type strain did not grow, even in the presence of sulfate, when sparging was applied. Nevertheless, the results suggest that growth

would not be possible for this organism, as only the periplasmic HynAB-1 Hase is essential for H_2 production from formate.

In conclusion, *D. vulgaris* has two apparent pathways for H_2 production from formate: a direct one only involving periplasmic enzymes, and another that involves transmembrane electron transfer and allows for energy conservation. In contrast, in *D. gigas* the electron transfer pathway occurs exclusively in the periplasm (Figure 3.6b) and formate is converted to H_2 without energy conservation. It seems likely that the presence of a high number of hydrogenases in *D. vulgaris*, with a capacity for functional redundancy, will confer an added advantage to this organism when faced with limitation or competition for nutrients and trace elements. This work demonstrates that the electron transfer mechanism involved in H_2 production from formate differs among *Desulfovibrio* strains.

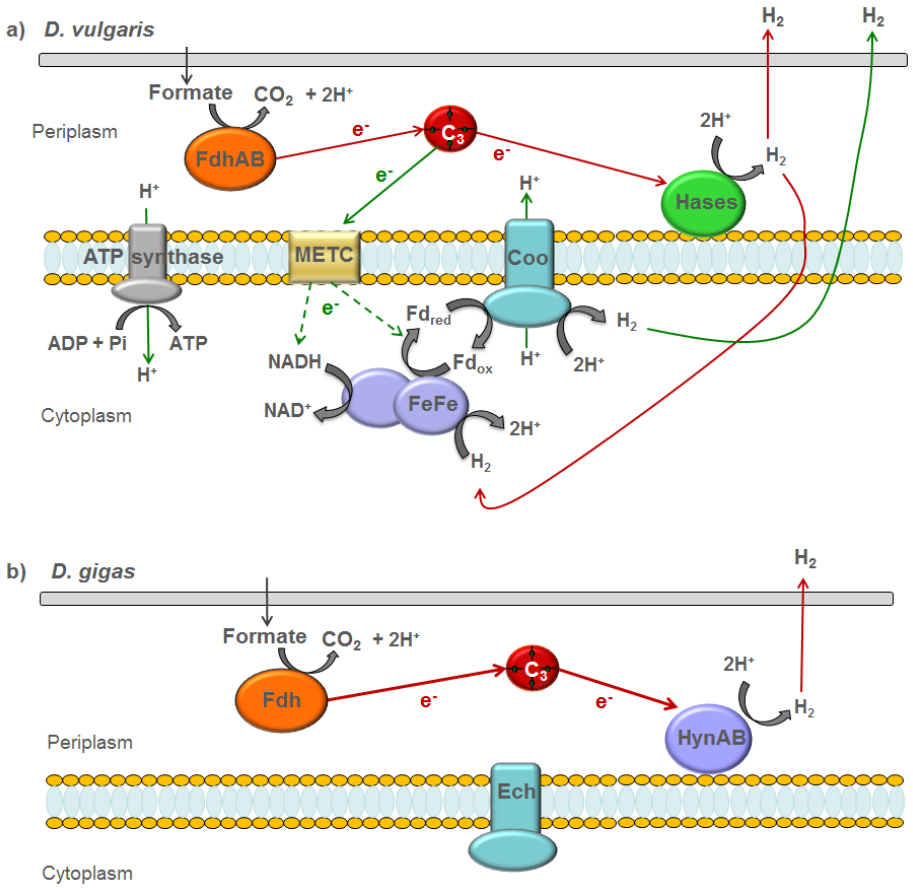

Figure 3.6. Proposed electron transfer pathways for formate-driven H_2 production, in the absence of sulfate, by *D. vulgaris* (a) and *D. gigas* (b). In *D. vulgaris*, two pathways can be involved in H_2 production: a direct one involving only periplasmic enzymes (red arrows), and a second one that involves transmembrane electron transfer and allows for energy conservation (green arrows). The relative weight of the two pathways is not known, so the stoichiometry of the reactions and the percentage of electrons transferred to each pathway are not considered in the figure. For the sake of simplicity, a single periplasmic Hase is depicted. In *D. gigas*, only the direct periplasmic pathway operates. Fdh formate dehydrogenase, Hase hydrogenase, Fd ferredoxin, c3 type I cytochrome c3, METC membrane-bound electron transfer complexes, Coo cytoplasmic [NiFe] Coo hydrogenase, Ech cytoplasmic [NiFe] Ech hydrogenase, FeFe cytoplasmic [FeFe] hydrogenase.

ACKNOWLEDGEMENTS

This research was supported by Post-Doc and PhD fellowships SFRH/BPD/76707/2011 and SFRH/BD/86442/2012, grants UID/Multi/04551/2013 and PTDC/BBB-BEP/2723/2014 funded by Fundação para a Ciência e Tecnologia (Portugal). The authors are grateful to Sebastien Dementin for supplying *D. fructosivorans* and Sofia Venceslau for genomic analysis of this organism.

REFERENCES

1. Boddien A, Mellmann D, Gärtner F, Jackstell R, Junge H, Dyson PJ, *et al*. Efficient dehydrogenation of formic acid using an iron catalyst. Science. 2011;333: 1733–1736.

2. Boddien A, Gärtner F, Federsel C, Sponholz P, Mellmann D, Jackstell R, *et al.* CO_2 -"neutral" hydrogen storage based on bicarbonates and formates. Angew Chemie. 2011;50: 6411–6414.

3. Enthaler S, von Langermann J, Schmidt T. Carbon dioxide and formic acid—the couple for environmental-friendly hydrogen storage? Energy Environ Sci. 2010;3: 1207–1217.

4. Bae SS, Kim TW, Lee HS, Kwon KK, Kim YJ, Kim MS, *et al*. H_2 production from CO, formate or starch using the hyperthermophilic archaeon, *Thermococcus onnurineus*. Biotechnol Lett. 2012;34: 75–79.

5. Bae SS, Lee HS, Jeon JH, Lee J-H, Kang SG, Kim TW. Enhancing bio-hydrogen production from sodium formate by hyperthermophilic archaeon, *Thermococcus onnurineus* NA1. Bioprocess Biosyst Eng. 2015;38: 989–993.

6. Kim YJ, Lee HS, Kim ES, Bae SS, Lim JK, Matsumi R, *et al.* Formate-driven growth coupled with H_2 production. Nature. Nature Publishing Group; 2010;467: 352–355.

7. Seol E, Jang Y, Kim S, Oh YK, Park S. Engineering of formate-hydrogen lyase gene cluster for improved hydrogen production in *Escherichia coli*. Int J Hydrogen Energy. 2012;37: 15045–15051.

8. Seol E, Manimaran A, Jang Y, Kim S, Oh Y-K, Park S. Sustained hydrogen production from formate using immobilized recombinant *Escherichia coli* SH5. Int J Hydrogen Energy. 2011;36: 8681–8686.

9. Shin J-H, Yoon JH, Lee SH, Park TH. Hydrogen production from formic acid in pH-stat fed-batch operation for direct supply to fuel cell. Bioresour Technol. 2010;101: S53–S58.

10. Yoshida A, Nishimura T, Kawaguchi H, Inui M, Yukawa H. Enhanced hydrogen

production from formic acid by formate hydrogen lyase-overexpressing *Escherichia coli* strains. Appl Environ Microbiol. 2005;71: 6762–6768.

11. Martins M, Pereira IAC. Sulfate-reducing bacteria as new microorganisms for biological hydrogen production. Int J Hydrogen Energy. 2013;38: 12294–12301.

12. Pereira IAC, Ramos AR, Grein F, Marques MC, da Silva SM, Venceslau SS. A comparative genomic analysis of energy metabolism in sulfate reducing bacteria and archaea. Front Microbiol. 2011;2: 1–18.

13. Walker CB, He Z, Yang ZK, Ringbauer JA, He Q, Zhou J, *et al*. The electron transfer system of syntrophically grown *Desulfovibrio vulgaris*. J Bacteriol. 2009;191: 5793–5801.

14. Boone DR, Bryant MP. Propionate-degrading bacterium, *Syntrophobacter wolinii* sp. nov. gen. nov., from methanogenic ecosystems. Applied and Environmental Microbiology. 1980. pp. 626–632.

15. Dolfing J, Jiang B, Henstra AM, Stams AJM, Plugge CM. Syntrophic growth on formate: a new microbial niche in anoxic environments. Appl Environ Microbiol. 2008;74: 6126–6131.

16. Martins M, Mourato C, Pereira IAC. *Desulfovibrio vulgaris* growth coupled to formate-driven H_2 production. Environ Sci Technol. 2015;49: 14655–14662.

17. Price MN, Ray J, Wetmore KM, Kuehl J V, Bauer S, Deutschbauer AM, *et al*. The genetic basis of energy conservation in the sulfate-reducing bacterium *Desulfovibrio alaskensis* G20. Front Microbiol. 2014;5: 577.

18. Caffrey SM, Park H-S, Voordouw JK, He Z, Zhou J, Voordouw G. Function of periplasmic hydrogenases in the sulfate-reducing bacterium *Desulfovibrio vulgaris* Hildenborough. J Bacteriol. 2007;189: 6159–6167.

19. Meyer B, Kuehl J V., Deutschbauer AM, Arkin AP, Stahl DA. Flexibility of syntrophic enzyme systems in *desulfovibrio* species ensures their adaptation capability to environmental changes. J Bacteriol. 2013;195: 4900–4914.

20. Meyer B, Kuehl J, Deutschbauer AM, Price MN, Arkin AP, Stahl DA. Variation among *Desulfovibrio* Species in electron transfer systems used for syntrophic growth. J Bacteriol. 2013;195: 990–1004.

21. Meyer B, Kuehl J V., Price MN, Ray J, Deutschbauer AM, Arkin AP, *et al*. The energy-conserving electron transfer system used by *Desulfovibrio alaskensis* strain G20 during pyruvate fermentation involves reduction of endogenously formed fumarate and cytoplasmic and membrane-bound complexes, Hdr-Flox and Rnf. Environ Microbiol. 2014;16: 3463–3486.

22. Voordouw G. Carbon monoxide cycling by *Desulfovibrio vulgaris* Hildenborough. J Bacteriol. 2002;184: 5903–5911.

23. da Silva SM, Pimentel C, Valente FMA, Rodrigues-Pousada C, Pereira IAC. Tungsten and molybdenum regulation of formate dehydrogenase expression in *Desulfovibrio vulgaris* Hildenborough. J Bacteriol. 2011;193: 2909–2916.

24. Sebban C, Blanchard L, Bruschi M, Guerlesquin F. Purification and characterization of the formate dehydrogenase from *Desulfovibrio vulgaris* Hildenborough. FEMS Microbiol Lett. 1995;133: 143–9.

25. Morais-Silva FO, Rezende AM, Pimentel C, Santos CI, Clemente C, Varela-Raposo A, *et al*. Genome sequence of the model sulfate reducer *Desulfovibrio giga*s: A comparative analysis within the *Desulfovibrio* genus. Microbiol Open. 2014;3: 513–530.

26. Morais-Silva FO, Santos CI, Rodrigues R, Pereira IAC, Rodrigues-Pousada C. Roles of HynAB and Ech, the only two hydrogenases found in the model sulfate reducer *Desulfovibrio gigas*. J Bacteriol. 2013;195: 4753–4760.

27. Rodrigues R, Valente FM., Pereira IA., Oliveira S, Rodrigues-Pousada C. A novel membrane-bound Ech [NiFe] hydrogenase in D*esulfovibrio gigas*. Biochem Biophys Res Commun. 2003;306: 366–375.

28. Caffrey SM. Functional genomics of periplasmic hydrogenases of *Desulfovibrio vulgaris* Hildenborough. [Ph.D. Thesis]. Alberta: University of Calgary. 2008.

29. da Silva SM, Voordouw J, Leitão C, Martins M, Voordouw G, Pereira IAC. Function of formate dehydrogenases in *Desulfovibrio vulgaris* Hildenborough energy metabolism. Microbiology. 2013;159: 1760–1769.

30. Keller KL, Bender KS, Wall JD. Development of a markerless genetic exchange system for *Desulfovibrio vulgaris* Hildenborough and its use in generating a strain with increased transformation efficiency. Appl Environ Microbiol. 2009;75: 7682–7691.

31. Valente FMA, Almeida CC, Pacheco I, Carita J, Saraiva LM, Pereira IAC. Selenium is involved in regulation of periplasmic hydrogenase gene expression in *Desulfovibrio vulgaris* Hildenborough. J Bacteriol. 2006;188: 3228–3235.

32. Hartmann T, Schwanhold N, Leimkühler S. Assembly and catalysis of molybdenum or tungsten-containing formate dehydrogenases from bacteria. Biochim Biophys Acta - Proteins Proteomics. 2015;1854: 1090–1100.

33. Maia LB, Moura JJG, Moura I. Molybdenum and tungsten-dependent formate dehydrogenases. J Biol Inorg Chem. 2015;20: 287–309.

34. Mota CS, Valette O, González PJ, Brondino CD, Moura JJG, Moura I, *et al*. Effects of molybdate and tungstate on expression levels and biochemical characteristics of formate dehydrogenases produced by *Desulfovibrio alaskensis* NCIMB 13491. J Bacteriol. 2011;193: 2917–2923.

35. Matias PM, Pereira IAC, Soares CM, Carrondo MA. Sulphate respiration from hydrogen in *Desulfovibrio* bacteria: A structural biology overview. Progress in Biophysics and Molecular Biology. 2005. pp. 292–329.

36. Pereira IA., Haveman SA, Voordouw G. Biochemical, genetic and genomic characterization of anaerobic electron transport pathways in sulphate-reducing Delta-proteobacteria. In: Barton WL, Hamilton WA, editors. Sulphate-reducing Bacteria - Environmental and Engineered systems. Cambridge: Cambridge University Press; 2007. pp. 215–240.

37. Rivas MG, González PJ, Brondino CD, Moura JJG, Moura I. EPR characterization of the molybdenum(V) forms of formate dehydrogenase from *Desulfovibrio desulfuricans* ATCC 27774 upon formate reduction. J Inorg Biochem. 2007;101: 1617–1622.

38. Brondino CD, Passeggi MCG, Caldeira J, Almendra MJ, Feio MJ, Moura JJG, *et al.* Incorporation of either molybdenum or tungsten into formate dehydrogenase from *Desulfovibrio alaskensis* NCIMB 13491; EPR assignment of the proximal iron-sulfur cluster to the pterin cofactor in formate dehydrogenases from sulfate-reducing bacteria. J Biol Inorg Chem. 2004;9: 145–151.

39. Almendra MJ, Brondino CD, Gavel O, Pereira AS, Tavares P, Bursakov S, *et al*. Purification and characterization of a tungsten-containing formate

dehydrogenase from *Desulfovibrio gigas*. Biochemistry. 1999;38: 16366–16372.

40. Carepo M, Baptista JF, Pamplona A, Fauque G, Moura JJG, Reis MAM. Hydrogen metabolism in *Desulfovibrio desulfuricans* strain New Jersey (NCIMB 8313) - Comparative study with D. vulgaris and D. gigas species. Anaerobe. 2002;8: 325–332.

41. Marques MC, Coelho R, De Lacey AL, Pereira IAC, Matias PM. The three-dimensional structure of [NiFeSe] hydrogenase from *Desulfovibrio vulgaris* Hildenborough: a hydrogenase without a bridging ligand in the active site in its oxidised, "as-isolated" state. J Mol Biol. 2010;396: 893–907. 13

42. Valente FMA, Oliveira ASF, Gnadt N, Pacheco I, Coelho A V., Xavier A V., *et al*. Hydrogenases in *Desulfovibrio vulgaris* Hildenborough: structural and physiologic characterisation of the membrane-bound [NiFeSe] hydrogenase. JBIC J Biol Inorg Chem. 2005;10: 667–682.

43. Fauque G, Peck HD, Moura JJG, Huynh BH, Berlier Y, DerVartanian D V., *et al*. The three classes of hydrogenases from sulfate-reducing bacteria of the genus *Desulfovibrio*. FEMS Microbiol Lett. 1988;54: 299–344.

44. Pereira PM, Teixeira M, Xavier A V., Louro RO, Pereira IAC. The Tmc complex from *Desulfovibrio vulgaris* Hildenborough is involved in transmembrane electron transfer from periplasmic hydrogen oxidation. Biochemistry. 2006;45: 10359–10367.

45. Venceslau SS, Lino RR, Pereira IAC. The Qrc membrane complex, related to the alternative complex III, is a menaquinone reductase involved in sulfate respiration. J Biol Chem. 2010;285: 22774–22783.

46. Venceslau SS, Matos D, Pereira IAC. EPR characterization of the new Qrc complex from sulfate reducing bacteria and its ability to form a supercomplex with hydrogenase and TpI *c3*. FEBS Lett. 2011;585: 2177–2181.

47. Buckel W, Thauer RK. Energy conservation via electron bifurcating ferredoxin reduction and proton/Na^+ translocating ferredoxin oxidation. Biochim Biophys Acta - Bioenerg. 2013;1827: 94–113.

CHAPTER 4

A CONTINUOUS SYSTEM FOR BIOCATALYTIC HYDROGENATION OF CO_2 TO FORMATE

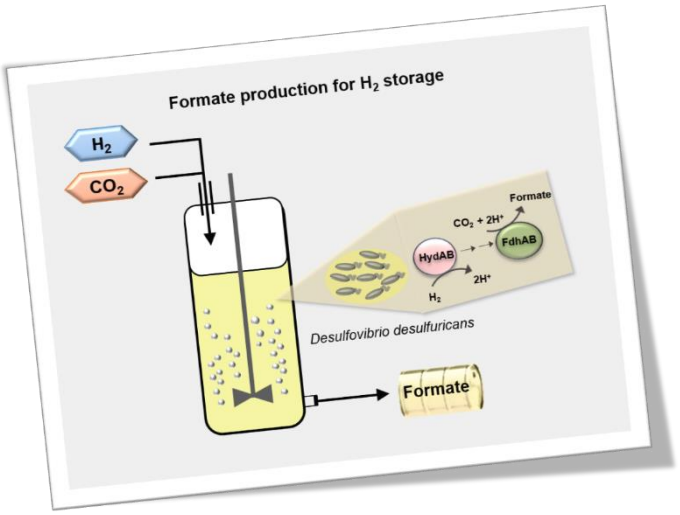

The work presented in this chapter was accepted in:

Cláudia Mourato, Mónica Martins, Sofia M. da Silva, Inês A. C. Pereira. A continuous system for biocatalytic hydrogenation of CO_2 to formate. Bioresource Technology. *Accepted.* (doi.org/10.1016/j.biortech.2017.03.091)

Cláudia Mourato was involved in the writing and in all the experimental procedures of this work.

4. ABSTRACT

In this work a novel biotechnological process for the hydrogenation of CO_2 to formate was developed, using whole cell biocatalysis by a sulfate-reducing bacterium. Three *Desulfovibrio* strains were tested (*D. vulgaris* Hildenborough, *D. alaskensis* G20, and *D. desulfuricans* ATCC 27774), of which *D. desulfuricans* showed the highest capacity to reduce CO_2 to formate, producing 12 mM of formate in serum bottles with a production rate of 0.09 mM h^{-1}. Gene expression analysis indicated that among the three formate dehydrogenases and five hydrogenases, the cytoplasmic FdhAB and the periplasmic HydAB [FeFe] are the main enzymes expressed in *D. desulfuricans* in these conditions. The new bioprocess for continuous formate production by *D. desulfuricans* had a maximum specific formate production rate of 14 mM g_{dcw}^{-1} h^{-1}, and more than 45 mM of formate were obtained with a production rate of 0.40 mM h^{-1}. This is the first report of a process for continuous biocatalytic production of formate.

4.1 INTRODUCTION

An increasing reliance on renewable energy sources for electricity production is a welcome reality, expected to further increase in the coming future. Albeit, the development of methods for storing excess electricity during periods of low consumption is an important requirement for the viability of a sustainable economy based on renewable energy [1]. A promising answer is the use of

hydrogen, produced by electrolysis of water, but the transport and storage of hydrogen is still a challenging issue. Formic acid has emerged as an ideal storage compound for H_2 as it is a safe liquid at room temperature, which can be easily stored and transported, and furthermore it allows the sequestration of CO_2 in a valuable commodity chemical [2–6]. Several chemical processes are known for reduction of CO_2 to formate, but these technologies require demanding and expensive conditions, like the use of precious metals and high temperatures and pressures [7–10]. In contrast, the use of biological catalysts, which work under mild conditions and with high specificity, provides an inexpensive and "greener" system for the conversion of CO_2 to formate, mainly through the hydrogenation of CO_2.

Formate production using whole cell catalysis is emerging as an attractive biotechnological application, and has been reported with several microorganisms, including *Acetobacterium woodii* [11], *Escherichia coli* [12] and *Methylobacterium extorquens* [13]. In the present work we tested sulfate-reducing bacteria (SRB) of the genus *Desulfovibrio* as novel biocatalysts for formate production through the hydrogenation of CO_2. SRB are anaerobic bacteria with important biotechnological applications in the bioremediation of heavy metals and wastewaters [14]. These bacteria live at low redox potentials and have a high content of formate dehydrogenases (FDHs) and hydrogenases (Hases), which play an important role in their energy metabolism [14,15]. In biologic systems, the hydrogenation of CO_2 to formate (equation 4.1) occurs by the action of these two types of enzymes. FDHs catalyze the reversible oxidation of formate to CO_2 (equation 4.2) [16,17] whereas Hases are responsible for the reversible oxidation of H_2 (equation 4.3) [18].

$$H_2 + CO_2 \leftrightarrow HCOOH \qquad \Delta G^{0'} = 3.5\ kJ\ mol^{-1} \qquad \text{(equation 4.1)}$$

$$HCOOH \overset{FDH}{\longleftrightarrow} CO_2 + 2e^- + H^+ \qquad \text{(equation 4.2)}$$

$$H_2 \overset{Hase}{\longleftrightarrow} 2H^+ + 2e^- \qquad \text{(equation 4.3)}$$

Due to the abundant presence of these enzymes [15], SRB are good candidates for formate production from CO_2 and H_2 and it was recently shown that these bacteria are good biocatalysts for H_2 production from formate [19–21]. In the acetogen *A. woodii* a cytoplasmic protein complex between a Hase and a FDH was shown to be involved in formate production [11]. In *Desulfovibrio* most of the Hases and FDHs are periplasmic and they share the same electron acceptor, the small tetraheme cytochrome c_3 [22,23]. This suggests that there can be direct electron transfer between these two kinds of enzymes through this cytochrome. In this work, formate production from CO_2 and H_2 was evaluated by three *Desulfovibrio* species in order to select the one with highest activity. Next, a column bioreactor was develop and optimized for formate production using *D. desulfuricans* ATCC 27774, followed by development of a continuous bioprocess for the production of formate. In parallel, expression analysis of genes coding for FDHs and Hases was also performed to investigate which enzymes are involved in formate production by this organism.

4.2 MATERIALS AND METHODS

4.2.1 BACTERIAL STRAINS AND GROWTH CONDITIONS

The bacterial strains used in this work were *Desulfovibrio vulgaris* Hildenborough (DSM 644), *Desulfovibrio desulfuricans* ATCC 27774 and *Desulfovibrio alaskensis* G20. All strains were grown in modified Postgate medium C containing 0.5 g L^{-1} KH_2PO_4, 1 g L^{-1} NH_4Cl, 2.5 g L^{-1} Na_2SO_4, 0.06 g L^{-1} $CaCl_2.2H_2O$, 0.06 g L^{-1} $MgSO_4.7H_2O$, 1 g L^{-1} yeast extract, 0.0071 g L^{-1} $FeSO_4.7H_2O$, 0.3 g L^{-1} sodium citrate tribasic dihydrate, 0.1 g L^{-1} ascorbic acid, 0.1 g L^{-1} sodium thioglycolate, 4.5 g L^{-1} sodium lactate and 0.3 mg L^{-1} resazurin. Bacterial growth was carried out at 37 ˚C in static conditions using 120 mL serum bottles with a working volume of 50 mL and N_2 as gas headspace. The bottles were sealed with butyl rubber stoppers and aluminum crimp seals.

4.2.2 FORMATE PRODUCTION BY WHOLE CELL IN SERUM BOTTLES

The production of formate by whole cell in serum bottles was performed using the modified Postgate medium C described above with a few modifications: medium without lactate was supplemented with sodium acetate (10 mM), nickel chloride (1 µM), sodium selenite (1 µM) and sodium molybdate (0.1 µM), sodium sulfate (8 mM instead of 17.6 mM), and yeast extract (0.2 g L^{-1} instead of 1 g L^{-1}), and the pH adjusted to 7.0 ± 0.1. This medium is designed as *Desulfovibrio* carbon dioxide (DCD) medium. Batch experiments were carried under anaerobic conditions at 37 °C using 120 mL serum bottles with

a working volume of 50 mL and H_2/CO_2 (80%/20%) as gas headspace, to a final overpressure of 1 bar. The bottles were sealed with butyl rubber stoppers and aluminum crimp seals. A 10 % (v/v) inoculum grown in modified Postgate medium C was used in all experiments, which were performed in triplicate.

4.2.3 FORMATE PRODUCTION IN A COLUMN BIOREACTOR

Formate production was studied using a sparging column bioreactor previously described [20]. This reactor was operated with a working volume of 0.5 L of DCD medium and a gas mixture of H_2/CO_2 (80%/20%) was used at a flow rate of 80 mL min^{-1}. The internal temperature was kept constant by a heating blanket. Two operation parameters were optimized for formate production: sulfate concentration (from 3 mM to 20 mM) and temperature (from 31 ˚C to 44 ˚C).

Continuous formate production was also investigated by the continuous addition of fresh DCD medium (without sodium sulfate and with 0.048 g L^{-1} $MgCl_2.6H_2O$ instead of 0.06 g L^{-1} $MgSO_4.7H_2O$). This fresh medium was also supplemented with MOPS buffer (2.5 M) and sodium sulfide (58 mM). Sulfide was added to ensure the maintenance of a low redox potential inside the bioreactor. After sulfate depletion, the fresh medium was fed to the bioreactor at a flow rate of 0.110 mL min^{-1}. Moreover, 20 mmol of bicarbonate were added daily to the bioreactor, as an additional source of CO_2 in the system, to a final concentration of 40 mM in fed batch mode (20 mL day^{-1}) . A 10 % (v/v) of inoculum was used to startup the bioreactor. Each experiment was carried out at least in duplicate.

4.2.4 RNA ISOLATION AND QUANTITATIVE RT-PCR ANALYSIS (qRT-PCR)

For the expression analysis of genes involved in formate production, *D. desulfuricans* ATCC 27774 was grown in the column bioreactor fed with CO_2 medium. Two types of experiments were conducted to compare the gene expression during hydrogen-sulfate respiration (Experiment I) with the expression when formate was produced in the absence of sulfate (Experiment II). In Exp. I, the cells were grown with a higher concentration of sulfate (20 mM) and collected when half of the initial sulfate was consumed (production of formate was not detected). In Exp. II the cells were collected at the stage where sulfate was depleted and formate production reached the maximum value. Cells were centrifuged for 12 min at 3000 xg, washed with cold (4 ˚C) sterile MilliQ water and frozen for later RNA extraction. Cell lysis and RNA extraction were performed as previously described [24]. RNA quality was assessed by inspecting the 16S and 23S rRNA bands after electrophoresis on agarose gel and quantified spectrophotometrically at 260 nm (NanoDrop 2000C ThermoScience). RNA samples were treated with DNase (TURBO™ DNase-free, Ambion) three times to avoid DNA contamination and RNA was cleaned up using the RNeasy minikit (Qiagen) according to the manufacturer's instructions.

Total RNA (3 µg) was reversed transcribed with Transcriptor Reverse Transcriptase (Roche). Primers were designed to amplify approximately 100 to 120 bp region of subunits of formate-dehydrogenases (*fdhA-p*, *fdhA-m*, *fdhA-cyt*) and hydrogenases genes (*hydA*, *hynA-p*, *hynA-m*, *echE*, *cooA*) and the reference ribosomal protein gene *rpls* (Table 4.1). The *rpls* gene was previously

validated as a reference gene [25] and was selected due to its similar levels of expression to the genes analyzed in this study. qRT-PCR reactions were performed in a Light Cycler 480 Real-Time PCR System (Roche), with LightCycler 480 SYBR Green I Master (Roche).

Relative standard curves and gene expression were calculated by the relative quantification method with efficiency correction, using the LightCycler Software 1.5. Values were normalized to the ones from the ribosomal protein gene *rpls*. Three biological replicates and three technical replicates were used for each condition.

Table 4.1. Primers used for qRT-PCR expression analysis of formate-dehydrogenases and hydrogenases in *D. desulfuricans* ATCC 27774.

Target gene/locus tag	Primers sequence (5' → 3')
Reference gene	
rRNA *rpls* (ddes_1790)	Fw - ATTGTGGAAGGCGAAAAACA Rv - TCAGAAATTTTGCGCACTGT
FDHs genes	
*fdhABD (fdhA-m/*ddes_0827*)*	Fw - AAAGCAAACGTGGCTCCATT Rv - TTGTAGCCGAAATGCATGGG
*fdhABC$_3$ (fdhA-p/*ddes_0555*)*	Fw - ATGCACTGGACGGACAAGTA Rv - CGCGCTTATAGGTCTTGTCG
*fdhAB (fdhA-cyt/*ddes_1545*)*	Fw - GGAGTATCCCTTCGTGCTCA Rv - AAATATCCGCCGTGTCATGC
Hases genes	
*coo (cooA/*ddes_1885*)*	Fw - GCCACTCCTTCACCTACAGC Rv - GAGGCGATACGCTTGATTTC
*ech (echE/*ddes_1669*)*	Fw - TTTCTGCGGGTTATCTGGTC Rv - GAACTGCTGGAACACGCTTT
*hydAB (hydA/*ddes_1503*)*	Fw - ACCATCAACGGTACGGAACT Rv - AGGCCATGAATTCGATGAAA
*hynAB (hynA-p/*ddes_1038*)*	Fw - TTGAAGACGCCATCAACAAG Rv - ATGCGTGGAGGTGGTAGAAG
*hynABC (hynA-m/*ddes_0836*)*	Fw - GACCGTTACTCCTGGCTCAA Rv - GCCCTTGATGTCGTCATTTT

4.2.5 ANALYTICAL METHODS

Cell growth was monitored by optical density at 600 nm (OD_{600}) with a Shimadzu UV/Vis spectrophotometer. *D. desulfuricans* biomass was determined by measuring the dry cell weight (dcw) correlated with OD_{600} values. One unit value of OD_{600} corresponded to 0.31 g_{dcw} L^{-1}. Liquid samples were periodically collected and filtered (0.22 µM) before sulfate and formate analysis. Sulfate was quantified by UV/Vis spectrophotometry at 450 nm using the method of SulfaVer®4 (Hach). Formate was quantified using the formate dehydrogenase of *Candida boidinii* (Sigma) as previously described in [11,26] using a 96-well plate. Each sample (20 µL) was placed in the plate and the reaction started by the addition of a solution containing of 1 mM NAD^+, 40 mM Tris-HCl buffer pH 8.0 (final concentrations) and 0.5 U of formate dehydrogenase to a final volume of 200 µL. Absorbance at the start and end of the reaction (after 1h of incubation at 37˚C) was monitored at 340 nm (for NADH formation) in a 96-well plate reader (ELx800 Absorvance Reader, BioTek).

4.2.6 THERMODYNAMIC AND SOLUBILITY CALCULATIONS

The Gibbs free energy in the bioreactor experiments was calculated using the Nernst equation (equation 4.4) and the measured values of formate. The standard Gibbs free energy was correct to the work temperatures using the

Gibbs-Helmholtz equation (equation 4.5) and the enthalpy energies of products and reactants formation [27].

$$\Delta G = \Delta G_T^0 + RTlnQ \qquad \text{(equation 4.4)}$$

$$\Delta G^0 = \Delta G_{T_{ref}}^0 \times \frac{T_{work}}{T_{ref}} + \Delta H_{T_{ref}}^0 \times \frac{T_{ref} - T_{work}}{T_{ref}} \qquad \text{(equation 4.5)}$$

The gas concentrations in solution at working conditions was calculated according to Henry's law (equation 4.6), where *c* is the concentration of the gas, K_H is the Henry's constant of solubility and *p* is the partial pressure [28]. The Henry's constant of solubility values were corrected to working temperature using the van't Hoff equation (equation 4.7) [28] and the Henry's Law constants of solubility at standard conditions (K_H^θ) and the values of $\frac{-\Delta_{sol}H}{R}$ were taken from [28].

$$c = K_H \times p \qquad \text{(equation 4.6)}$$

$$K_H = K_H^\theta \times \frac{-\Delta_{sol}H}{R}\left(\frac{1}{T} - \frac{1}{T^\theta}\right) \qquad \text{(equation 4.7)}$$

4.2.7 STATISTICAL ANALYSIS

The production of formate by the different strains and in different bioreactor conditions was analyzed using one-way analysis of variance (ANOVA) and the multiple comparative pairwise Tukey test (confidence of 95%). The statistical analyses were performed with SigmaStat 3.0 and a *p*-value less than 0.05 was considered statistically significant.

4.3 RESULTS AND DISCUSSION

4.3.1 FORMATE PRODUCTION BY *DESULFOVIBRIO* WHOLE CELLS IN BATCH CONDITIONS

The potential of three *Desulfovibrio* spp. to act as biocatalysts for the production of formate from CO_2 reduction with H_2 was investigated during 10 days (Figure 4.1). The three strains showed similar initial formate production rates (from 0.086 to 0.092 mM h^{-1}, p=0.257), but different amounts of formate were produced between days 4 and 10 (p<0.002). *D. vulgaris* and *D. alaskensis* accumulated 8 mM and 10 mM of formate, respectively, whereas 12 mM was obtained with *D. desulfuricans* after 10 days. These results indicate that 36 to 55 % of the CO_2 available (1.1 mmol) was used for formate production.

Formate production by *Desulfovibrio* spp. Was reported for *D. vulgaris,* which produced 10 mM of formate when grown with CO_2 and H_2 [26]. This value agrees with the present results for the same organism. The differences in

formate production between the three strains may be related to the differences in Hases and especially FDHs present in these strains. It is known that the expression of FDHs is dependent on the metals available [16,29,30]. In this work, molybdenum was used as a metal supplement in the growth medium. The genome of *D. desulfuricans* codes for three FDHs, in which one was characterized as a FDH that incorporates Mo (Mo-FdhABC$_3$) [15,31]. *D. vulgaris*, which produced less formate, has also three FDHs, two of which have been described as Mo-dependent FDHs (Mo-FdhABC$_3$), and a third FDH that can incorporate either Mo or tunsgten (Mo/W-FdhAB) [15,29]. Previous studies showed that the *D. vulgaris* FdhAB has a higher catalytic activity than FdhABC$_3$ [29] and that this protein is mainly involved in formate oxidation [21]. The lowest formate production was observed for *D. alaskensis.* This organism has three FDHs, two of which have been characterized as W-FDHs, and a third that can incorporate either Mo or W [30,32], similarly to *D. vulgaris.* Interestingly, these three microorganisms showed a similar H_2 production profile from formate, with the maximum H_2 production obtained from *D. desulfuricans* and *D. vulgaris*, followed by *D. alaskensis* (with Mo) [21].

In conclusion, *D. desulfuricans* was selected for further studies aiming to develop and optimize a new bioreactor process for formate production.

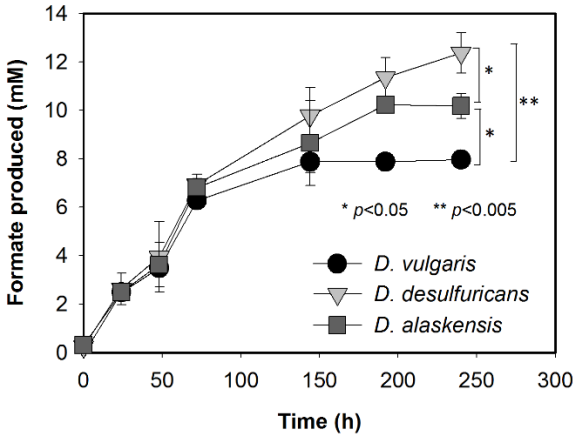

Figure 4.1. Formate production from CO_2 and H_2 by three *Desulfovibrio* species. The assays were conducted in serum bottles under an atmosphere of 20% CO_2/80% H_2 to a final overpressure of 1 bar. Data are the average of triplicate incubations and error bars indicate the standard deviations.

4.3.2 FORMATE PRODUCTION BY *D. DESULFURICANS* IN A BIOREACTOR

To develop a bioprocess for formate production, a column bioreactor with gas sparging was tested and optimized using *D. desulfuricans* as biocatalyst. This bioreactor was first designed and optimized for H_2 production in a previous study, where it led to a great improvement in H_2 production from formate [20]. This bioreactor and its gas sparging system allows for a constant and efficient delivery of CO_2 and H_2 to the cells.

4.3.2.1. FORMATE PRODUCTION PROFILE

Growth of *D. desulfuricans* in the bioreactor fed with CO_2 and H_2 was initially promoted by the presence of an initial sulfate concentration of 10 mM (Figure 4.2). Growth was observed in the first 14 hours of study until sulfate was completely reduced, reaching a maximum OD_{600} of 0.35, representing 0.12 g_{dcw}^{-1} L^{-1}. The production of formate started after sulfate depletion. The initial production rate was 0.6 mM h^{-1} and a maximum amount of 12 mM of formate was achieved at 48 h of study. A specific formate production of 245 mM g_{dcw}^{-1} and a maximum specific production rate of 11 mM g_{dcw}^{-1} h^{-1} were obtained in this process.

A formate production of 12 mM was similar to that obtained with *D. desulfuricans* in serum bottles. In the bioreactor, the concentration of substrates is not limiting since there is a continuous delivery of CO_2 and H_2. The calculated ΔG at the bioreactor conditions also showed a favorable thermodynamic reaction for formate production, with ΔG values between -32 and -26 kJ mol^{-1} (Figure 4.2). It should be noted that these ΔG values apply to the solution conditions, and not to the intracellular milieu, where the concentrations of the metabolites may be different. Although the amount of formate produced in the bioreactor was similar to that in batch conditions, the initial production rate was 6-fold higher. This demonstrates a better catalytic performance of the cells in the bioreactor, which was probably due to the continuous feeding of H_2 and CO_2. To further optimize formate production, the effect of initial sulfate concentration and temperature were also evaluated.

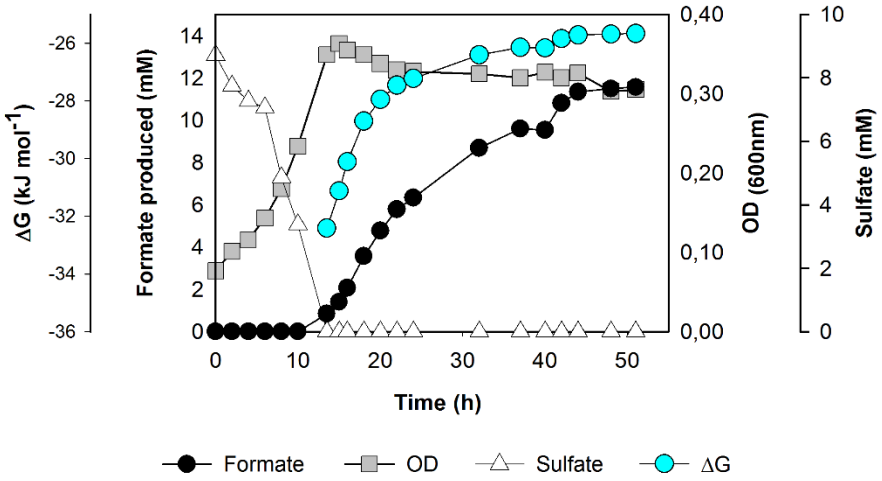

Figure 4.2. Formate production and bacterial growth profiles of *D. desulfuricans* in a column bioreactor. The bioreactor was fed with medium containing 10 mM of sulfate and operated at 37˚C with a gas sparging (20 %CO_2/80%H_2) flow rate of 80 mL min^{-1}.

4.3.2.2. OPTIMIZATION OF BIOREACTOR CONDITIONS

In order to investigate the effect of cell load on formate production, *D. desulfuricans* was grown in the bioreactor with CO_2 and H_2 in the presence of different initial sulfate concentrations (Table 4.2). As expected, the increase of initial sulfate concentration promoted growth expressed in the increase of maximum OD_{600}. In all conditions, formate production started only after sulfate was depleted. The production of formate increased almost 3-fold (from 4.5 to 12 mM) when the initial sulfate concentration was increased from 3 to 10 mM (p<0.05) (Table 4.2). However, when the bioreactor was operated with

20 mM of sulfate, only a slight improvement of formate production was observed, reaching 14 mM (Table 4.2). This may have been due to inefficient substrate uptake in the presence of a higher cell load. A similar effect was observed in previous studies of H_2 production [19,33,34]. The highest specific formate production of 245 mM g_{dcw}^{-1} was obtained when the initial sulfate concentration was 10 mM. A maximum specific formate production rate of 11 mM g_{dcw}^{-1} h^{-1} was also observed in this condition. Thus, 10 mM of sulfate was used in subsequent experiments.

To test the effect of temperature on formate production, the bioreactor was operated at different temperatures from 31 ˚C to 44 ˚C. An improvement of formate production from 7 mM to 12 mM was observed when the temperature increased from 31 ˚C to 37 ˚C (Table 4.2). At 40 ˚C, a lower amount of formate was observed (8.4 mM), whereas at 44 ˚C no formate was produced. The maximum specific formate production and formate production rates were also higher at 37 ˚C (Table 4.2). Although formate production decreased with temperatures higher than 37 ˚C, the cells were still able to grow, even at 44 ˚C, where no formate was produced. The calculated ΔG is favorable for the production of formate at all temperatures (Table 4.2). The reduced production of formate above 37 ˚C may be due to a specific effect of temperature on formate metabolism of *D. desulfuricans*, since the concentrations of CO_2 and H_2 in solution are only slightly reduced (the calculated variation is from 5.6 $x10^{-5}$ M at 31 ˚C to 4.1 $x10^{-5}$ M at 44 ˚C for CO_2 and 6$x10^{-6}$ M at 31 ˚C to 5.6 $x10^{-6}$ M at 44 ˚C for H_2).

Table 4.2. Formate production by *D. desulfuricans* in a bioreactor at different initial sulfate concentrations and temperatures.

	OD[a]		Formate produced (mM)	Specific formate production (mM g_{dcw}^{-1})	Formate production rate (mM h^{-1})	Maximum specific production rate (mM g_{dcw}^{-1} h^{-1})	ΔG[d] (kJ mol^{-1})
	OD[b]	OD[c]					
Sulfate concentration							
3 mM	0.21	0.21	4.5	137	0.3	9.5	-67.6
10 mM	0.36	0.30	12	245	0.6	11	-67.6
20 mM	0.50	0.46	14	204	0.4	5.3	-67.6
Temperature							
31˚C	0.32	0.32	7	124	0.2	3	-66.9
37˚C	0.36	0.30	12	245	0.6	11	-67.6
40˚C	0.32	0.30	8.4	46	0.3	1.6	-68.0
44˚C	0.29	0.29	0	0	0	0	-68.4

[a] Initial OD of 0.078 ± 0.003 in all conditions.

[b] Maximum OD after sulfate depletion.

[c] OD at maximum formate production.

[d] The Gibbs free energy (kJ mol^{-1}) at working conditions was calculated using the equation $\Delta G = \Delta G^{0}_{(T)} + RT\ln Q$ and considering the formate concentration of 10^{-3} mM, pH 7 and a P_{H2} of 0.8 atm and a P_{CO2} of 0.2 atm.

4.3.3 FORMATE PRODUCTION IN CONTINUOUS CONDITIONS

The capacity of *D. desulfuricans* for production of formate in continuous mode was further investigated (Figure 4.3). In this setup fresh medium was continuously fed to the bioreactor after sulfate depletion (13 h), with a flow rate of 0.11 mL min^{-1}, and 20 mmol of bicarbonate were added daily, in fed-batch mode, as additional source of CO_2. The concentration of formate in the bioreactor increased until 64 h where maximum steady state value of 30 mM of formate production was achieved. This concentration was maintained in the

bioreactor until the end of the experiment. In the steady state (64 to 184 h) formate was produced at a rate of 0.40 mM h^{-1}. Overall, in this state, more than 45 mM of formate was produced. This value is almost 4-fold higher than that produced in fed-batch mode. This improvement is probably due to: i) the addition of bicarbonate as additional source of CO_2; ii) the continuous addition of sulfide in the fresh medium, which helps to maintain a low redox potential in the bioreactor, and iii) the continuous removal of formate, which helps to lower product inhibition.

Bacterial growth occurred during the initial sulfate reduction period reaching an OD of 0.28 after 13 h. After depletion of sulfate, the continuous feeding and removal of medium was responsible for the decrease in bacterial growth observed between 47 and 116 h (from OD of 0.27 to 0.18). Interestingly, from 116 h onwards the cell density remained constant (OD around 0.18). The bioreactor worked with a hydraulic retention time (HRT) of 76 h, which means that the medium was completely renewed more than once after 116 h. Since the cell density was constant after 116 h this suggests that *D. desulfuricans* was able to grow during the formate production phase with a maximum growth rate of 0.013 h^{-1} and a maximum specific formate production rate of 14 mM g_{dcw}^{-1} h^{-1}. This growth may be due to the small amount of sulfate present as iron sulfate (25 µM) in the fresh medium fed to bioreactor with a molar flow rate of 0.17 µmol h^{-1}. Another explanation would be that *D. desulfuricans* can grow during the production of formate from hydrogenation of CO_2, similarly to what was observed by Martins *et al.* for the growth of *D. vulgaris* by H_2 production from formate, in the absence of sulfate, in a bioreactor with gas sparging [20].

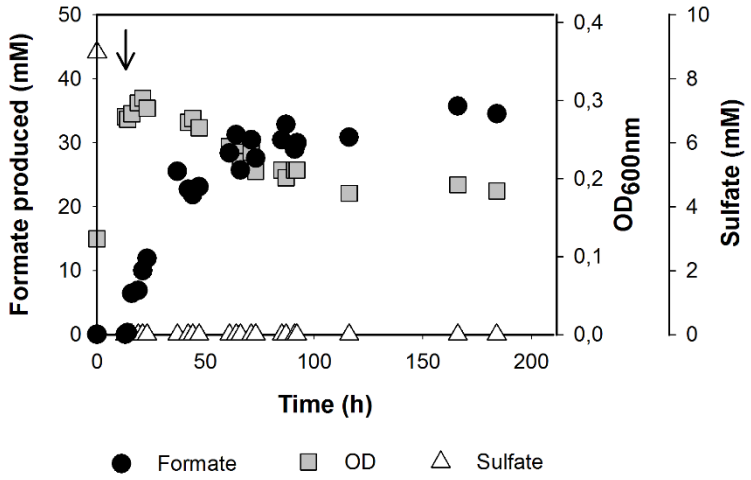

Figure 4.3. Continuous production of formate by *D. desulfuricans* in a sparging column bioreactor at 37˚C with a sparging gas mixture (20% CO_2/80% H_2) at a flow rate of 80 mL min^{-1}. Fresh medium was fed to the reactor with a flow rate of 0.110 mL min^{-1} after sulfate depletion (starting at 13 h), as indicated by the arrow.

4.3.4 EXPRESSION ANALYSIS OF FDHS AND HASES

The identification of the enzymes involved in formate production is very important for future optimization of this process through genetic manipulation. So far, no studies on the metabolism of formate production from H_2 and CO_2 have been reported in *D. desulfuricans*. The genome of this organism encodes three FDHs, two of which are periplasmic: a membrane-bound FDH (FdhABD) and a soluble one ($FdhABC_3$), which was characterized as a Mo-containing enzyme [15,31]. A cytoplasmic FDH (FdhAB) is also present

[15], but was never characterized. *D. desulfuricans* also contains five Hases, belonging to the [FeFe] and [NiFe] families [15]. Three periplasmic Hases are present in this bacterium, the soluble [FeFe] HydAB and [NiFe] HynAB, and a membrane-bound [NiFe] HynABC. The two cytoplasmic Hases are the membrane-bound [NiFe] Ech and Coo Hases. In order to investigate which FDHs and Hases may be involved in the production of formate an expression analysis by real time qRT-PCR was performed. The mRNA levels were analyzed in cells grown with CO_2 and H_2 and collected in two growth conditions: 1) when the cells were growing by sulfate reduction (i.e., when there is no formate production) and 2) in the absence of sulfate where maximum formate production is observed.

4.3.4.1 FORMATE DEHYDROGENASES GENES

The relative expression of the catalytic subunit genes (*fdhA*) is shown in Figure 4.4a. During hydrogen-sulfate respiration, a higher level of expression was observed for the *fdhA-p* gene of the periplasmic $FdhABC_3$, than for the *fdhA-m* and *fdhA-cyt* genes of the membrane-associated and cytoplasmic FDHs, respectively. In contrast, when the cells were producing formate in the absence of sulfate, a drastic decrease in the mRNA levels of *fdhA-p* was observed, whereas the expression of *fdhA-cyt* was about 2-fold increased. The expression level of *fdhA-m* did not change between the two conditions tested. The physiological function of FDHs is usually correlated with their cellular location and in general, cytoplasmic FDHs are thought to act as CO_2

reductases, whereas the periplasmic FDHs are mainly involved in the oxidation of formate [16,17]. The results obtained agree with this concept, as they suggest that the main FDH involved in formate production is the cytoplasmic enzyme, whereas the periplasmic FDH is down-regulated in these conditions. In a previous *in vivo* study, a higher formate production from CO_2 and H_2 was also reported for a $FdhABC_3$ deletion mutant of the *D. vulgaris* periplasmic FDH, confirming a formate oxidation role for this enzyme [26]. The relative expression of the *fdhA-m* gene of the membrane-associated FdhABD does not change between the two conditions analyzed, so the involvement of this enzyme is uncertain.

A role of cytoplasmic FDHs for the reduction of CO_2 to formate has been reported in other organisms [11,35]. In fermentative conditions, the oxidation of formate to H_2 and CO_2 by *E. coli* is performed by a cytoplasmic FDH, FDH-H, which is part of the membrane-bound formate-hydrogen lyase complex (FHL) [36,37]. However, this enzyme is also capable of catalyzing the reduction of CO_2 to formate either as an isolated enzyme [38] or as part of FHL complex [39]. The interconversion of CO_2 to formate in *A. woodii* is performed by a cytoplasmic complex where a Hase and a FDH are coupled [11]. A cytoplasmic FDH from *Rhodobacter capsulatus* was also shown to catalyze the reduction of CO_2 to formate [35]. These observations are in accordance with the results obtained in this work, in which the cytoplasmic FDH seems to be the main enzyme involved in CO_2 reduction to formate.

4.3.4.2 HYDROGENASES GENES

The expression levels of the Hase genes was also analyzed (Figure 4.4b) Concerning the periplasmic Hases, it was observed that during hydrogen-sulfate respiration, the transcript levels of the catalytic subunit *hydA* (of the [FeFe] HydAB Hase) and *hynA-m* (of the membrane [NiFe] HynABC enzyme) were higher than that of *hynA-p* gene (of the [NiFe] HynAB Hase). In the absence of sulfate, a high increase (9-fold) was observed for the expression of *hydA*, whereas a strong decrease occured for *hynA-m* and *hynA-p*. The expression levels of *echE* and *cooA* genes of the cytoplasmic [NiFe] Hases Ech and Coo, respectively (Figure 4.4c), were higher during hydrogen-sulfate respiration than in formate producing conditions, with *echE* showing higher expression than *cooA*. In the absence of sulfate, the expression level of these genes decreased to almost undetectable levels.

Hases are usually reversible enzymes able to catalyze both H_2 oxidation and production reactions, and their physiological function is often dependent on the growth conditions. This expression study revealed that the most important Hase oxidizing H_2 during formate production is the periplasmic [FeFe] HydAB Hase. On the other hand, the HynAB and HynABC enzymes play a more important role in H_2 oxidation during hydrogen-sulfate respiration. Previous studies reported a down-regulation of *D. vulgaris hydA* in hydrogen-sulfate respiration versus lactate-sulfate [40,41], whereas mutants lacking *hydAB* from both *D. vulgaris* and *D. alaskensis* G20 showed a reduced growth in this condition [40,42,43]. The cytoplasmic Ech and Coo Hases have apparently no role during formate production, whereas the Ech Hase has a high expression

level during hydrogen-sulfate respiration. The predominant role of Ech during hydrogen-sulfate growth was also observed previously in *D. vulgaris* [41].

The expression results allow us to propose a metabolic pathway for formate production from CO_2 and H_2 in *D. desulfuricans* (Figure 4.5). H_2 is oxidized by the periplasmic [FeFe] HydAB Hase and the electrons are transferred to the electron acceptor Type I cytochrome c_3, which is the most abundant cytochrome in the periplasm of *Desulfovibrio* and is known to accept electrons from both Hases and FDHs [22,23]. Then, electrons are transferred from this cytochrome either to membrane-associated redox complexes that shuttle them across the membrane to reach the cytoplasmic FDH, or directly to the periplasmic FdhABD.

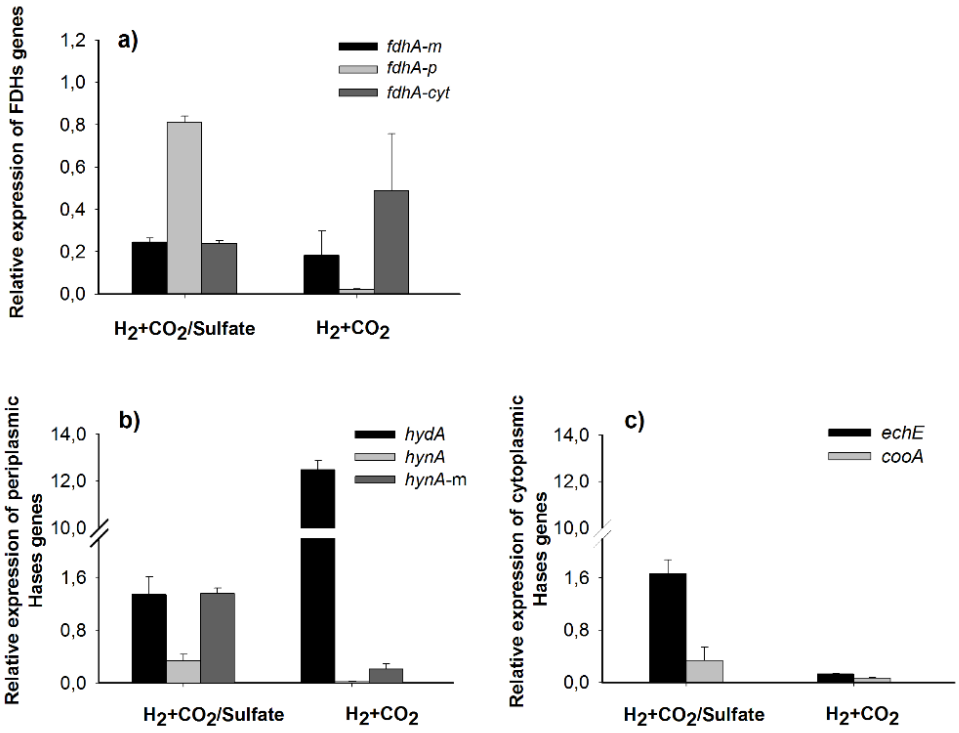

Figure 4.4. Relative expression of *D. desulfuricans* FDH (a), periplasmic (b) and cytoplasmic Hase (c) genes by qRT-PCR in cells grown in a bioreactor with CO_2 and H_2 in the presence or in the absence of sulfate. The expression of the genes was normalized to that of the *rpls* gene. Results are from three independent biological experiments (means ± standard deviations).

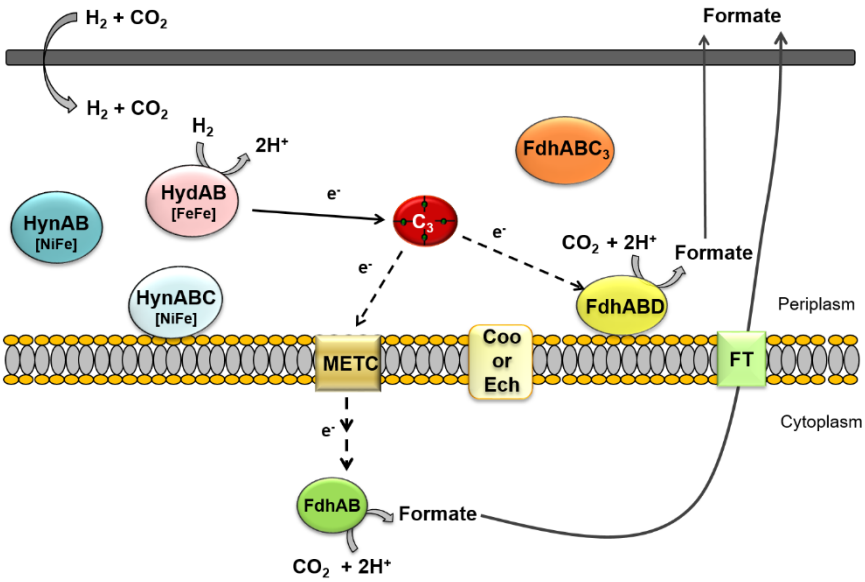

Figure 4.5. Proposed metabolic pathway for formate production in *D. desulfuricans* (in dashed lines). FdhAB, cytoplasmic formate dehydrogenase; $FdhABC_3$, periplasmic formate dehydrogenase; FdhABD, membrane-bound periplasmic formate dehydrogenase; HydAB, periplasmic [FeFe] hydrogenase; HynAB, periplasmic [NiFe] hydrogenase; HynABC, membrane-bound periplasmic [NiFe] hydrogenase; c_3, type I cytochrome c_3; METC, membrane-bound electron transfer complexes; Coo and Ech, cytoplasmic [NiFe] hydrogenases; FT, formate transporter.

4.3.5 Overview of Formate Production Studies

Recent work on formate production involved different approaches and different microorganisms as biocatalysts [11–13]. In 2013, Schuchmann and Müller showed that cell extracts of the acetogenic bacterium *A. woodii* could

produce 10 mM of formate from H_2 and CO_2 and up to 50 mM of formate when H_2 and bicarbonate were used [11]. However, formate was only produced after blocking the energy metabolism for acetate production. The metabolism of *A. woodii* is strictly sodium ion-dependent, with acetate as the final product. The use of a sodium ionophore or the absence of sodium ions allowed the blockage of acetate production so that electrons could be diverted to formate production [11]. A different approach was taken by Hwang *et al*. who developed a bioelectrocatalytic system to generate formate using oxygen-stable cells of *Methylobacterium* [13]. This electrochemical reactor was operated with CO_2 as carbon source and electricity as a reductant instead of H_2. In that work, a maximum formate concentration of 60 mM was obtained after 80 h using *M. extorquens* AM1, in the presence of methyl viologen as electron mediator [13]. In another study, non-engineered *E. coli* cells showed a formate production of only 2.5 mM after 24 h [12]. This was improved by genetic engineering to create strains harboring FDHs from different species (*Clostridium carboxidivorans*, *Pyrococcus furiosus* and *Methanobacterium thermoformicicum*), displaying high catalytic activity for CO_2 reduction. The recombinant strains produced between 10 to 20 mM of formate in 5 h [12]. In addition, the recombinant *E. coli* cells with a FDH from the thermophile *P. furiosus* was able to reach a concentration of 44 mM of formate after 2 h, in batch conditions, when H_2 sparging was used [12]. In the present work, no recombinant strains or electron mediators were used for formate production and still the values of formate produced were comparable or even higher than those reported with non-genetically modified organisms, demonstrating the

potential of *D. desulfuricans* for formate production from hydrogenation of CO_2, which may be further enhanced by genetic engineering.

4.4 CONCLUSIONS

In this study a bioreactor operating in continuous mode for formate production was developed using *D. desulfuricans* as biocatalyst. This is the first process described for continuous production of formate, using CO_2 and H_2 gas sparging. Furthermore, the FDHs and Hases involved in formate production by *D. desulfuricans* were identified, which may contribute to improving formate production efficiency by genetic manipulation of the biocatalyst. The contribution towards innovation of bioprocess and their optimization is an important step towards efficient biocatalytic hydrogenation using CO_2 as feedstock for the generation of formate.

ACKNOWLEDGMENTS

This research was supported by Fundação para a Ciência e Tecnologia (Portugal) through R&D unit, UID/Multi/04551/2013 (GreenIT), grant PTDC/BBB-EBB/2723/2014 and fellowships numbers SFRH/BPD/76707/2011 and SFRH/BD/86442/2012. The authors are grateful to Catarina Pimentel for help with qRT-PCR experiments.

REFERENCES

1. Sternberg A, Bardow A. Power-to-What? – Environmental assessment of energy storage systems. Energy Environ Sci. 2015;8: 389–400.

2. Enthaler S, von Langermann J, Schmidt T. Carbon dioxide and formic acid—the couple for environmental-friendly hydrogen storage? Energy Environ Sci. 2010;3: 1207–1217.

3. Hawkins AS, McTernan PM, Lian H, Kelly RM, Adams MW. Biological conversion of carbon dioxide and hydrogen into liquid fuels and industrial chemicals. Curr Opin Biotechnol. 2013;24: 376–384.

4. Pereira IAC. An enzymatic route to H_2 storage. Science. 2013;342: 1329–1330.

5. Yuan Z, Eden MR, Gani R. Toward the development and deployment of large-scale carbon dioxide capture and conversion processes. Ind Eng Chem Res. 2016;55: 3383–3419.

6. Yishai O, Lindner SN, Gonzalez de la Cruz J, Tenenboim H, Bar-Even A. The formate bio-economy. Curr Opin Chem Biol. 2016;35: 1–9.

7. Boddien A, Gärtner F, Federsel C, Sponholz P, Mellmann D, Jackstell R, *et al.* CO_2 -"neutral" hydrogen storage based on bicarbonates and formates. Angew Chemie. 2011;50: 6411–6414.

8. Appel AM, Bercaw JE, Bocarsly AB, Dobbek H, DuBois DL, Dupuis M, *et al*. Frontiers, opportunities, and challenges in biochemical and chemical catalysis of CO_2 fixation. Chem Rev. 2013;113: 6621–6658.

9. Moret S, Dyson PJ, Laurenczy G. Direct synthesis of formic acid from carbon dioxide by hydrogenation in acidic media. Nat Commun. 2014;5: 4017.

10. Aresta M, Dibenedetto A, Quaranta E. State of the art and perspectives in catalytic processes for CO_2 conversion into chemicals and fuels: The distinctive contribution of chemical catalysis and biotechnology. J Catal. 2016;343: 2–45.

11. Schuchmann K, Muller V. Direct and reversible hydrogenation of CO_2 to formate by a bacterial carbon dioxide reductase. Science. 2013;342: 1382–1385.

12. Alissandratos A, Kim HK, Easton CJ. Formate production through carbon dioxide hydrogenation with recombinant whole cell biocatalysts. Bioresour Technol. 2014;164: 7–11.

13. Hwang H, Yeon YJ, Lee S, Choe H, Jang MG, Cho DH, *et al.* Electro-biocatalytic production of formate from carbon dioxide using an oxygen-stable whole cell biocatalyst. Bioresour Technol. 2015;185: 35–39.

14. Rabus R, Venceslau SS, Wöhlbrand L, Voordouw G, Wall JD, Pereira IAC. A post-genomic view of the ecophysiology, catabolism and biotechnological relevance of sulphate-reducing prokaryotes. In: Poole RK, editor. Advances in Microbial Physiology. 2015. pp. 55–321.

15. Pereira IAC, Ramos AR, Grein F, Marques MC, da Silva SM, Venceslau SS. A comparative genomic analysis of energy metabolism in sulfate reducing bacteria and archaea. Front Microbiol. 2011;2: 1–18.

16. Hartmann T, Schwanhold N, Leimkühler S. Assembly and catalysis of molybdenum or tungsten-containing formate dehydrogenases from bacteria. Biochim Biophys Acta - Proteins Proteomics. 2015;1854: 1090–1100.

17. Maia LB, Moura JJG, Moura I. Molybdenum and tungsten-dependent formate dehydrogenases. J Biol Inorg Chem. 2015;20: 287–309.

18. Lubitz W, Ogata H, Rudiger O, Reijerse E. Hydrogenases. Chem Rev. 2014;114: 4081–4148.

19. Martins M, Pereira IAC. Sulfate-reducing bacteria as new microorganisms for biological hydrogen production. Int J Hydrogen Energy. 2013;38: 12294–12301.

20. Martins M, Mourato C, Pereira IAC. *Desulfovibrio vulgaris* growth coupled to formate-driven H_2 production. Environ Sci Technol. 2015;49: 14655–14662.

21. Martins M, Mourato C, Morais-Silva FO, Rodrigues-Pousada C, Voordouw G, Wall JD, *et al.* Electron transfer pathways of formate-driven H_2 production in *Desulfovibrio*. Appl Microbiol Biotechnol. Applied Microbiology and

Biotechnology; 2016;100: 8135–8146.

22. Matias PM, Pereira IAC, Soares CM, Carrondo MA. Sulphate respiration from hydrogen in Desulfovibrio bacteria: A structural biology overview. Progress in Biophysics and Molecular Biology. 2005. pp. 292–329.

23. da Silva SM, Pacheco I, Pereira IAC. Electron transfer between periplasmic formate dehydrogenase and cytochromes c in *Desulfovibrio desulfuricans* ATCC 27774. JBIC J Biol Inorg Chem. 2012;17: 831–838.

24. Reddy KJ, Gilman M. Preparation of bacterial RNA. In: Ausubel FM, Brent R, Kingston RE, Moore DD, Seidman JG, Smith JA, *et al.*, editors. Current Protocols in Molecular Biology. Hoboken, NJ, USA: John Wiley & Sons, Inc.; 2001. p. 4.4.1-4.4.7.

25. Christensen GA, Zane GM, Kazakov AE, Li X, Rodionov DA, Novichkov PS, *et al*. Rex (Encoded by DVU_0916) in *Desulfovibrio vulgaris* Hildenborough is a repressor off sulfate adenylyl transferase and is regulated by NADH. J Bacteriol. 2015;197: 29–39

26. da Silva SM, Voordouw J, Leitão C, Martins M, Voordouw G, Pereira IAC. Function of formate dehydrogenases in *Desulfovibrio vulgaris* Hildenborough energy metabolism. Microbiology. 2013;159: 1760–1769.

27. Hanselmann KW. Microbial energetics applied to waste repositories. Cell Mol Life Sci. 1991;47: 645–687.

28. Sander R. Compilation of Henry's law constants (version 4.0) for water as solvent. Atmos Chem Phys. 2015;15: 4399–4981.

29. da Silva SM, Pimentel C, Valente FMA, Rodrigues-Pousada C, Pereira IAC. Tungsten and molybdenum regulation of formate dehydrogenase expression in *Desulfovibrio vulgaris* Hildenborough. J Bacteriol. 2011;193: 2909–2916.

30. Mota CS, Valette O, González PJ, Brondino CD, Moura JJG, Moura I, *et al*. Effects of molybdate and tungstate on expression levels and biochemical characteristics of formate dehydrogenases produced by *Desulfovibrio alaskensis* NCIMB 13491. J Bacteriol. 2011;193: 2917–2923.

31. Costa C, Teixeira M, Moura I, LeGall J, Moura JJG. Formate dehydrogenase from *Desulfovibrio desulfuricans* ATCC 27774: isolation and spectroscopic characterization of the active sites (heme, iron-sulfur centers and molybdenum). J Biol Inorg Chem. 1997;2: 198–208.

32. Brondino CD, Passeggi MCG, Caldeira J, Almendra MJ, Feio MJ, Moura JJG, *et al.* Incorporation of either molybdenum or tungsten into formate dehydrogenase from *Desulfovibrio alaskensis* NCIMB 13491; EPR assignment of the proximal iron-sulfur cluster to the pterin cofactor in formate dehydrogenases from sulfate-reducing bacteria. J Biol Inorg Chem. 2004;9: 145–151.

33. Wang J, Wan W. Effect of temperature on fermentative hydrogen production by mixed cultures. Int J Hydrogen Energy. 2008;33: 5392–5397.

34. Seol E, Manimaran A, Jang Y, Kim S, Oh Y-K, Park S. Sustained hydrogen production from formate using immobilized recombinant *Escherichia col*i SH5. Int J Hydrogen Energy. 2011;36: 8681–8686.

35. Hartmann T, Leimkühler S. The oxygen-tolerant and NAD^+-dependent formate dehydrogenase from *Rhodobacter capsulatus* is able to catalyze the reduction of CO_2 to formate. FEBS J. 2013;280: 6083–6096.

36. Sawers RG. Formate and its role in hydrogen production in Escherichia coli. Biochem Soc Trans. 2005;33: 42–46.

37. McDowall JS, Murphy BJ, Haumann M, Palmer T, Armstrong FA, Sargent F. Bacterial formate hydrogenlyase complex. Proc Natl Acad Sci U S A. 2014;111: E3948–E3956.

38. Bassegoda A, Madden C, Wakerley DW, Reisner E, Hirst J. Reversible interconversion of CO_2 and formate by a molybdenum-containing formate dehydrogenase. J Am Chem Soc. 2014;136: 15473–15476.

39. Pinske C, Sargent F. Exploring the directionality of *Escherichia coli* formate hydrogenlyase: a membrane-bound enzyme capable of fixing carbon dioxide to organic acid. Microbiol Open. 2016;5: 721–737.

40. Caffrey SM, Park H-S, Voordouw JK, He Z, Zhou J, Voordouw G. Function of periplasmic hydrogenases in the sulfate-reducing bacterium *Desulfovibrio*

vulgaris Hildenborough. J Bacteriol. 2007;189: 6159–6167.

41. Pereira PM, He Q, Valente FMA, Xavier A V, Zhou J, Pereira IAC, *et al.* Energy metabolism in *Desulfovibrio vulgaris* Hildenborough: insights from transcriptome analysis. Antonie Van Leeuwenhoek. 2008;93: 347–362.

42. Pohorelic BKJ, Voordouw JK, Lojou E, Dolla A, Harder J, Voordouw G. Effects of deletion of genes encoding Fe-only hydrogenase of *Desulfovibrio vulgaris* hildenborough on hydrogen and lactate metabolism. J Bacteriol. 2002;184: 679–686.

43. Li X, Luo Q, Wofford NQ, Keller KL, McInerney MJ, Wall JD, *et al.* A molybdopterin oxidoreductase is involved in H_2 oxidation in *Desulfovibrio desulfuricans* G20. J Bacteriol. 2009;191: 2675–2682.

CHAPTER 5

CONCLUDING REMARKS

5. CONCLUDING REMARKS

H_2 is as an energy carrier of the future, due to its clean combustion but many research efforts must still be carried out to achieve a H_2 economy. The search for an efficient and safe H_2 storage system is probably one of the most crucial step. In this sense, the use of formate as H_2 storage system might act as a simple and efficient concept, with CO_2 as the only byproduct.

Due to the importance of implementing a H_2 and formate economy, there is a need to find alternative suitable processes to the use of the currently chemical, expensive and exhaustible processes for the production of these two biofuels. Thus, biologic systems, based on using whole cell biocatalysts, have been investigated and developed for biological H_2 and formate production and in this work we focused on evaluating the potential of a new group of anaerobic microorganisms to be used as biocatalysts in these two processes.

In this thesis, two main investigations were conducted: an applied study where the potential of SRB as biocatalysts for H_2 and formate production was evaluated and new technologies were developed; and fundamental studies in which the aim was to investigate the capacity of SRB to grow by the conversion of formate to H_2 in the absence of sulfate and to understand the metabolic pathways involved in H_2 and formate production.

The present work clearly demonstrated that SRB are capable of producing H_2 from formate and also capable of producing formate from the hydrogenation

of CO_2. In these studies, the H_2 and formate production capacity of SRB was evaluated in different *Desulfovibrio* species since this genus is the most thoroughly studied among SRB. In H_2 production studies, *D. vulgaris* showed to be the strain with the highest H_2 production performance, whereas in the production of formate, *D. desulfuricans* was the strain producing the highest amount of formate. Moreover, the potential of new design bioreactors for continuous H_2 and formate production using these microorganisms as biocatalysts was demonstrated for the first time. The developed bioreactors constitute a simple and low cost technology for H_2 and formate production, especially when compared to the actual processes for the generation of these compounds.

Furthermore, in the H_2 production studies, it was also demonstrated for the first time that a single mesophilic organism, *D. vulgaris*, can grow by the conversion of formate to H_2 in the absence of sulfate, which had only been observed before in a single hyperthermophile organism or in syntrohic association. Although in the study of formate production, the growth coupled to formate production from H_2 and CO_2 was not investigated, the results obtained highlighted the potential of *D. desulfuricans* cells to grow by the conversion of H_2 and CO_2 to formate in the bioreactor. Thus, this could be further evaluated in future work.

Since it was shown that SRB have potential to be used as biocatalysts for H_2 and formate production, it was also important to understand the metabolic pathways involved in these processes. SRB possess a high content of FDHs and

Hases, and the role of these enzymes in the reversible reactions of H_2 and formate production was elucidated in this thesis. Regarding formate-driven H_2 production, it was demonstrated that the electron transfer pathways vary among *Desulfovibrio* sp. In *D. vulgaris*, the periplasmic FdhAB showed to be the key enzyme for formate oxidation and two pathways are involved in the production of H_2 from formate: a direct one only involving periplasmic enzymes, in which the Hys [NiFeSe] Hase is the main enzyme responsible for H_2 production; and a second one that involves transmembrane electron transfer and may allow for energy conservation. In contrast, the H_2 production in *D. gigas* occurs exclusively in the periplasm not involving the cytoplasmic Ech Hase. Concerning the hydrogenation of CO_2 to formate, it was concluded that the cytoplasmic FdhAB and the periplasmic HydAB [FeFe] are the main enzymes expressed in *D. desulfuricans*.

Overall, the research presented in this thesis contributed to the emerging field of biological H_2 and formate production as energy sustainable resources and showed the potential of SRB as whole cells biocatalysts in the interconversion of H_2 and formate. SRB whole cells as biocatalysts was shown to be a promising approach for large scale H_2 and formate production due to their high energy efficiency and stability in bioreactors. Nevertheless, further studies should be performed in order to improve H_2 or formate productivity by process optimization such as whole cell immobilization in a continuous process or through genetic engineering of the biocatalysts.

♪ We'll have the days we break,
And we'll have the scars to prove it,
We'll have the bonds that we saved,
But we'll have the heart not to lose it.

For all of the times we've stopped,
For all of the things I'm not.

We put one foot in front of the other
We move like we ain't got no other,
We go where we go, we're marchin on, marchin on.

There's so many wars we fought
There's so many things we're not
But with what we have,
I promise you that
We're marchin on
(We're marchin on)
(We're marchin on) ♪ (“Marchin on” by One Republic)